Conformal Properties of Spacetime

Peter James Cameron

St John's College

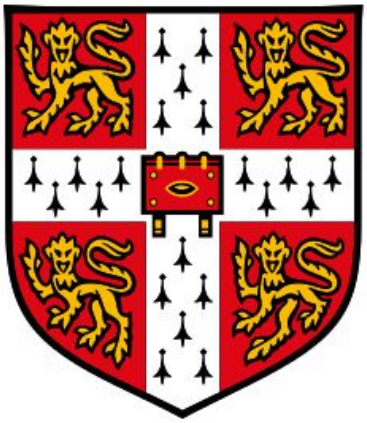

Department of Applied Mathematics and Theoretical Physics

University of Cambridge

Supervisor: Maciej Dunajski

This thesis is submitted for the degree of

Doctor of Philosophy

October 2022

This thesis is the result of my own work and includes nothing which is the outcome of work done in collaboration except as declared in the preface and specified in the text. It is not substantially the same as any work that has already been submitted before for any degree or other qualification except as declared in the preface and specified in the text.

The research presented in Chapters 2, 3, 4, 5 and 6 is based on the following papers respectively:

- P. Cameron, M. Dunajski *On Schwarzschild causality in higher dimensions*, Class. Quant. Grav. **37** (2020) 225002
- P. Cameron *The Penrose property with a cosmological constant*, Class. Quant. Grav. **39** (2022) 115002
- P. Cameron *Positivity of mass in higher dimensions*, Annales Henri Poincaré (2022), arXiv:2010.05086.
- P. Cameron, P. T. Chruściel *Asymptotic flatness in higher dimensions*, J. Math. Phys. **63**, (2022) 032501
- P. Cameron, M. Dunajski, K. P. Tod *Conformal geodesics cannot spiral*, arXiv:2205.07978, submitted to J. Differ. Geom.

These are papers [14–18] in the bibliography.

To my Mum.

Acknowledgements

Firstly I would like to thank my supervisor, Maciej Dunajski, for giving me the opportunity to complete this PhD and for all your help over the last four years. Thank you for introducing me to so many interesting topics and allowing me to chart my own course through them. You have encouraged me to take every opportunity and for that I am grateful. I would also like to thank Paul Tod and Piotr Chruściel for their helpful comments and collaboration, as well as Mihalis Dafermos, Roger Penrose, Greg Galloway, Harvey Reall, Claude Warnick and Eric Woolgar for conversations which have contributed greatly to various parts of this thesis. Thanks also to my undergraduate Director of Studies, Matthias Dörrzapf, for all his help and support in my first few years in Cambridge (and even before) and to Marion McGurk at Trinity Academy for offering me safe haven, even when I wasn't her problem.

I am also grateful to all of the friends I have made during my time in Cambridge, in particular through the Cambridge University Hare and Hounds. Without your support and love for adventure I would almost certainly never have returned to Cambridge.

Finally, I would like to thank my family. To my Dad for always being a voice of reason and to my brother for always being a voice. To my Mum for getting me into this subject in the first place and to my Grandad, who lived in a house full of Penrose tiles and Escher prints.

Abstract

We begin by studying a property first introduced by Penrose as a consistency condition for possible constructions of quantum gravity. In an asymptotically flat spacetime, this property, which we call the Penrose property, is satisfied if for any two endless timelike curves λ, ν in the same domain of outer dependence, there exists a future directed timelike curve from λ to ν. Penrose showed that this property is equivalent to the entirety of future null infinity being contained in the timelike future of every point in past null infinity. We will investigate how the Penrose property is affected by the mass and dimensionality of spacetime. By considering various examples, we find that this property appears to be a property of positive mass spacetimes in 3 and 4 dimensions.

We will then move on to study the Penrose property in greater generality. In particular we will consider how this property can be generalised to spacetimes with a non-zero cosmological constant. We find that in asymptotically de Sitter spacetimes the property can remain essentially unchanged, however in asymptotically anti-de Sitter spacetimes it is necessary for it to be re-stated in a way which is more suited to spacetimes with a timelike boundary. In the latter case we arrive at a property previously considered by Gao and Wald. Curiously, this property was shown to fail in spacetimes which focus null geodesics. This is in contrast to our findings in asymptotically flat and asymptotically de Sitter spacetimes.

Next we show how some of the methods established in the study of the Penrose property can be used to prove a version of the positive mass theorem in higher dimensions. This proof is inspired by an argument of Penrose, Sorkin and Woolgar in 3+1 dimensions. This argument relied on causality arguments to show that spacetimes which focus null geodesics (a feature we expect to be indicative of positive mass spacetimes) cannot have negative ADM mass.

Penrose has argued that the Penrose property is a property of spacetime near i^0. We have also demonstrated how this property appears to depend on the dimensionality of spacetime. Motivated by this, we study more generally the nature of possible conformal completions at spatial infinity. In particular, we show that $(d+1)$-dimensional Myers-Perry metrics $(d \geq 4)$

have a conformal completion at spatial infinity of $C^{d-3,1}$ differentiability class, and that this result is optimal in even spacetime dimension in the sense that no C^{d-2} completion exists unless the ADM mass is zero. We also present the associated asymptotic symmetries.

Finally, we will study conformal geodesics. We will show that these curves cannot spiral towards a point. This resolves a major unsolved problem in the field. We will begin by developing a proof of the same result for metric geodesics which does not rely on length minimisation arguments, before showing how this proof can be generalised to rule out spiralling of conformal geodesics.

Contents

Chapter1

Introduction

1.1 Conformal Transformations in General Relativity

General relativity is a geometric theory of gravity defined on a manifold, M, known as *spacetime*, equipped with a Lorentzian signature metric g. The metric is responsible for describing the curvature of spacetime, which in turn is related to the distribution of matter through the Einstein field equations[1] [70].

$$G_{ab} + \Lambda g_{ab} = \frac{8\pi G}{c^4} T_{ab} \tag{1.1.1}$$

It is postulated that massive particles travel along timelike curves whose tangent vector X satisfies[2] $g(X, X) > 0$, while massless particles (such as photons) travel along null curves, whose tangent vector satisfies $g(X, X)$=0. Points which cannot be connected by a causal (i.e. timelike or null) curve are said to be spacelike separated. Such points have the physical interpretation that communication between them is impossible.

From this it follows that the causal structure of spacetime is invariant under a conformal

[1] In the remainder of this thesis we will set $c = G = 1$.
[2] For consistency with [59], we will use the 'mostly minus' signature $(+, -, \ldots, -)$.

re-scaling of the metric:

$$g_{ab} \mapsto \Omega^2 g_{ab} \tag{1.1.2}$$

where $\Omega : M \to \mathbb{R}^+$ is a nowhere vanishing function. For this reason, if we are interested only in the causal structure of spacetime then we are free to perform a conformal re-scaling.

Conformal transformations are useful if one is interested in the asymptotic properties of spacetime. In [55,56], Penrose showed how certain spacetimes could be conformally embedded into the interior of a compact manifold with boundary. This boundary, known as *conformal infinity*, then represents points "at infinity" in the physically relevant spacetime. One benefit of this construction is that it provides an arena in which certain problems of physical relevance can be posed. For example, initial data for scattering problems can be posed on the subset of conformal infinity representing null rays in the far past. One then aims to solve a Goursat problem to find the outgoing data in the far future [35,51]. Conformal infinity is also useful as the location where many global quantities, such as the total mass and momentum contained in a spacetime, can be defined.

1.2 A Quantum Gravity Consistency Condition

In [59], Penrose studies a property which arises from considering a 'Lorentz covariant' approach to quantum gravity. In such an approach, the theory is constructed with respect to some background Minkowski metric, η, and the physical field tensors, including the metric, g, are constructed as an infinite sum of tensors defined with respect to this background metric. For example, we write a physical operator as a sum

$$\mathcal{O}_g\left(x^\mu\right) = \mathcal{O}_\eta^{(0)}\left(x^\mu\right) + \mathcal{O}_\eta^{(1)}\left(x^\mu\right) + \mathcal{O}_\eta^{(2)}\left(x^\mu\right) + \ldots \tag{1.2.1}$$

where the operators $\mathcal{O}_\eta^{(\alpha)}$ are Lorentz covariant operators such that for any states $|\psi\rangle$, $|\psi'\rangle$ and any point x^μ, we have $\left|\langle\psi'|\,\mathcal{O}_\eta^{(\alpha)}(x^\mu)\,|\psi\rangle\right| \to 0$ sufficiently quickly as $\alpha \to \infty$ to ensure this sum converges.

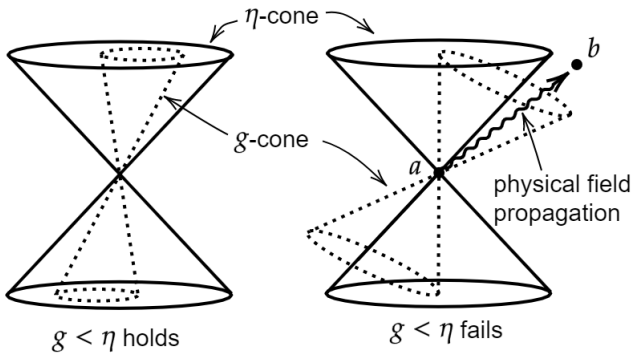

Figure 1.1: $g < \eta$ is a necessary condition for the 'Lorentz covariant' approach to be consistent with QFT

This construction places restrictions on the physical theory one can write down. In particular, the physical metric, g, defines the causal structure of the theory and we need to ensure this causal structure is consistent with the standard rules of quantum field theory. For example, any two operators evaluated at spacelike separated points must commute, while operators evaluated at timelike separated points should have non-zero commutator in general (where we evaluate this condition using η for the background operators and g for the physical operators). This leads to a consistency condition on the theory. In order for the 'Lorentz covariant' approach to remain valid, the lightcones defined by g must be contained inside the lightcones defined by η. If this condition fails, then there are points a, b as shown on the right in Figure 1.1 which are timelike separated with respect to g but spacelike separated with respect to η. This means we require the background Lorentz covariant operators defined at these points to commute, but the physical operators should have non-zero commutator in general. This is clearly incompatible with the Lorentz covariant expansion (1.2.1). Following [59], we will denote this condition by $g < \eta$, since it tells us that if a curve is timelike with respect to g, then it must also be timelike with respect to η.

Furthermore, in order for problems involving data specified "at infinity" (for example scattering problems) to be posed on the spacetime (M, g), it is necessary for (M, g) to have the same asymptotic behaviour as the background Minkowski spacetime. By this we mean that whichever Minkowski metric we choose to define the background structure, it should be possible to conformally embed both spacetimes in the same compact manifold using the

same embedding map, with all null geodesics which escape to the asymptotic region having endpoints on the null hypersurfaces which comprise the conformal boundary at infinity (see Section 2.1 for definitions). For example, as discussed in [59], if we consider (M, g) to be the Schwarzschild spacetime in 3+1 dimensions with metric

$$ds^2 = \left(1 - \frac{2m}{r}\right) dt^2 - \frac{dr^2}{1 - \frac{2m}{r}} - r^2 \left(d\theta^2 + \sin^2\theta d\phi^2\right) \tag{1.2.2}$$

then the Minkowski metric obtained by setting $m = 0$ satisfies the condition $g < \eta$, however the two spacetimes cannot be compactified using the same procedure. Any attempt to compactify (M, g) using a procedure suitable for this Minkowski spacetime will result in g–null geodesics which escape to the asymptotic region but do not have endpoints on the conformal boundary at infinity (these endpoints will instead lie at timelike or spacelike infinity depending on the sign of m).

Motivated by this, Penrose [59] introduces a property we call the *non-timelike boundary version of the Penrose Property* (Definition 2.1.5). This property involves past and future null infinity, $\mathscr{I}^{\pm}$, however Penrose shows (Theorem 2.1.7) that in asymptotically flat spacetimes it can equivalently be stated as a property which does not refer to $\mathscr{I}^{\pm}$ (Definition 2.1.6) which we call the *finite version of the Penrose property*. This equivalence allows us to refer to both versions concurrently as the *Penrose Property*. Penrose goes on to show (Theorem 2.1.9) that if an asymptotically flat spacetime (M, g) satisfies the Penrose property, then then there is no Minkowski metric, η, on M with compatible asymptotics (in the sense outlined above) such that quantum gravity consistency condition, $g < \eta$, is satisfied. The main result of [59] is to show that the Penrose property is satisfied by the positive mass Schwarzschild spacetime in 3+1 dimensions. This example, coupled with Theorem 2.1.9, provides strong evidence against the validity of a 'Lorentz covariant' theory of quantum gravity.

Despite its original quantum gravity motivations, the Penrose property can also be considered an interesting and important property in its own right. The arguments presented in [59] suggest that this property should be thought of as a statement about the asymptotic behaviour of null rays near spatial infinity. For example, in Minkowski spacetime the only points on

$\mathscr{I}^{\pm}$ which cannot be timelike connected are antipodal points in some neighbourhood of i^0 (Proposition 2.2.3). In 3+1 dimensional Schwarzschild spacetime, it is precisely the extent to which null geodesics are focused and retarded by the positive point mass (which can be thought of as living at i^0) which results in these points being in timelike communication. Studying the Penrose property leads to a better understanding of the effect of the ADM mass and dimensionality of spacetime on null geodesics near infinity. In particular this allows a version of the positive mass theorem to be proved (see [61] and Chapter 4 for further discussion).

Not only does the Penrose property fail in Minkowski spacetime, it is also impossible to connect certain antipodal points using a null curve through the interior of the spacetime. It is however possible to connected these points using null curves which lie entirely on the conformal boundary and pass through i^0. This suggests an alternative interpretation of the Penrose property which instead views it as a statement about which points on the conformal boundary can be causally connected using curves restricted to this boundary, and which can be causally connected using curves entering the interior spacetime (Definition 3.3.2). This interpretation provides a link between the Penrose property and a result of Gao and Wald (Theorem 3.3.3) for spacetimes which are asymptotically anti-de Sitter. This result says that if the spacetime satisfies a suitable focusing theorem then null geodesics passing through the bulk spacetime are "delayed" relative to those restricted to conformal infinity. Consequently there are pairs of points on the conformal boundary which can be timelike connected by curves restricted to the boundary but not by curves through the bulk. Curiously, this is precisely the opposite to what is observed in the asymptotically flat case in 3+1 dimensions, where the positive mass Schwarzschild spacetime satisfies both a focusing theorem and the Penrose property.

1.3 Mass in General Relativity

Mass in general relativity is a surprisingly subtle issue. One of the key features of the theory is its diffeomorphism invariance, however this also means that no local definition of mass-energy can exist. Such a quantity would be obtained by integrating some energy density function over a spacetime volume. This energy density would in turn be defined in terms of the metric and its first derivatives. However, general covariance of the theory allows us to set

$$\begin{aligned} g_{\mu\nu} &= \eta_{\mu\nu} \\ \partial_\rho g_{\mu\nu} &= 0 \end{aligned} \tag{1.3.1}$$

at any point $p \in M$. Consequently, any such local energy density must be co-ordinate dependent and hence cannot hold any physical meaning.

There have been attempts (for example in [12,43,49,60]) to construct a "quasi-local" definition of mass. This would involve assigning an energy-momentum vector to any spacelike sphere bounding some compact portion of a spacelike hypersurface. However, these attempts have also run into various problems (see for example [53, 71]).

We will focus on the global definition of mass given by Arnowitt, Deser and Misner in [3]. In this set-up it is assumed that $(d+1)$-dimensional spacetime is foliated by spacelike hypersurfaces, Σ_t, and that the metric takes the form

$$ds^2 = Ndt^2 - h_{ij}(dx^i + N^i dt)(dx^j + N^j dt) \tag{1.3.2}$$

where the lapse function N satisfies

$$N = 1 + O(r^{-(d-2)}), \tag{1.3.3}$$

the shift vector N^i satisfies

$$N^i = O(r^{-(d-2)}), \tag{1.3.4}$$

and the metric h_{ij} defined on the spacelike hypersurfaces, Σ_t, satisfies

$$\begin{aligned} h_{ij} &= \delta_{ij} + O(r^{-(d-2)}) \\ \partial_k h_{ij} &= O(r^{-(d-1)}). \end{aligned} \tag{1.3.5}$$

Definition 1.3.1. For a spacetime satisfying the above conditions, the ADM mass is defined to be

$$m_{ADM} := \frac{1}{2(d-1)A_{S^{d-1}}} \lim_{r\to\infty} \int_{S_r^{d-1}} n_i \left(\partial_j h_{ij} - \partial_i h_{jj}\right) d\mathrm{A} \tag{1.3.6}$$

where S_r^{d-1} denotes the $(d-1)$-sphere of Euclidean radius r (with S^{d-1} denoting the corresponding unit $(d-1)$-sphere and $A_{S^{d-1}}$ its area), and n_i denotes the unit outward normal from S_r^{d-1}.

This definition can be motivated by considering a Hamiltonian formulation of general relativity, however in order for it to be taken seriously there are a number of criteria we expect it to satisfy. In particular, it should be non-negative under physically reasonable assumptions, and zero if and only if the spacetime is isometric to a subset of Minkowski. It is clearly possible to construct spacetimes for which the ADM mass is negative, for example Schwarzschild with $m < 0$, so it is also an issue to establish exactly what one means by "physically reasonable".

The positive mass theorem for 3+1 dimensional spacetimes admitting a maximal slice and arising from initial data which satisfies the dominant energy condition was first proved by Schoen and Yau [64–66] using minimal surface arguments. This result was later extended to spacetimes of dimension up to seven by Eichmair, Huang, Lee and Schoen [33]. A more complete proof, based on spinors, which did not rely on a maximal slicing assumption was given by Witten [72].

An alternative argument given by Penrose, Sorkin and Woolgar [61] has the advantage of relying more clearly on features of spacetime we expect to be associated with positive mass, in particular the focusing and retarding of null geodesics. In [61] it is argued that spacetimes which satisfy a suitable null geodesic focusing theorem cannot have negative mass. The disadvantage of this method is that it requires global assumptions on spacetime. Since general

relativity is more naturally viewed as an evolution problem, it would be preferable to have assumptions posed at the level of initial data, as was done in previous proofs.

1.4 Structure at Spatial Infinity

One of the major questions in general relativity is that of the behaviour of the gravitational field when receding to infinity in spacelike directions. This has been studied in detail for four dimensional spacetimes in many works, see for example [5–7, 9, 10, 21, 22, 36, 40, 41, 55]. In particular, as is well known, Minkowski spacetime has a conformal completion which includes a point at spacelike infinity, called i^0, such that the conformally extended metric is smooth near this point. It is also well known that the usual extension of the Minkowskian construction to four-dimensional Schwarzschild spacetime leads to a conformal completion with a metric which is continuous [5, 9, 22] at i^0, but no C^1 extension is known. In standard examples of higher dimensional spacetimes the metric decays faster to the Minkowski metric at spacelike infinity, and therefore one expects that such constructions will lead to metrics with better differentiability properties at i^0. The question then arises about the precise degree of differentiability one can achieve.

The conformal method of constructing solutions of the general relativistic constraint equations shows that the decay of the metric towards Minkowski when receding in spacelike directions can be arbitrarily slow. Therefore nothing striking can be said in this generality. However the study of the asymptotics of initial data sets, and thus of the associated spacetimes, has been given new life by the work of Corvino and Schoen [29] (compare [25]), who show that rather general initial data sets can be deformed at large distances to members of any family of metrics which contains a complete set of asymptotic charges. A particularly useful such family is provided by the Myers-Perry metrics, to which boosts have been applied. The glued metric is then stationary near i^0. This provides useful information concerning the resulting evolution and leads one naturally to consider the conformal properties near i^0 of spacetimes within this family.

1.5 Conformal Geodesics

A manifold with (Riemannian or Lorentzian) metric, (M, g) defines a distinguished set of curves known as metric geodesics. These curves are solutions to a set of 2nd order ODEs and are uniquely specified locally by an initial point and initial unit tangent direction. However, with the exception of null geodesics in the Lorentzian case, there is in general no relation between the metric geodesics of two conformally related metrics. By analogy with metric geodesics, conformal geodesics can be thought of as a distinguished set of curves defined on a conformal manifold $(M, [g])$. These curves are solutions to a set of (conformally invariant) 3rd order ODEs and are uniquely specified locally by an initial position, unit tangent direction and perpendicular acceleration. Although metric geodesics have been studied extensively, much less is known about conformal geodesics.

Conformal geodesics were systematically introduced into general relativity by Friedrich and Schmidt [37]. Their motivation was to construct good co-ordinate systems for the local study of conformal boundaries, as discussed in Section 1.1. Normal or Gaussian co-ordinates based on timelike geodesics cannot be expected to behave well near such conformal boundaries - recall for example how, in compactified Minkowski space, timelike geodesics do not pass through null infinity but instead all focus at timelike infinity. It was shown in [37] (following an earlier suggestion in [63]) that one could instead define conformal normal or conformal Gaussian co-ordinates constructed from conformal geodesics. These would provide good co-ordinates near the conformal boundary of asymptotically Minkowskian, asymptotically de Sitter or asymptotically anti-de Sitter spacetimes.

An unresolved issue stemming from this earlier work, which was also known as an unsolved problem in Riemannian-signature conformal geometry, was the question of spiralling for conformal geodesics. A curve can be said to spiral at a point p if it enters and remains in every neighbourhood of p but does not pass through p itself. It is a classical result, based on the existence of geodesically-convex neighbourhoods [19] that metric geodesics cannot spiral. Until now this has not been shown for conformal geodesics. It is a question of interest both

abstractly and because spiralling raises the possibility of a new kind of co-ordinate singularity to guard against.

1.6 Overview of This Work

We begin in Chapter 2 by introducing the two versions of the Penrose property, which we refer to as the *non-timelike boundary version* and the *finite version*. We review the results obtained by Penrose in [59], including the proof of the equivalence of both versions of the Penrose property in asymptotically flat spacetimes. In Section 2.2 we consider in more detail the Penrose property in Minkowski spacetime, before moving on in Section 2.3 to study Schwarzschild spacetime in both higher and lower dimensions and with positive or negative mass. Our results are summarised in Theorem 2.3.7, which suggests that the Penrose property is a property of positive mass spacetimes in 3 and 4 dimensions.

In Section 2.4 we consider the Penrose property in the Ellis-Bronnikov wormhole spacetime. This is an example of a spacetime with multiple asymptotically flat ends, which leads to a more complicated result when we attempt to timelike connect points on $\mathscr{I}^{\pm}$ which lie in different ends. We then investigate in Section 2.5 how to generalise a key result of [59] regarding the effect on null geodesic endpoints of allowing the impact parameter to become infinitely large. We use this to explain the results of [2], which discusses the unique continuation of the linear wave equation in 4 or more spacetime dimensions. Finally, in Section 2.6 we derive a necessary and sufficient condition for the Penrose property to be satisfied in an asymptotically flat, spherically symmetric, static spacetime.

In Chapter 3 we study the Penrose property in greater generality. In particular we consider how this property can be generalised to spacetimes which are not asymptotically flat but instead have a positive or negative cosmological constant, Λ. In Section 3.2 we study the asymptotically de Sitter case ($\Lambda > 0$), where we find that the two versions of the Penrose property are once again equivalent and are satisfied in $d+1$ dimensional Schwarzschild-de Sitter spacetime ($d \geq 3$) of mass m if and only if $m > 0$. This is the same result as was

found in the asymptotically flat case in 3 and 4 spacetime dimensions, although the results in higher dimensions are different. In the asymptotically anti-de Sitter case ($\Lambda < 0$), studied in Section 3.3, we find that the finite version of the Penrose property is trivially satisfied and does not generalise to an interesting property. However, the non-timelike boundary version can be re-interpreted to give a non-trivial property in asymptotically AdS spacetimes. We refer to this as the *timelike boundary version of the Penrose property*. In fact, this property was previously considered in [39], where it was shown to fail in spacetimes which satisfy a focusing theorem on null geodesics. Schwarzschild-AdS with positive mass is an example of a spacetime satisfying such a focusing theorem, however in the negative mass case we find that the timelike boundary version of the Penrose property is satisfied. The main results of Sections 3.2 and 3.3 are summarised in Theorems 3.1.1 and 3.1.2.

In Section 3.4 we consider the Penrose property in spacetimes which are the product of an asymptotically flat Lorentzian manifold and a compact Riemannian manifold. We discuss the conformal compactification of such spacetimes before showing that the the two (equivalent) versions of the Penrose property are satisfied in the product spacetime if and only if they are satisfied in the Lorentzian spacetime only.

Next we move on to consider more generally how causal properties of spacetime can be related to the ADM mass. In particular, in Chapter 4 we prove a version of the positive mass theorem for higher dimensional spacetimes using arguments inspired by those of Penrose, Sorkin and Woolgar [61]. We begin in Section 4.1 with a review of these arguments, which were specific to 3+1 dimensions. As in [61], our proof involves showing that in negative mass spacetimes it is possible to construct a "fastest causal curve", γ, between antipodal generators $\Lambda^- \subset \mathscr{I}^-$ and $\Lambda^+ \subset \mathscr{I}^+$. By this we mean a causal curve with the property that no other causal curve departs Λ^- later and arrives on Λ^+ earlier than γ. This curve would necessarily be a null line - an endless null geodesic without conjugate points. In Section 4.3 we derive an estimate for the time of flight along a null geodesic escaping to the asymptotically flat region. This is analogous to the result derived in [61] for null geodesics in 3+1 dimensional spacetimes. In Section 4.4 we show how a fastest causal curve can be constructed in certain negative mass, higher dimensional spacetimes. This argument relies on the estimate obtained in the previous

section. Finally, in Section 4.5 we discuss assumptions which allow a global focusing theorem to be proved. Such a theorem would rule out the existence of a null line, which allows us to conclude that spacetimes satisfying these assumptions must have non-negative mass.

In Chapter 5 we discuss conformal completions of spacetimes at spatial infinity, and in particular how the regularity of the metric near this point depends on the dimensionality of spacetime. We begin with a short discussion of three dimensional spacetimes in Section 5.1 before considering the Schwarzschild metric in all spacetime dimensions $d+1 \geq 4$ in Section 5.2. The Myers-Perry metrics are analysed in Section 5.3, where it is shown that a conformal completion at i^0 exists so that $\mathscr{I}^{\pm}$ form the past and future null cones emanating from this point and the metric is of $C^{d-3,1}$ differentiability class near this point. In Section 5.4 we show that the ADM mass provides an obstruction to C^{d-2}-differentiability in even spacetime dimensions. The asymptotic symmetries of metrics with $C^{d-3,1}$-conformal completions are also discussed.

Finally, in Chapter 6 we prove a no-spiralling theorem for conformal geodesics in Riemannian signature conformal manifolds. We begin in Section 6.1 by establishing a proof of this result in the metric geodesic case which does not rely on any length minimisation arguments. We then show how this proof can be adapted to the conformal geodesic setting. This involves defining, in Section 6.2, a conformal geodesic analogue of the exponential map. This is used to understand the local properties of conformal geodesics. Whereas in the metric geodesic case it is a standard result [19, Proposition 2.9] that for any $p \in M$, the exponential map is a bijection (in fact a diffeomorphism) from a neighbourhood of $0 \in T_pM$ to a neighbourhood of $p \in M$, we will find that the result for conformal geodesics is more complicated. In fact, we will show that the exponential map we define is a bijection from some open ball in $T_{u_0}T_pM$ (where u_0 is a fixed unit vector in T_pM) to a set in M with "heart shaped" cross-sections. In Section 6.3 we discuss how to measure the size of these image sets. Finally, in Section 6.4 we show how, despite some additional complications, the results of this Chapter can be combined to prove a no-spiralling theorem for conformal geodesics using the same logic as was outlined in Section 6.1 for the metric geodesic case.

Chapter2

The Penrose Property

In this Chapter we will introduce the two versions of the Penrose property for asymptotically flat spacetimes first discussed in [59]. We will summarise Penrose's proof of their equivalence, before studying in detail precisely how they fail in Minkowski spacetime of any spacetime dimension $d+1 \geq 3$. We then move on to consider Schwarzschild spacetime in higher and lower dimensions and with positive and negative mass. The main result of this section is Theorem 2.3.7.

Next we will consider the Penrose property in a wormhole spacetime. This is an example of a spacetime with two asymptotically flat ends and will be more complicated because it will also be necessary to consider points on $\mathscr{I}^{\pm}$ in different ends.

Finally we will see how the methods we have used to study the Penrose property can help explain results regarding the unique continuation of the linear wave equation obtained in [2]. We will finish by proving a general result regarding the Penrose property in static, spherically symmetric spacetimes.

2.1 Introduction to the Penrose Property

Throughout this thesis we will be interested in spacetimes which admit a conformal compactification. We make the following definitions.

Definition 2.1.1. A time- and space-orientable spacetime (M, g) is *partially asymptotically simple* if there is a strongly causal spacetime $(\tilde{M}, \overline{g})$ and an embedding $\varphi : M \to \tilde{M}$ which embeds M as a manifold with smooth boundary $\partial\overline{M}$ in $\tilde{M}$ such that:

1. there is a smooth function Ω on $\tilde{M}$, with $\Omega > 0$ and $\varphi^*(\overline{g}) = \varphi^*(\Omega)^2 g$ on M;
2. $\Omega = 0$ and $d\Omega \neq 0$ on $\partial\overline{M}$.

We shall write $\overline{M} \equiv M \cup \partial\overline{M}$ and refer to $(\overline{M}, \overline{g})$ as the conformal compactification of (M, g). Definition 2.1.1 ensures that such a conformal compactification exists. For brevity we will often omit the embedding map φ, for example writing $\overline{g} = \Omega^2 g$ for condition 1 above.

In a partially asymptotically simple spacetime, we define $\mathscr{I}^+$ to be elements of $\partial\overline{M}$ which are future endpoints of null geodesics and we define $\mathscr{I}^-$ to be elements of $\partial\overline{M}$ which are past endpoints of null geodesics. The union of these two sets will be referred to as the *conformal boundary at infinity*, denoted $\mathscr{I}$. Note that $\mathscr{I}^+$ and $\mathscr{I}^-$ may have non-empty intersection. For example in the compactification of anti-de Sitter spacetime (Section 3.3), we have $\mathscr{I} = \mathscr{I}^+ = \mathscr{I}^-$.

In the remainder of this Chapter as well as in Chapter 3, we will often consider spacetimes satisfying one of the following additional conditions .

Definition 2.1.2. A time- and space-orientable spacetime (M, g) is *asymptotically flat* if it is partially asymptotically simple and $R_{ab} = 0$ on some neighbourhood of $\mathscr{I}$ in $\overline{M}$.

Definition 2.1.3. A time- and space-orientable spacetime (M, g) is *asymptotically de Sitter* if it is partially asymptotically simple and $R_{ab} = \Lambda g_{ab}$ on some neighbourhood of $\mathscr{I}$ in $\overline{M}$, for some $\Lambda > 0$.

Definition 2.1.4. A time- and space-orientable spacetime (M, g) is *asymptotically anti-de Sitter* if it is partially asymptotically simple and $R_{ab} = \Lambda g_{ab}$ on some neighbourhood of $\mathscr{I}$ in $\overline{M}$, for some $\Lambda < 0$.

Using these definitions, we introduce the first version of the Penrose property to be considered.

Definition 2.1.5 (Penrose property - non-timelike boundary version)**.** An asymptotically flat or asymptotically de Sitter spacetime, (M, g), with conformal compactification $(\overline{M}, \overline{g})$ satisfies the *non-timelike boundary version of the Penrose property* if any $p \in \mathscr{I}^-$ and any $q \in \mathscr{I}^+$ can be connected by a smooth timelike curve in $\overline{M}$.

This definition will be adapted in the case of spacetimes with timelike boundary (see Definition 3.3.2).

Besides defining this property, Penrose also shows in [59] that there is an equivalent version which does not make reference to a conformal compactification but instead relates to endless timelike curves. Before continuing, it will be helpful to define the following sets (for some $p \in \overline{M}$):

$$\begin{aligned} J^+(p) &= \{q \in \overline{M} | \exists \text{ a smooth future-directed causal curve in } \overline{M} \text{ from } p \text{ to } q\} \\ J^-(p) &= \{q \in \overline{M} | p \in J^+(q)\} \\ I^+(p) &= \{q \in \overline{M} | \exists \text{ a smooth future-directed timelike curve in } \overline{M} \text{ from } p \text{ to } q\} \\ I^-(p) &= \{q \in \overline{M} | p \in I^+(q)\}. \end{aligned} \tag{2.1.1}$$

In these definitions we include curves in the boundary of $\overline{M}$ and determine the causal nature of such curves using the conformal metric, $\overline{g}$, which extends to $\partial\overline{M}$. For non-compact spacetimes, (M, g), we can define the same sets as subsets of M rather than as subsets of $\overline{M}$. We also define single points to be curves of zero length, so $p \in J^{\pm}(p)$ but $p \notin I^{\pm}(p)$.

As in [59] we will concern ourselves only with inextendible timelike curves contained in the domain of outer dependence $\mathcal{D} = J^-(\mathscr{I}^+) \cap J^+(\mathscr{I}^-)$.

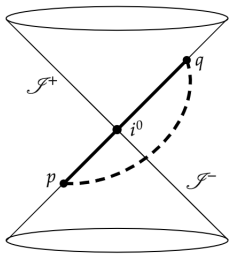

Figure 2.1: The non-timelike boundary version of the Penrose property asks whether the properties of the spacetime near i^0 allow all points on $\mathscr{I}^-$ and $\mathscr{I}^+$ to be connected using timelike curves. This figure shows $\mathscr{I}^-$ and $\mathscr{I}^+$ as the past and future lightcones emanating from i^0, as described in [5].

Definition 2.1.6 (Penrose Property - finite version)**.** A partially asymptotically simple spacetime (M, g) satisfies the *finite version of the Penrose property* if for any endless timelike curves $\lambda, \nu \subset J^-(\mathscr{I}^+) \cap J^+(\mathscr{I}^-)$, there exists $p \in \lambda$ and $q \in \nu$ such that p can be connected to q by a future pointing timelike curve in M.

The condition that $\lambda, \nu \subset J^-(\mathscr{I}^+) \cap J^+(\mathscr{I}^-)$ ensures that these curves do not cross any event horizons.

Theorem 2.1.7 (Penrose: Theorem IV.4 [59])**.** The two versions of the Penrose property, Definitions 2.1.5 and 2.1.6, are equivalent for asymptotically flat spacetimes.

To study the Penrose property it is helpful to begin with Minkowski spacetime in $d+1$ dimensions ($d \geq 1$), which we denote $\text{Mink}_{d,1}$.

Theorem 2.1.8 (Penrose [59], Thm. IV.5)**.** The Penrose property is not satisfied by $\text{Mink}_{d,1}$, for any $d \geq 1$.

Proof: With respect to co-ordinates $(t, x_1, x_2, \ldots, x_d)$, the Minkowski line element in $d+1$ dimensions can be written as

$$ds^2 = dt^2 - dx_1^2 - dx_2^2 - \cdots - dx_d^2 \tag{2.1.2}$$

Now consider the hyperbola in the $x_1 - t$ plane defined by $x_1^2 - t^2 = 1$, $x_2 = \cdots = x_d = 0$. We see (Figure 2.2) that the two branches of this hyperbola are endless timelike curves which are

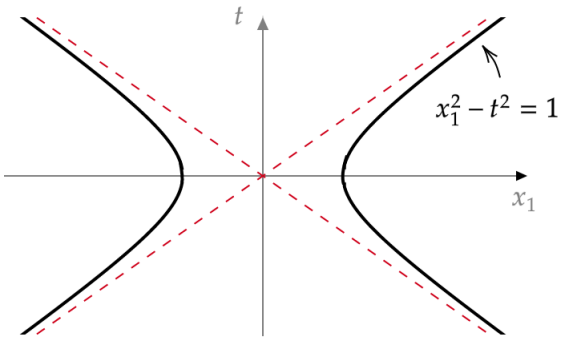

Figure 2.2: Two everywhere spacelike-separated branches of the hyperbola $x_1^2 - t^2 = 1$. These branches tend towards null lines as we approach infinity.

everywhere spacelike separated. We therefore conclude, by Theorem 2.1.7, that the Penrose property does not hold for Minkowski spacetime in any dimension. □

Penrose's motivation for studying the Penrose property in [59] is that it can be related to the condition $g < \eta$, which it was argued in Section 1.2 was a consistency condition for a "Lorentz covariant" quantum gravity construction.

Theorem 2.1.9 (Penrose: Theorem IV.5 [59])**.** Let $(\overline{M}, \overline{g})$ be the conformal compactification of an asymptotically flat spacetime which satisfies the Penrose property and let $\mathscr{I}$ denote its conformal boundary at infinity. Suppose a subset of conformally compactified Minkowski spacetime which includes a neighbourhood of i^0 can be embedded into a subset of $\overline{M}$, as in Definition 2.1.1, such that this embedding contains a neighbourhood of i^0 and has a subset of $\mathscr{I}$ as its conformal boundary at infinity. Then there is no neighbourhood of i^0 on which the inequality $\overline{g} \leq \overline{\eta}$ holds.

Proof: Suppose there does exist a neighbourhood, $U \subset \overline{M}$, of i^0, on which the condition $\overline{g} \leq \overline{\eta}$ holds. Minkowski spacetime does not satisfy the Penrose property (Theorem 2.1.8), hence we can choose $p \in \mathscr{I}^-$ and $q \in \mathscr{I}^+$ to be points which cannot be connected by a $\overline{\eta}$-timelike curve and which are sufficiently close to i^0 so that any $\overline{g}$ causal curve between them must lie entirely in U. Since $(\overline{M}, \overline{g})$ satisfies the Penrose property, we therefore have a $\overline{g}$-timelike curve $\lambda \subset U$ from p to q. The condition $\overline{g} \leq \overline{\eta}$ implies that this curve is also timelike with respect to the metric $\overline{\eta}$. This is a contradiction. □

In the remainder of this Chapter and in Chapter 3 we will primarily consider the Penrose property as a property in its own right, rather than as a tool to constrain possible theories of quantum gravity. It will turn out that a useful way to prove results relating to this property will be to use a similar trick of comparing the metric of interest to some other metric, defined on the same manifold, whose properties we do understand.

We will consider the Penrose property in Schwarzschild spacetime in both higher and lower dimensions and with positive or negative mass. Our results can be summarised by the following theorem:

Theorem 2.3.7: The Penrose property is satisfied by Schwarzschild spacetime of mass m and varying spacetime dimension according to the following table

Spacetime dimension	$m > 0$	$m \leq 0$
3	✓	✗
4	✓	✗
≥ 5	✗	✗

This result can be understood intuitively as follows. Minkowski spacetime in $(d+1)$–dimensions can be compactified as in Section 2.3.2. In this compactification, certain pairs of points on $\mathscr{I}^-$ and $\mathscr{I}^+$ which project to antipodal points on S^{d-1} cannot be connected by timelike curves (Proposition 2.2.3). They can however be connected by a null curve passing through i^0, as shown in Figure 2.1. As explained in [5], spacetimes with positive ADM mass can be thought of as containing a point mass at i^0. If the ADM mass is positive, we expect this point mass to focus null geodesics. This may allow all antipodal points on $\mathscr{I}^-$ and $\mathscr{I}^+$ to be timelike connected. However, this focusing is offset by the time delay of null geodesics in positive mass spacetimes which we might expect to prevent us from timelike connecting points near spatial infinity. Whether or not the non-timelike boundary version of the Penrose property is satisfied depends on the interplay between these two effects. This in turn depends on the dimensionality of spacetime. We will find in fact that in the 3+1 dimensional positive mass case, null geodesics passing further from the source are time advanced relative to those

passing nearer. Moreover, this advancement becomes infinite as we let the impact parameter diverge. This effect was discussed in [59] where it was used to show that the Penrose property is satisfied in this case.

We also seek to clear up some apparent contradictions in the literature. For example, in a footnote in section 2 of [74], Witten states that one can leave the dimension arbitrary when studying the causal properties of spacetimes and that restricting to 4 spacetime dimensions 'does not introduce any complications'. This is in contradiction with [13], where in section 2.1 the authors outline an argument which suggests that the causal properties of higher dimensional asymptotically flat spacetimes are different to those in 4 dimensions. The results of Theorem 2.3.7 agree that the causal structure of spacetime is affected by dimensionality.

2.2 Minkowski Causality

Before looking at more complicated situations, we should first make sure we fully understand Minkowski spacetime. We have seen from the hyperbola example in Theorem 2.1.8 that in compactified Minkowski space, some points on $\mathscr{I}^-$ cannot be timelike connected to certain points on $\mathscr{I}^+$. To understand exactly which points this applies to, we will require the following result about spherically symmetric spacetimes.

Lemma 2.2.1. Consider a static, spherically symmetric, asymptotically flat spacetime (M, g) in $d+1$ dimensions. Let γ be a timelike curve with endpoints $p \in \mathscr{I}^-$ and $q \in \mathscr{I}^+$. Then we can choose polar co-ordinates $(t, r, \theta_1, ..., \theta_{d-2}, \phi)$, where $t \in \mathbb{R}$, r is defined on some subset of $\mathbb{R}$, $\phi \in [0, 2\pi)$ and θ_1,...$\theta_{d-2} \in [0, \pi]$, as well as a timelike curve, γ', from p to q such that $\theta_1 = ... = \theta_{d-2} = \pi/2$ along γ'.

In other words, if we are trying to timelike connect two points in a spherically symmetric spacetime, it suffices to consider only curves lying in the equatorial plane defined with respect to suitable co-ordinates.

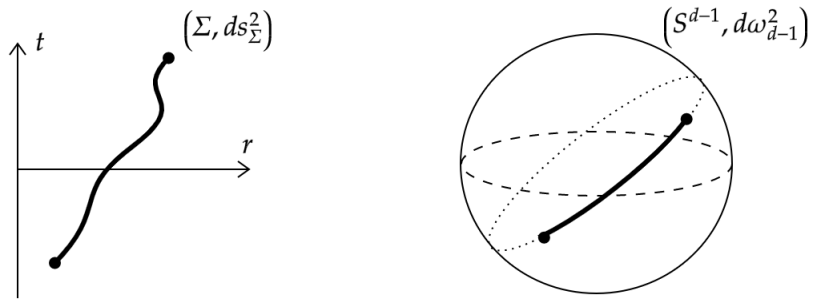

Figure 2.3: A curve in $d+1$-dimensional, spherically symmetric, static spacetime can be thought of as a pair of curves in Σ and S^{d-1} described by a common parameter.

Proof: Let the metric take the form

$$ds^2 = A(r)^2 dt^2 - B(r)^2 dr^2 - r^2 d\omega^2_{d-1}.$$

We follow [46] and consider the conformally re-scaled metric

$$\overline{ds}^2 = r^{-2} g = ds^2_\Sigma - d\omega^2_{d-1},$$

defined on the product space $\Sigma \times S^{d-1}$, where ds^2_Σ is a Lorentzian metric on the surface Σ. An endless non–spacelike curve in the $d+1$ dimensional spacetime therefore corresponds to a pair of curves described by a common parameter, s. One of these is an endless curve in Σ and the other is a curve in S^{d-1} (which may be a single point) with endpoints which come from looking at the points on S^{d-1} at which γ meets $\mathscr{I}^{\pm}$ [1].

If the full curve in M is timelike, then the line element evaluated at each point along it satisfies

$$\bar{ds}^2 = ds^2_\Sigma - d\omega^2_{d-1} > 0. \tag{2.2.1}$$

Now consider the curve in $(S^{d-1}, d\omega^2_{d-1})$. The metric $d\omega^2_{d-1}$ is a Riemannian metric, so $d\omega^2_{d-1}(s) \geq 0$ for each value of the parameter s (with equality corresponding to a radial line segment in M). We can modify this curve, keeping the endpoints the same, so that it becomes a geodesic. This reduces the value of $d\omega^2_{d-1}(s)$ at each value of s and ensures that the curve in

[1] Recall that both $\mathscr{I}^+$ and $\mathscr{I}^-$ are topologically $\mathbb{R} \times S^{d-1}$ - this is a straightforward extension of Prop. 6.9.4 in [44])

the full spacetime remains timelike. Furthermore, the geodesic in S^{d-1} is a segment of a great circle, so we can choose spherical co-ordinates $(\theta_1, \ldots, \theta_{d-2}, \phi)$ (where $\theta_1, \ldots, \theta_{d-2} \in [0, \pi]$, $\phi \in [0, 2\pi)$) such that $\theta_1 = \cdots = \theta_{d-2} = \pi/2$ along the geodesic. This means that the curve in the full spacetime is restricted to the surface $\theta_1 = ... = \theta_{d-2} = \pi/2$. □

The following result is used by Penrose in his construction in [59] and we also be used repeatedly throughout this thesis.

Proposition 2.2.2. (Penrose [58], Prop. 2.20, Prop. 2.23 and comments after Remark 2.24) Let γ_1 and γ_2 be future pointing causal curves from a to b and from b to c respectively. Then either there exists a smooth timelike curve from a to c or the union of these geodesics, $\gamma = \gamma_1 \cup \gamma_2$, is itself a null geodesic.

We now return to considering Minkowski spacetime in $d+1$ dimensions, $\text{Mink}_{d,1}$. Since this spacetime is spherically symmetric, Lemma 2.2.1 ensures that if two points can be connected by a timelike curve then we can choose this curve to lie in a 3-dimensional surface with induced metric equal to that of $\text{Mink}_{2,1}$. It therefore suffices to consider only the compactification of Minkowski spacetime in 2+1 dimensions. The Minkowski line element in $2+1$ dimensions can be written as

$$ds^2 = dt^2 - dr^2 - r^2 d\phi^2 \tag{2.2.2}$$

where $t \in (-\infty, \infty)$ and (r, ϕ) are the usual plane polar co-ordinates.

First we define retarded and advanced time co-ordinates respectively by

$$u = t - r, \quad v = t + r \tag{2.2.3}$$

We then compactify the metric by defining

$$u = \tan P, \quad v = \tan Q \tag{2.2.4}$$

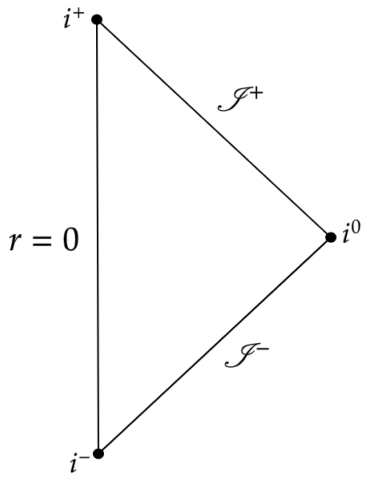

Figure 2.4: The Penrose diagram of Minkowski spacetime in $d+1$ dimensions. Each point on this diagram represents a copy of S^{d-1}

Finally, we define new co-ordinates

$$T = Q + P \in (-\pi, \pi), \quad \chi = Q - P \in [0, \pi) \tag{2.2.5}$$

which we can think of as "time" and "radial" co-ordinates respectively in the compactified spacetime.

We then consider the conformally related metric, $\overline{g}$, given by

$$\overline{g} = \Omega^2 g = (2\cos P \cos Q)^2 \, g. \tag{2.2.6}$$

This gives the line element

$$\overline{ds}^2 = dT^2 - d\chi^2 - \sin^2\chi d\phi^2. \tag{2.2.7}$$

The Penrose diagram for Minkowski spacetime in $d+1$ dimensions is shown in Figure 2.4. In 2+1 dimensions, the compactified manifold, $\overline{M}$, is a double cone (as shown in Figure 2.5), where we can think of time as moving upwards.

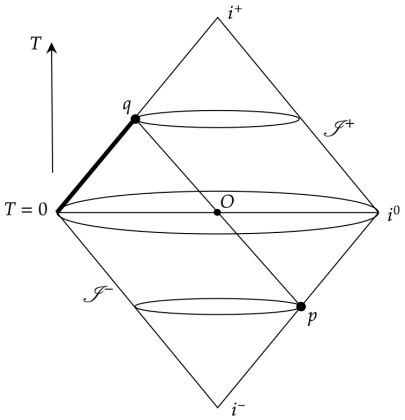

Figure 2.5: The points $p \in \mathscr{I}^-$ and $q \in \mathscr{I}^+$ are connected by a radial null geodesic through the origin. The point p can be timelike connected to all points in $\mathscr{I}^+$ except those that lie to the past of q and on the same null generator of $\mathscr{I}^+$. These points correspond to the shaded region.

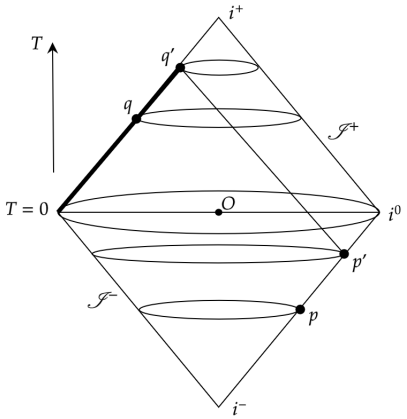

Figure 2.6: The point $p' \in \mathscr{I}^-$ can be connected to all points on $\mathscr{I}^+$ except those that lie to the past of q' and on the same null generator of $\mathscr{I}^+$ (i.e. the shaded region), where q' is the unique future endpoint of null geodesics from p' which enter M.

The antipodal points p and q in Figure 2.5 correspond to the past and future endpoints of different branches of the hyperbola shown in Figure 2.2. They have T and χ co-ordinates $(T,\chi) = \left(-\frac{\pi}{2},\frac{\pi}{2}\right)$, $\left(\frac{\pi}{2},\frac{\pi}{2}\right)$ respectively. The radial null geodesic between these points is a straight line in this diagram. Moreover, any null geodesic from p which enters the interior spacetime, M, has future endpoint at q. By a simple translation, it follows that for a general point $p' \in \mathscr{I}^-$ there is a unique $q' \in \mathscr{I}^+$ which is the future endpoint of null geodesics from p' which enter M.

Proposition 2.2.3. Let $p \in \mathscr{I}^-$ and let q be the unique point in $\mathscr{I}^+$ which is connected to p by a null geodesic through M. Then

$$I^+(p) \cap \mathscr{I}^+ = \mathscr{I}^+ \setminus \left(J^-(q) \cap \mathscr{I}^+\right) \tag{2.2.8}$$

This says that the only points in $\mathscr{I}^+$ which cannot be timelike connected to p are the points in $\mathscr{I}^+$ which can be reached from q by a past pointing null geodesic, including the point q itself.

Proof: Consider $p \in \mathscr{I}^-$ with co-ordinates $(T,\chi,\phi) = (-\frac{\pi}{2},\frac{\pi}{2},0)$, so q has co-ordinates

$(\frac{\pi}{2}, \frac{\pi}{2}, \pi)$. This is shown in Figure 2.5. The results for arbitrary $p' \in \mathscr{I}^-$ follow by a simple translation (Figure 2.6).

First note that none of the points $J^-(q) \cap \mathscr{I}^+$ lie in the interior of the future lightcone of p. If they did, then using Proposition 2.2.2 we could construct a smooth timelike curve from p to q. But these points correspond to the past and future endpoints of opposite branches of the hyperbola introduced in the proof of Theorem 2.1.8. In this proof it was shown that p and q cannot be timelike connected.

Next observe that there is a timelike curve from p to points such as $\hat{q}$ in Figure 2.7 which lie on $\mathscr{I}^+$ with T co-ordinate greater than or equal to that of q (and excluding q itself). To see this, note that such points can be connected using two radial null geodesics intersecting at the origin O as well as a radial null geodesic up $\mathscr{I}^+$ if necessary. Since $\hat{q} \neq q$, the full curve is not a null geodesic, so we can use Proposition 2.2.2 to deduce that there exists a smooth timelike curve from p to $\hat{q}$. By using a curve which is both constant in ϕ and a straight line in the (T, χ) co-ordinates, we are also able to timelike connect p to any point in $\mathscr{I}^+$ which has the same ϕ co-ordinate as p. This means we can concentrate on points on $\mathscr{I}^+$ with larger χ co-ordinates than p, i.e. which are closer to spacelike infinity, and whose ϕ co-ordinate differs from that of p by a value in $(0, \pi)$.

It is helpful to look at the double cone from above, as in Figure 2.8. The circles shown correspond to surfaces $\chi =$ constant, with the larger circle $\chi = \pi$ representing spatial infinity. To show that all non-antipodal points can be timelike connected, we will follow an argument similar to the one used by Penrose in [59]. This argument, which will be used again in Section 2.3.2, relies on repeated applications of Proposition 2.2.2 to a curve which is composed of segments of null geodesics. More specifically, the curve is based on several radial null geodesics, as well as a single non-radial one, which we use to achieve the desired change in the angular co-ordinate ϕ.

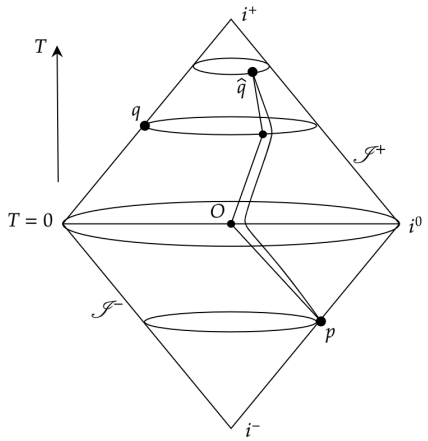

Figure 2.7: p can be timelike connected to any point on $\mathscr{I}^+$ with T co-ordinate greater than or equal to that of q (other than q itself). The path shown consists of two radial null lines through the origin as well as a null line up $\mathscr{I}^+$. Proposition 2.2.2 then implies the existence of a smooth timelike curve between p and $\hat{q}$.

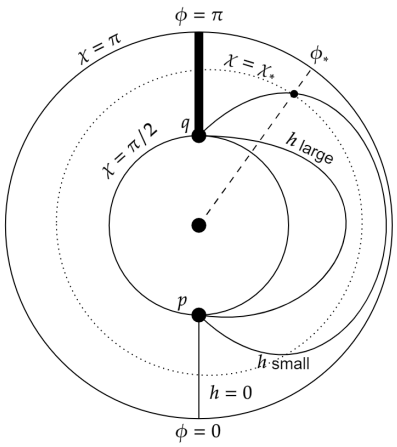

Figure 2.8: The double cone of compactified Minkowski spacetime viewed from above.

Solving the geodesic equations, we have

$$\begin{aligned} \dot{T} &= 1 \text{ (wlog)} \\ \sin^2(\chi)\dot{\phi} &= h = \text{constant} \\ \dot{\chi}^2 &= 1 - \frac{h^2}{\sin^2\chi} \end{aligned} \tag{2.2.9}$$

where overdots denote differentiation with respect to some parameter which we have re-scaled so that $\dot{T} = 1$.

We can integrate these equations to find explicit expressions for χ and ϕ in terms of T. Firstly we have

$$\tan^2 T = \frac{\sin^2\chi - h^2}{\cos^2\chi} \tag{2.2.10}$$

where we have chosen the geodesic to intersect $\mathscr{I}^-$ at $(T, \chi) = (-\pi/2, \pi/2)$. This ensures that the maximum value of χ is achieved at $T = 0$ and that the geodesic intersects $\mathscr{I}^+$ at $(T, \chi) = (\pi/2, \pi/2)$. Using this, we can solve for ϕ along the curve (assuming $h \neq 0$). We

have

$$\begin{aligned} &\sin^2\chi\dot{\phi} = h \\ \implies &\dot{\phi} = \frac{h\,(1+\tan^2 T)}{h^2+\tan^2 T} \\ \implies &\phi = \tan^{-1}\left(\frac{\tan T}{h}\right) + \frac{\pi}{2} \end{aligned} \tag{2.2.11}$$

Where we have chosen our geodesic to have $\phi = 0$ at $\mathscr{I}^-$. This ensures that $\phi = \pi$ on $\mathscr{I}^+$.

Consider a point $\tilde{q} \in \mathscr{I}^+$ at which $\chi = \chi_* \in (\pi/2, \pi)$ and $\phi = \phi_* \in (0, \pi)$ (for $\phi_* \in (\pi, 2\pi)$ we simply reverse the sign of h in what follows). It suffices to show that a null geodesic with past endpoint at p reaches a point in M with these same values of the χ and ϕ co-ordinates. This is because we could then reach $\tilde{q}$ by following this null geodesic until we reach such a point before switching to a timelike geodesic of constant χ, ϕ. This construction is shown as the bold path in Figure 2.8. Finally we could then apply Proposition 2.2.2 to obtain a smooth timelike curve with endpoints at p and $\tilde{q}$.

Re-arranging equation (2.2.11), the null geodesic intersects the required point provided we choose

$$h^2 = \frac{\sin^2\chi_*}{1+\cos^2\chi_*\tan^2(\phi_* - \pi/2)} \tag{2.2.12}$$

where we choose the positive sign for h since we assumed $\phi_* \in (0, \pi)$.

Choosing this value of h gives us the required null geodesic and we conclude that points in $\mathscr{I}^-$ with $\chi = T = \frac{\pi}{2}$ are timelike connected to all non-antipodal points in $\mathscr{I}^+$. $\square$

2.3 The Penrose Property in Schwarzschild Spacetime

We now consider the effect of adding mass. In particular, we will consider the Schwarzschild spacetime in various dimensions and for both positive and negative mass.

2.3.1 2+1 Dimensions

We begin by focusing on the 2+1 dimensional case, where we prove the following result.

Proposition 2.3.1. The Penrose property is satisfied by the Schwarzschild spacetime of mass m in 2+1 dimensions if and only if $m > 0$.

Proof: We first note that the failure of the Penrose property when $m = 0$ has already been established in section 2.2 (since the spacetime in this case is Minkowski with a point removed). We now consider the case where the mass is non-zero.

In 2+1 dimensions, the symmetries of the Riemann tensor are highly constraining, and we have [68]

$$R_{abcd} = \left(R^{mn} - \frac{1}{2} R g^{mn} \right) \epsilon_{mab} \epsilon_{ncd} \tag{2.3.1}$$

where ϵ_{abc} is the fully anti-symmetric tensor of rank 3 with $\epsilon_{123} = 1$.

Away from sources, the Einstein equations imply $R_{ab} = 0$ and equation (2.3.1) it follows that spacetime is flat. We see that, in 2+1 dimensions, spacetime curvature is fully determined by the Einstein equations and there is no propagating field of gravity. This is in contrast to general relativity in 4 or more spacetime dimensions.

The stress-energy tensor for a point source of mass m at the origin is

$$T^{00} = m\delta(r), \; T^{0i} = T^{ij} = 0. \tag{2.3.2}$$

The spacetime is static and spherically symmetric, so we can write the metric in isotropic co-ordinates as

$$ds^2 = N(r)dt^2 - \varphi(r)(dr^2 + r^2 d\phi^2) \tag{2.3.3}$$

for some functions $N(r)$ and $\varphi(r)$.

Solving the Einstein equations in vacuum ($R_{ab} = 0$), we find [30, Eq. 2.4] that N is a constant,

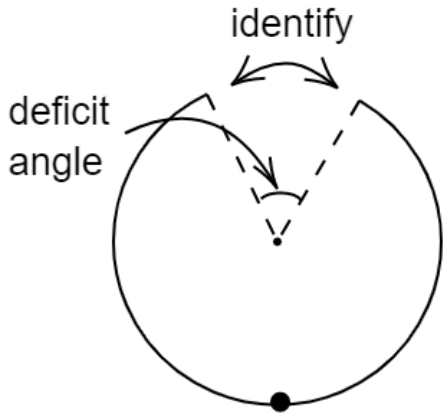

Figure 2.9: The deficit angle resulting from inserting a positive point means that all points have $\tilde{\phi}$ co-ordinates which differ by strictly less than π.

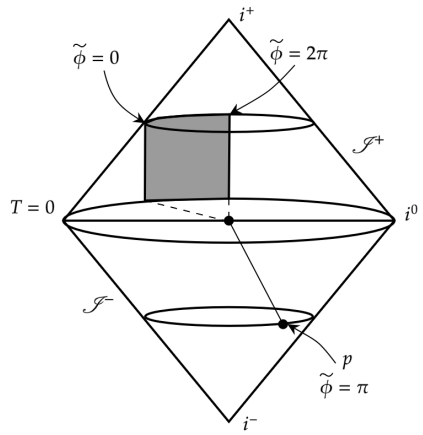

Figure 2.10: The surplus angle resulting from inserting a negative point mass means that given any point p on $\mathscr{I}^-$ there is now a wedge of points on $\mathscr{I}^+$ which cannot be reached by a timelike curve.

which we can choose to be 1 by a re-scaling of t. We also find [30, Eq. 2.6] that

$$\varphi(r) = r^{-8m} \tag{2.3.4}$$

Making the change of variables[2] $\tilde{r} = \alpha^{-1} r^{\alpha}$, $\tilde{\phi} = \alpha\phi$, where $\alpha = 1 - 4m$, we arrive at the metric

$$ds^2 = dt^2 - d\tilde{r}^2 - \tilde{r}^2 d\tilde{\phi}^2 \tag{2.3.5}$$

We recognise this as the Minkowski metric (2.2.2). The important thing to note is that the co-ordinates (t, r, ϕ) do not cover all of $\mathbb{R}^3$. This is because the range of $\tilde{\phi}$ is now $0 \leq \tilde{\phi} < 2\pi\alpha$, so there is a conical singularity at the origin.

If $m > 0$, the range of $\tilde{\phi}$ is strictly less than 2π. There is a deficit angle of $8\pi m$. This means that any two points on $\mathscr{I}^-$ and $\mathscr{I}^+$ will have $\tilde{\phi}$ co-ordinates which differ by strictly less than π (mod 2π). By Proposition 2.2.3, this means we are able to connect any pair of points on $\mathscr{I}^-$ and $\mathscr{I}^+$ with a timelike curve, so the Penrose property is satisfied.

[2]We are actually restricting here to $m < \frac{1}{4}$. The case $m > \frac{1}{4}$ corresponds to a 'mass at infinity', while $m = \frac{1}{4}$ gives a cylinder in the spatial dimensions. See [30] for a discussion of this. We will not consider these cases further.

On the other hand, inserting a negative mass yields the opposite effect. We now have a surplus angle and $\tilde{\phi}$ has a range strictly greater than 2π. The result of this is that given any initial point $p \in \mathscr{I}^-$, there is a wedge of points on $\mathscr{I}^+$ which cannot be reached by a timelike curve (see Figure 2.10). At these points, the $\tilde{\phi}$ co-ordinate differs by at least π from the value at p. The Penrose property is not satisfied by this negative mass spacetime. In fact, the situation is worse than in Minkowski, since the set of points on $\mathscr{I}^+$ which cannot be reached by a timelike curve from p now forms a 2 dimensional area (as opposed to the 1 dimensional line segment we found in Minkowski spacetime). $\square$

So it appears that the Penrose property is linked to the presence of positive mass. This is not wholly unsurprising since we expect a positive mass source to focus null geodesics. This should help us timelike connect antipodal points which cannot be timelike connected in Minkowski spacetime. Our results in 2+1 dimensions, along with this intuition, suggest that we should look at positive mass spacetimes if we wish satisfy the Penrose property by timelike connecting the antipodal points near i^0 which could not be connected in Minkowski.

2.3.2 Positive Mass in 3+1 Dimensions

We now consider the Schwarzschild solution in 3+1 dimensions, beginning with the positive mass case.

The positive mass Schwarzschild metric in 3+1 dimensions is

$$ds^2 = V(r)dt^2 - \frac{dr^2}{V(r)} - r^2\left(d\theta^2 + \sin^2\theta d\phi^2\right) \tag{2.3.6}$$

where $V(r) = 1 - \frac{2m}{r}$ and m is the ADM mass of the spacetime.

We can conformally compactify this metric using the same procedure as was used in section 2.2 for Minkowski spacetime, the only difference being we now use the tortoise co-ordinate, r_*, which satisfies

$$dr_* = \frac{dr}{V(r)} \tag{2.3.7}$$

in order to define the retarded and advanced time co-ordinates

$$\begin{aligned} u &= t - r_* = t - r - 2m\log(r/2m - 1) \\ v &= t + r_* = t + r + 2m\log(r/2m - 1) \end{aligned} \tag{2.3.8}$$

where we have set the arbitrary integration constant in the definition of r_* (equation (2.3.7)) to zero.

Just as in Section 2.2, we can compactify the spacetime by defining co-ordinates $T, \chi \in (-\pi, \pi)$ by

$$\begin{aligned} T &= \arctan v + \arctan u \\ \chi &= \arctan v - \arctan u. \end{aligned} \tag{2.3.9}$$

The conformally compactified metric is then

$$\overline{ds}^2 = \Omega^2 ds^2 = dT^2 - d\chi^2 - \frac{r^2}{V(r)r_*^2}\sin^2\chi\left(d\theta^2 + \sin^2\theta d\phi^2\right), \tag{2.3.10}$$

where $\Omega = \frac{2\cos\left(\frac{T+\chi}{2}\right)\cos\left(\frac{T-\chi}{2}\right)}{\sqrt{V(r)}}$.

This compactification procedure maps the region $\{r > 2m\}$ to the interior of the manifold with boundary

$$\overline{M} = \{(T, \chi) \in [-\pi, \pi] \times [-\pi, \pi) : |T| \leq \pi - |\chi|\} \times S^2. \tag{2.3.11}$$

Importantly, a subset of Schwarzschild spacetime (corresponding to $\{r_* > 0\}$) is mapped to the interior of the same manifold with boundary on which compactified Minkowski spacetime was defined in Section 2.2.

Theorem 2.3.2. (Penrose [59]) Positive mass Schwarzschild spacetime in $3+1$ dimensions satisfies the Penrose property.

Proof: We follow the method of Penrose in [59] to connect points $p \in \mathscr{I}^-$ and $q \in \mathscr{I}^+$, while also filling in some details.

As in 2+1 dimensions, we will use a piecewise null geodesic construction, with the existence of a smooth timelike curve with the same endpoints guaranteed by Proposition 2.2.2. We choose co-ordinates (t, r, θ, ϕ) such that $\theta = \pi/2$ at p and q. The Schwarzschild metric is static and spherically symmetric, so by Lemma 2.2.1 it suffices to consider curves restricted to the hypersurface $\theta = \pi/2$. All points and curves referred to in this proof will be assumed to lie in this plane. Up to shifts in t and ϕ, Schwarzschild geodesics in this plane which are null and inextendible (so in particular $r \geq 2m$) are uniquely determined by their impact parameter, R, defined to be the minimal value of r along the curve. A translation in t allows us to assume that $r = R$ at $t = 0$. The geodesic Lagrangian is

$$L = V(r)\dot{t}^2 - V(r)^{-1}\dot{r}^2 - r^2\dot{\phi}^2$$

so that, in the null case,

$$\begin{aligned} L &= 0 \\ r^2\dot{\phi} &= h = \text{ constant} \\ V(r)\dot{t} &= 1 \text{ (wlog)} \end{aligned} \tag{2.3.12}$$

where the final equation is our choice of the parametrisation.

For a null geodesic, we have

$$\begin{aligned} \dot{r}^2 &= 1 - \left(1 - \frac{2m}{r}\right)\frac{h^2}{r^2} \\ &\leq 1 - \left(1 - \frac{2m}{R}\right)\frac{h^2}{r^2} \\ &= 1 - \frac{R^2}{r^2} \end{aligned} \tag{2.3.13}$$

where we use the fact that $\dot{r} = 0$ at $r = R$ to solve for $h^2 = R^2\left(1 - \frac{2m}{R}\right)^{-1}$.

Using this, we can obtain a lower bound for $|\Delta\phi|$, the magnitude of the change in ϕ along

the null geodesic:

$$\begin{aligned}
\frac{d\phi}{dr} &= \frac{\dot{\phi}}{\dot{r}} \\
\implies |\Delta\phi| &= 2h \int_R^\infty \frac{dr}{\dot{r} r^2} \\
&\geq 2R \left(1 - \frac{2m}{R}\right)^{-1/2} \int_R^\infty \frac{dr}{(1 - R^2/r^2)^{1/2} r^2} \\
&= \left[-2 \left(1 - \frac{2m}{R}\right)^{-1/2} \tan^{-1} \left(\frac{R}{\sqrt{r^2 - R^2}} \right) \right]_{r=R}^{\infty} \\
&= (1 - 2m/R)^{-1/2} \, \pi \\
&\geq \pi
\end{aligned} \tag{2.3.14}$$

Therefore $|\Delta\phi| \geq \pi$ along a null geodesic in the $\theta = \frac{\pi}{2}$ plane. This was to be expected near a positive mass source (see Figure 2.11).

Consider $p \in \mathscr{I}^-$ with $v = v_0$, $\phi = \phi_0$ and $q \in \mathscr{I}^+$ with $u = u_1$, $\phi = \phi_1$. The construction described below to timelike connect these points is illustrated in Figure 2.12.

Suppose we are able to choose the impact parameter, R, of a null geodesic such that its past and future endpoints have $v = v_* > v_0$ and $u = u_* < u_1$ respectively. Along this geodesic, we choose points p' and q' (with $q' \in J^+(p')$) at which $\phi = \phi_0$ and $\phi = \phi_1$ respectively (we know this is possible because we have shown that $|\Delta\phi| \geq \pi$ and we can choose the angular momentum h to be positive or negative). We use this segment of geodesic to vary the value of ϕ. We connect p to p' using two null geodesics with zero angular momentum (so ϕ is constant along them), one of which runs along null infinity towards i^0. We connect q to q' similarly. This gives us a piecewise null geodesic curve from p to q. We deduce, using repeated applications of Proposition 2.2.2, that a smooth timelike curve from p to q must exist.

We have therefore reduced the Penrose property to a problem concerning the endpoints of null geodesics. The construction described above will allow us to connect all pairs of points on $\mathscr{I}^-$ and $\mathscr{I}^+$ if we are able to choose null geodesic endpoints arbitrarily close to spatial

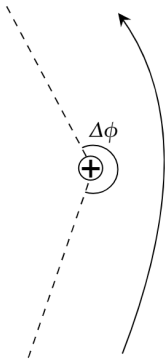

Figure 2.11: $|\Delta\phi| > \pi$ along null geodesics in the $\theta = \pi/2$ plane in positive mass Schwarzschild.

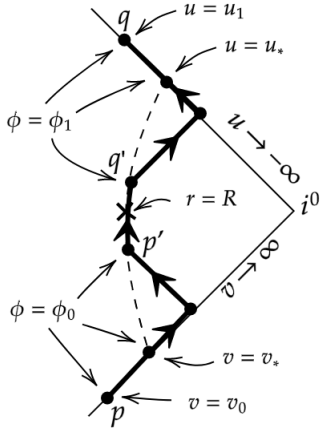

Figure 2.12: Construction used in [59] to timelike connect points $p \in \mathscr{I}^-$ and $q \in \mathscr{I}^+$. This is based on using a null geodesic (dashed line) to vary the angular co-ordinate ϕ (working in the hypersurface $\theta = \frac{\pi}{2}$). We then complete the path using null geodesics with zero angular momentum. The existence of a smooth timelike curve from p to q is guaranteed by Proposition 2.2.2.

infinity. This also demonstrates how the Penrose property is a property of neighbourhoods of spatial infinity. If we know that we can connect all points arbitrarily close to i^0 then this construction shows that the Penrose property is satisfied.

The u co-ordinate, u_*, at the future endpoint of a non-radial null geodesic, chosen to be symmetric about $t = 0$, is given in terms of the u co-ordinate at $r = R$, denoted u_R, by

$$\begin{aligned} u_* &= u_R + \int_R^\infty \frac{du}{dr} dr \\ &= -R - 2m \log\left(\frac{R}{2m} - 1\right) + \int_R^\infty \frac{du}{dr} dr \end{aligned} \tag{2.3.15}$$

In [59], Penrose shows that

$$\int_R^\infty \frac{du}{dr} dr = R + \mathcal{O}(1) \tag{2.3.16}$$

where $\mathcal{O}(1)$ denotes terms which are bounded as $R \to \infty$. This proves that $u_* \to -\infty$ as $R \to \infty$. A similar argument also shows that $v_* \to \infty$ as $R \to \infty$. This is exactly what we wanted. We can therefore use the above construction to connect any pairs of points on $\mathscr{I}^-$

and $\mathscr{I}^+$ using a timelike curve. We simply need to use a geodesic with sufficiently large impact parameter. $\square$

We see that quantum gravity consistency condition Theorem 2.1.9, is not satisfied. This provides strong evidence against a "Lorentz covariant" quantum gravity construction (see Section 1.2).

2.3.3 Negative Mass in 3+1 Dimensions

We now consider the Schwarzschild metric in 3+1 dimensions with negative mass. The compactified metric is now as in (2.3.10) except with

$$\begin{aligned} V(r) &= 1 + \frac{\mu}{r} \\ \implies r_* &= r - \mu \log(r/\mu + 1) \end{aligned} \tag{2.3.17}$$

where $\mu = 2|m|$ and the compact manifold covers the full spacetime $\{r > 0\}$ outside the naked singularity. This naked singularity will not be relevant for our discussion because, as explained in the positive mass case, we are concerned only with properties of the spacetime near i^0 (and hence at large values of r).

Proposition 2.3.3. Negative mass Schwarzschild spacetime in $3 + 1$ dimensions does not satisfy the Penrose property.

Proof: The compactified Schwarzschild line element (2.3.10) differs from the compactified Minkowski metric (2.2.7) only by the function $\frac{r^2}{V(r)r_*^2}$ which appears in front of the angular terms (this function is identically 1 for Minkowski). In fact, the similarity is deeper than this. Not only do the metrics look similar, we also note that the negative mass Schwarzschild spacetime is mapped to the interior of the same same compact manifold as the $r > 0$ portion of Minkowski. This means that, by identifying the co-ordinates (T, χ, θ, ϕ) defined on both these manifolds, we have a bijection between curves in compactified Schwarzschild and curves in compactified Minkowski (with $r > 0$). It does not matter that these will correspond to

different curves when we map back to the physically relevant non-compact spacetimes.

To further this comparison, we need to understand the relationship between the two compactified metrics. This means looking more closely at the function $\frac{r^2}{V(r)r_*^2}$. We consider the large r asymptotics of this function. Expanding $V(r)$ and $r_*(r)$ to leading order, we have

$$\begin{aligned}\frac{r^2}{r_*^2 V(r)} &= \left[1+\frac{2\mu}{r}\log\left(r/\mu+1\right)+O\left(\frac{\mu^2}{r^2}\left(\log\left(r/\mu+1\right)\right)^2\right)\right]\left[1-\frac{\mu}{r}+O\left(\frac{\mu^2}{r^2}\right)\right] \\ &= 1+\left(2\log\left(r/\mu+1\right)-1\right)\frac{\mu}{r}+O\left(\frac{r^2}{r_s^2}\left(\log\left(r/\mu+1\right)\right)^2\right) \\ &> 1 \text{ for large } r\end{aligned} \tag{2.3.18}$$

Hence the conformally compactified negative mass Schwarzschild metric in 3+1 dimensions can be bounded above by the conformally compactified Minkowski metric, i.e. $\overline{g} < \overline{\eta}$ (for large r).

We conclude from this that the Penrose property does not hold for negative mass 3+1 dimensional Schwarzschild. In particular, antipodal points on $\mathscr{I}^-$ and $\mathscr{I}^+$ sufficiently near i^0 cannot be timelike connected. To see this, suppose we could connect such points using a Schwarzschild timelike curve. By choosing these points sufficiently close to i^0, we can ensure that such a curve is restricted to large enough r to ensure that inequality (2.3.18) holds (recall that curves near i^0 in compactified Schwarzschild are restricted to large values of r_* and that $r \to \infty$ as $r_* \to \infty$). This curve would then also be timelike in compactified Minkowski spacetime and would connect the same points on $\mathscr{I}^{\pm}$. By choosing our points even closer to i^0 if necessary, we obtain a contradiction Proposition 2.2.3 (which says that antipodal points sufficiently near spatial infinity in Minkowski spacetime cannot be timelike connected). We conclude that the Penrose property does not hold for negative mass Schwarzschild in 3+1 dimensions. □

This argument is similar to the argument used for negative mass in 2+1 dimensions. The difference is that the constant $\alpha \in (0,1)$ which created the deficit angle has now been replaced by the function $\frac{r^2}{V(r)r_*^2} \in (0,1)$ which depends on r.

2.3.4 Positive Mass in Higher Dimensions

It is tempting to try to show that the Penrose property is satisfied in higher dimensional positive mass Schwarzschild using the same construction as was used in the 3+1 dimensional case in [59] (and summarised in section 2.3.2). However, this construction no longer works because the endpoints of non-radial null geodesics do not approach i^0 as we let the impact parameter $R \to \infty$. In fact, the situation for positive mass Schwarzschild in higher dimensions is similar to the negative mass case in 3+1 dimensions, as we see below.

Proposition 2.3.4. Positive mass Schwarzschild spacetime in $d+1$ dimensions ($d > 3$) does not satisfy the Penrose property.

Proof: The Schwarzschild metric in $d+1$ dimensions ($d > 3$) is

$$ds^2 = V(r)dt^2 - \frac{dr^2}{V(r)} - r^2 d\omega_{d-1}^2 \tag{2.3.19}$$

where $V(r) = 1 - \frac{\mu}{r^n}$ and $n = d-2$. We have also introduced the *mass parameter*, μ, which is related to the ADM mass, m, by

$$\mu = \frac{16\pi m}{(d-1)A_{S^{d-1}}}. \tag{2.3.20}$$

We can conformally compactify this metric as in lower dimensions to obtain (2.3.10) with $d\omega_2^2$ replaced by $d\omega_{d-1}^2$.

Once again we consider the large r asymptotics of the metric. We have

$$\begin{aligned} dr_* &= \frac{dr}{V(r)} \\ &= \left(1 + \frac{\mu^n}{r^n} + O\left(\frac{\mu^{2n}}{r^{2n}}\right)\right) dr \\ \implies r_* &= r\left(1 - \frac{\mu^n}{(n-1)r^n} + O\left(\frac{\mu^{2n}}{r^{2n}}\right)\right) \end{aligned} \tag{2.3.21}$$

So the crucial term in equation (2.3.10) can be expanded as

$$\begin{aligned} \implies \frac{r^2}{r_*^2 V(r)} &= \left(1 + \frac{2\mu}{(n-1)r^n} + O\left(\frac{\mu^{2n}}{r^{2n}}\right)\right)\left(1 + \frac{\mu}{r^n} + O\left(\frac{\mu^{2n}}{r^{2n}}\right)\right) \\ &= 1 + \frac{(n+1)\mu}{(n-1)r^n} + O\left(\frac{\mu^{2n}}{r^{2n}}\right) \\ &> 1 \text{ for large } r. \end{aligned} \tag{2.3.22}$$

Hence we obtain the same bounds as in section 2.3.2, and the same argument tells us that the Penrose property does not hold in this spacetime (again noting that curves near i^0 in Schwarzschild are restricted to large values of r_* and that $r \to \infty$ as $r_* \to \infty$). $\square$

2.3.5 Negative Mass in Higher Dimensions

The negative mass Schwarzschild metric in spacetime of dimension $d+1$ ($d > 3$) is as in equation (2.3.19) except with $\mu < 0$. The bound we obtained in (2.3.4) is now reversed, so we cannot use this method to conclude that the Penrose property fails. In fact, the lightcones of the naturally associated Minkowski metric (i.e. the one obtained by setting $\mu = 0$) are now contained inside the Schwarzschild lightcones (at least at large r). This suggests that the spacetime may have a chance of satisfying the Penrose property. We should at least be able to timelike connect all the same points as we could in Minkowski by using curves restricted to large r where this bound holds. However, as we let $r \to \infty$, the Schwarzschild and Minkowski lightcones converge towards each other. This means that we may be unable to connect antipodal points sufficiently near i^0, as is the case in Minkowski spacetime, since such curves would be restricted to increasingly large values of r. It turns out that this is indeed the case - the deflection of null geodesics away from the negative point mass prevents us from timelike connecting certain pairs of antipodal points near i^0.

Theorem 2.3.5. Negative mass Schwarzschild spacetime in $d+1$ dimensions ($d > 3$) does not satisfy the Penrose property.

To prove this theorem we will require the following result (which we will not prove).

Theorem 2.3.6. [24, Thm. 2.8.5] Let (M, g) be a spacetime with $g \in C^2$ and let $a, b \in M$ be such that the causal diamond $J^+(a) \cap J^-(b)$ is non-empty and globally hyperbolic. Then there exists a causal geodesic from a to b.

Proof of Theorem 2.3.5: Suppose we are aiming to timelike connect the points $p \in \mathscr{I}^-$ and $q \in \mathscr{I}^+$. We choose co-ordinates $(t, r, \theta_1, ..., \theta_{d-2}, \phi)$ such that $\theta_1 = ... = \theta_{d-2} = \pi/2$ at p and q. Once again we can exploit the staticity and spherical symmetry of the metric and argue using Lemma 2.2.1 that it suffices to consider curves restricted to the surface $\theta_1 = ... = \theta_{d-2} = \pi/2$. All curves and points referred to in this proof will be assumed to lie on this surface.

A negative point mass will be repulsive and will deflect null geodesics away. We therefore expect that, in contrast to positive mass, causal geodesics will undergo an angular change of strictly less than π (Figure 2.13). This is what we now prove. Solving the geodesic equations, we find

$$\begin{aligned} V(r)\dot{t} &= 1 \text{ (wlog)} \\ r^2\dot{\phi} &= h = \text{constant} \\ \dot{r}^2 &= 1 - V(r)\left(k^2 + \frac{h^2}{r^2}\right) \end{aligned} \tag{2.3.23}$$

where the first equation is our choice of the parametrisation and $k \geq 0$ is a constant such that $k = 0$ for a null geodesic and $k > 0$ for a timelike geodesic. We can determine h^2 by solving $\dot{r} = 0$ at $r = R$, where R denotes the minimum value of r along the geodesic. We find that

$$\begin{aligned} h^2 &= \frac{R^2}{V(R)}\left(1 - k^2 V(R)\right) \\ \implies \frac{\dot{r}^2}{h^2} &= \frac{V(R)}{R^2}\frac{1 - k^2 V(r)}{1 - k^2 V(R)} - \frac{V(r)}{r^2} \\ &\geq \frac{V(R)}{R^2} - \frac{V(r)}{r^2} \\ &\geq \frac{V(R)}{R^2}\left(1 - \frac{R^2}{r^2}\right) \end{aligned} \tag{2.3.24}$$

where we have used the fact that $V(r) \leq V(R)$ for $r \geq R$. We also assume that $h \neq 0$. If

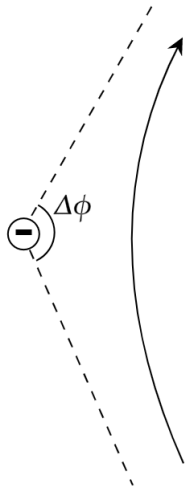

Figure 2.13: $|\Delta\phi| < \pi$ along null geodesics in negative mass Schwarzschild.

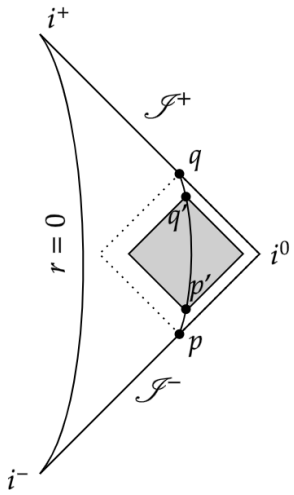

Figure 2.14: The interior of the causal diamond (shaded) formed by the points p' and q' is non-empty and globally hyperbolic, so we can apply Theorem 2.3.6.

$h = 0$ then trivially ϕ is constant (and furthermore the geodesic is incomplete). Note that the first inequality above tells us that, as expected, among all causal geodesics with fixed h, $|\Delta\phi|$ is maximised by null geodesics (for which $k = 0$).

We obtain an upper bound for the magnitude of the change in ϕ along a causal geodesic, denoted $|\Delta\phi|$, as follows

$$\begin{aligned} |\Delta\phi| &= 2|h| \int_R^\infty \frac{dr}{\dot{r} r^2} \\ &\leq \frac{2R}{V(R)^{1/2}} \int_R^\infty \frac{dr}{(1 - R^2/r^2)^{1/2} r^2} \\ &= \frac{\pi}{V(R)^{1/2}} \\ &< \pi \end{aligned} \tag{2.3.25}$$

where the final inequality is obtained from the fact that $V(R) = 1 - \frac{\mu}{R^n} > 1$.

We aim to use Theorem 2.3.6 to show that it suffices to restrict our attention to geodesics when attempting to timelike connect points on $\mathscr{I}^\pm$. However, since we are interested in connecting these points using curves which pass through the interior spacetime, we cannot

apply this theorem to the causal diamond formed by points on $\mathscr{I}^{\pm}$ since this may give us a geodesic lying entirely in the conformal boundary. Furthermore, in 4 spatial dimensions, the results of Chapter 5 tell us that the conformal metric at i^0 fails to be C^2, so the results of Theorem 2.3.6 are not be applicable. It is also necessary to make sure that any causal diamond on which we hope to apply Theorem 2.3.6 does not include the naked singularity at $r = 0$.

We begin by choosing $p \in \mathcal{I}^-$ at $\phi = 0$ and $q \in \mathscr{I}^+$ at $\phi = \pi$, with p, q sufficiently close to i^0 that $J^+(p) \cap J^-(q)$ does not intersect the $r = 0$ singularity (see Figure 2.14). Note in particular that the causal diamond formed by any two points in $J^+(p) \cap J^-(q)$ will also not intersect this singularity. Now if the Penrose property were satisfied in this spacetime then there would exist a timelike curve from p to q. Since the metric is invariant under $\phi \mapsto -\phi$, we can assume without loss of generality that ϕ is increasing along this curve. Now for any point $a \in \overline{M}$, $I^{\pm}(a)$ are open sets [58, Prop 2.8], so we must be able to modify this curve to obtain a new timelike curve, with the same u and v values at its endpoints, except with $\phi = -\epsilon$ on $\mathscr{I}^-$ and $\phi = \pi + \epsilon$ on $\mathscr{I}^+$ (for some $\epsilon > 0$) and such that ϕ is still increasing along this new curve. By restricting to a segment of this curve, we obtain a timelike curve between points p' and q' in the interior spacetime, where $\phi = 0$ at p' and $\phi = \pi$ at q'. The set $J^+(p') \cap J^-(q')$ then satisfies the conditions of Theorem 2.3.6 (in particular the conformal metric is C^2), so we conclude that there exists a causal geodesic from p' to q'. But we also know that such a geodesic cannot exist. In particular, it would necessarily have $\Delta\phi \geq \pi$ along its full length. We therefore have a contradiction with inequality (2.3.25), so we conclude that the Penrose property is not satisfied by negative mass Schwarzschild in higher dimensions. □

2.3.6 Summary of the Penrose Property

We summarise Propositions 2.3.1, 2.3.3, 2.3.4, 2.3.5 and Theorem 2.3.2 with the following theorem.

Theorem 2.3.7. The Penrose property is satisfied by Schwarzschild spacetime of mass m and varying spacetime dimension according to the following table

Spacetime dimension	$m > 0$	$m \leq 0$
3	✓	✗
4	✓	✗
≥ 5	✗	✗

We observe that the Penrose property appears to be a property of positive mass in low dimensions. We have seen that adding positive mass in 3 or 4 dimensions gives us the inequality

$$\overline{ds}_S^2 \geq \overline{ds}_M^2 \tag{2.3.26}$$

at large r, where $\overline{ds}_M^2$ is the naturally associated compactified Minkowski metric. This tells us that the lightcone condition $g < \eta$ fails. This is also the case for negative mass in higher dimensions. However in this case, rather than diverging, the Schwarzschild and Minkowski lightcones converge at infinity and the effect of the mass is not strong enough for the failure of the Penrose property in Minkowski to be overcome. For negative mass in 3 and 4 dimensions as well as positive mass in higher dimensions, the inequality (2.3.26) is now reversed at large r and the Penrose property fails (by comparison with Minkowski space). It is curious that positive and negative mass seem to have the opposite effect on lightcones in higher dimensions compared with 3 and 4 dimensions.

Since the Penrose property is concerned only with the asymptotic behaviour of the metric near spatial infinity, these results can be immediately applied to a number of other spacetimes. For example, the Reissner-Nordström line element in $d+1$ dimensions ($d \geq 3$) is

$$ds^2 = \left(1 - \frac{\mu}{r^{d-2}} + \frac{Q^2}{r^{2d-4}}\right) dt^2 - \left(1 - \frac{\mu}{r^{d-2}} + \frac{Q^2}{r^{2d-4}}\right)^{-1} dr^2 - r^2 d\omega_{d-1}^2 \tag{2.3.27}$$

where Q is the charge of the black hole. Just like Schwarzschild, this spacetime satisfies the Penrose property only when $d = 3$ and $m > 0$ (regardless of the value of Q). The case where $m = 0$ and $Q \neq 0$ is notable because the large r asymptotics are now the same as those of negative mass Schwarzschild in $2d-2$ spatial dimensions.

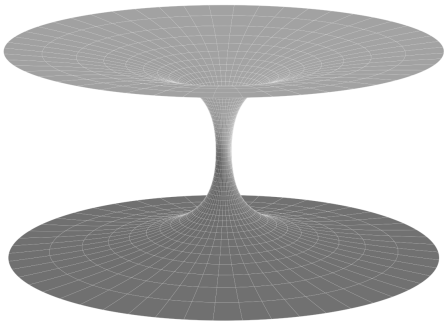

Figure 2.15: The Ellis-Bronnikov wormhole consists of two asymptotically flat "universes" separated by a "throat". The wormhole is called "traversable" because timelike observers can pass through it from one universe to the other. This figure shows the equatorial plane in a $t =$ constant slice of the spacetime, embedded in 3d Euclidean space.

2.4 Wormhole Spacetime

The Ellis-Bronnikov wormhole spacetime in $(d+1)$-dimensions ($d \geq 2$) has metric

$$ds^2 = dt^2 - dr^2 - (r^2 + a^2)d\omega_{d-1}^2 \tag{2.4.1}$$

where $a > 0$ is a constant.

In this spacetime it is possible to extend r through the "throat" at $r = 0$ and consider negative values of r. The constant a corresponds to the width of this throat. An illustration of this spacetime is given in Figure 2.15.

It will be more convenient to consider the non-timelike boundary version of the Penrose property (Definition 2.1.5) rather than the equivalent finite version (Definition 2.1.6), so we begin by compactifying the spacetime. We can do this using the same method as was used for Minkowski spacetime in section 2.2, the only change being we now define the retarded and advanced time co-ordinates to be $u = t - |r|$ and $v = t + |r|$ respectively. We obtain the conformally related metric

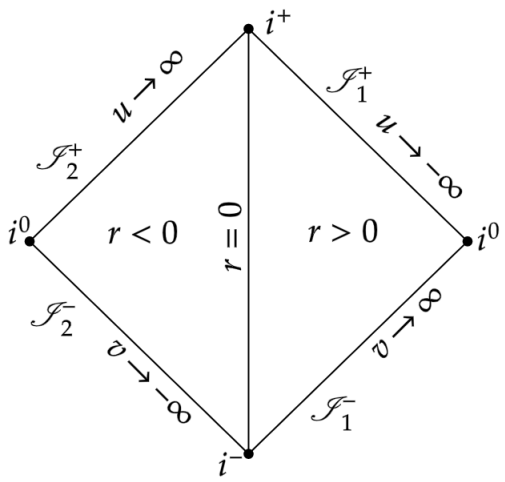

Figure 2.16: The Penrose diagram for the Ellis-Bronnikov wormhole spacetime. This diagram consists of two copies of compactified Minkowski spacetime, each corresponding to one of the two universes $r < 0$ and $r > 0$.

$$\overline{ds}^2 = dT^2 - d\chi^2 - \left(1 + \frac{a^2}{r^2}\right) \sin^2 \chi d\omega_{d-1}^2 \tag{2.4.2}$$

Note that we have $r \in (-\infty, \infty)$, so the range of χ is now $\chi \in [-\pi, \pi]$ (for Minkowski we had $r \in [0, \infty)$ and hence $\chi \in [0, \pi]$). We also have $T \in [-\pi, \pi]$ and $|T| \leq \pi - |\chi|$. This means we obtain a Penrose diagram consisting of two copies of the Minkowski diagram (Figure 2.4) - one for each of the two "'universes" $r < 0$ and $r > 0$. This is shown in Figure 2.16, where each point with $r \neq 0$ represents a manifold which is topologically S^{d-1}.

The problem of timelike connecting points on $\mathscr{I}^-$ and $\mathscr{I}^+$ can be split into two cases. The first is when both points lie in the same universe, so either $r = \infty$ at both or $r = -\infty$ at both. The second case is when the two points lie in different universes: one is at $r = \infty$ and the other is at $r = -\infty$. We use subscripts 1 and 2 to denote the two universes $r > 0$ and $r < 0$ respectively.

We begin by dealing with the case where both points lie in the same universe, which we choose without loss of generality to be the one with $r > 0$. For a curve restricted to this universe, let R denote its impact parameter. It will be also helpful to make the following definition.

Definition 2.4.1. The *time of flight* along a curve with endpoints is defined to be the difference between the retarded time at its future endpoint, denoted u_∞, and the advanced time at its past endpoint, denoted v_∞.

Note that the time of flight along a curve need not be positive or finite (for example any timelike curve with future endpoint at i^+ has infinite time of flight).

Proposition 2.4.2. Let $p \in \mathscr{I}_1^-$ and let $q \in \mathscr{I}_1^+$ be antipodal points such that any curve from p to q has zero time of flight. Then

$$I^+(p) \cap \mathscr{I}_1^+ = \mathscr{I}_1^+ \setminus \left(J^-(q) \cap \mathscr{I}_1^+\right) \tag{2.4.3}$$

That is, the only points in $\mathscr{I}_1^+$ which cannot be timelike connected to p are the antipodal points where the time of flight would be ≤ 0.

Note that this is the same result as was obtained for Minkowski spacetime (Proposition 2.2.3), since all null geodesics in Minkowski have zero time of flight.

Proof: We begin by showing that as the impact parameter $R \to \infty$, the future endpoints of null geodesics from p tend to the antipodal point on the S^{d-1} part of the spacetime and the time of flight tends to zero.

Solving the geodesic equations, we find that the change in the retarded time co-ordinate, $u = t$, along a null geodesic from $r = R$ to its future endpoint at $r = \infty$ is

$$u_\infty - u_R = \int_R^\infty \left[\left(1 - \frac{R^2 + a^2}{\rho^2 + a^2}\right)^{-1/2} - 1\right] d\rho \tag{2.4.4}$$

Similarly, the change in the advanced time co-ordinate, v, from the past endpoint to the point where $r = R$ is

$$v_R - v_\infty = \int_R^\infty \left[\left(1 - \frac{R^2 + a^2}{\rho^2 + a^2}\right)^{-1/2} - 1\right] d\rho \tag{2.4.5}$$

Hence the time of flight along this null geodesic is

$$\begin{aligned} u_\infty - v_\infty &= 2\int_R^\infty \left[\left(1 - \frac{R^2+a^2}{\rho^2+a^2}\right)^{-1/2} - 1\right] d\rho + u_R - v_R \\ &= 2R\int_1^\infty \left[\left(1 - \frac{1+a^2/R^2}{x^2+a^2/R^2}\right)^{-1/2} - 1\right] dx - 2R \\ &= \frac{2af(b)}{b} \end{aligned} \tag{2.4.6}$$

where we have made the substitution $x = \rho/R$ and defined $b = a/R$ and $f(b) = \int_1^\infty \left[\left(\frac{x^2+b^2}{x^2-1}\right)^{1/2} - 1\right] dx - 1$.

Now $f(0) = 0$, so we can use l'Hôpital's rule to determine the limit of $u_\infty - v_\infty$ as $b \to 0$ (i.e. as $R \to \infty$). We have

$$\begin{aligned} \lim_{R\to\infty}(u_\infty - v_\infty) &= \lim_{b\to 0} 2af'(b) \\ &= \lim_{b\to 0} 2ab\int_1^\infty \left(x^2-1\right)^{-1/2}\left(x^2+b^2\right)^{-1/2} dx \\ &= 0 \end{aligned} \tag{2.4.7}$$

since

$$\int_1^\infty \left(x^2-1\right)^{-1/2} x^{-1} dx = \frac{\pi}{2} \tag{2.4.8}$$

We also need to check the angular change along a null geodesic with endpoints on $\mathscr{I}_1^-$ and $\mathscr{I}_1^+$. We choose co-ordinates so that our null geodesic lies in the equatorial plane. Then

$$\begin{aligned} \frac{d\phi}{dr} &= \frac{(R^2+a^2)^{1/2}}{(r^2-R^2)^{1/2}(r^2+a^2)^{1/2}} \\ \implies \Delta\phi &= 2(R^2+a^2)^{1/2}\int_R^\infty (r^2-R^2)^{-1/2}(r^2+a^2)^{-1/2} dr \\ &\geq 2R\int_R^\infty r^{-1}(r^2-R^2)^{-1/2} dr \\ &= \pi \end{aligned} \tag{2.4.9}$$

We conclude that $p \in \mathscr{I}_1^-$ can be connected to any point $q \in \mathscr{I}_1^-$ where the time of flight is

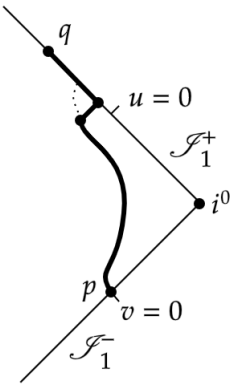

Figure 2.17: This figure shows the construction of a timelike path with strictly positive time of flight between $p \in \mathscr{I}_1^-$ and $q \in \mathscr{I}_1^+$. We follow a null geodesic in the same plane as p and q which reaches $\mathscr{I}_1^+$ at an earlier retarded time than q. Once we reach the same angular co-ordinate as q, we switch to an outgoing radial null geodesic until we reach $\mathscr{I}_1^+$ and then another radial null geodesic up $\mathscr{I}_1^+$ until we reach q. We then smooth this path (without changing its endpoints) so that it becomes timelike everywhere.

strictly positive using the following construction (illustrated in Figure 2.17).

Choose co-ordinates such that p and q lie in the equatorial plane. By the above result, we can choose a null geodesic, lying in the equatorial plane, from p with sufficiently large impact parameter to ensure that it reaches $\mathscr{I}_1^+$ at an earlier retarded time than q. We follow this null geodesic until we have reached the ϕ co-ordinate of q (reversing the angular momentum if necessary so that the required change in $|\phi|$ is at most π) before switching to an outgoing radial null geodesic until we reach $\mathscr{I}_1^+$ and then finally another null geodesic up $\mathscr{I}_1^+$ until we reach q. This path can then be smoothed (without changing its endpoints) so that it becomes timelike everywhere (Proposition 2.2.2).

Next we consider points separated by a curve with non-positive time of flight. It is straightforward to see that antipodal points cannot be timelike connected by using a comparison argument similar to those used throughout this Chapter. Indeed, we note that the compactified wormhole metric (equation (2.4.1)) can be bounded from above by the compactified Minkowski metric (which corresponds to setting $a = 0$ in (2.4.2)).

$$\overline{ds}^2_{E-B} \leq \overline{ds}^2_{Mink} \tag{2.4.10}$$

This tells us that if two points on $\mathscr{I}_1^{\pm}$ cannot be connected using a Minkowski timelike curve then they also cannot be connected using a curve which is timelike with respect to the wormhole metric (since any such curve would be Minkowski timelike). From Proposition 2.2.3, we conclude that in the wormhole spacetime, antipodal points separated by curves with time of flight ≤ 0 cannot be timelike connected.

We now consider the case where p and q are non-antipodal. We once again choose co-ordinates so that these points lie in the equatorial plane.

For $r \geq R$, we have

$$\begin{aligned} \overline{ds}^2 &= dT^2 - d\chi^2 - \left(1 + \frac{a^2}{r^2}\right) \sin^2 \chi d\phi^2 \\ &\geq dT^2 - d\chi^2 - \left(1 + \frac{a^2}{R^2}\right) \sin^2 \chi d\phi^2 \\ &= dT^2 - d\chi^2 - \sin^2 \chi d\overline{\phi}^2 \\ &= \overline{ds}^2_{Mink} \end{aligned} \tag{2.4.11}$$

where $\overline{\phi} = \phi \left(1 + \frac{a^2}{R^2}\right)^{1/2} \in \left[0, 2\pi\sqrt{1 + \frac{a^2}{R^2}}\right)$.

From the proof of Proposition 2.2.3, we see that given any R it is possible to connect any non-antipodal points using a Minkowski timelike curve which remains at $r > R$. Suppose the ϕ co-ordinate of such a curve in the equatorial plane is given by the function $\overline{\phi}(s)$, where s is some affine parameter. The above inequality tells us that if this function is replaced by $\phi(s) = \overline{\phi}(s) \left(1 + \frac{a^2}{R^2}\right)^{-1/2}$, then the curve will be timelike with respect to the compactified wormhole metric. This method allows us to timelike connect any points in the equatorial plane whose angular difference is

$$\Delta\phi < \frac{\pi}{\sqrt{1 + \frac{a^2}{R^2}}} \tag{2.4.12}$$

By choosing R sufficiently large, we conclude that all non-antipodal points can be timelike connected. □

Next we consider points on $\mathscr{I}^-$ and $\mathscr{I}^+$ which lie in different universes. As in previous

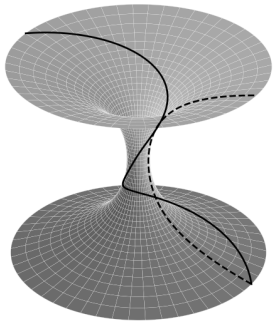

Figure 2.18: The dashed line shows a null geodesic with zero angular momentum ($h = 0$) which passes through the throat. The case $0 < h < a$ is shown as a solid line. This geodesic passes through the throat and intersects $\mathscr{I}_2^+$.

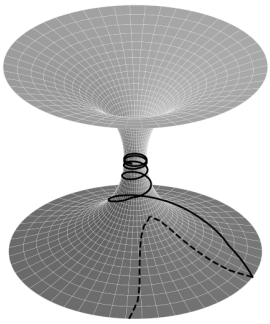

Figure 2.19: The solid line shows a null geodesic with angular momentum $h = a$. This geodesic asymptotes towards the throat at $r = 0$ and has an endpoint at future timelike infinity i^+. The case $h > a$ is shown as a dashed line. This geodesic does not pass through the throat and has future endpoint on $\mathscr{I}_1^+$.

constructions we will rely on null geodesics. We begin by asking which null geodesics cross the wormhole throat and which remain in one universe.

Lemma 2.4.3. Let γ be a null geodesic in the equatorial plane with past endpoint $p \in \mathscr{I}_1^-$. Then γ crosses the wormhole throat of width a if and only if it has angular momentum $h = (r^2 + a^2)\dot{\phi}$ satisfying $h^2 < a^2$ (where $\dot{}$ denotes differentiation with respect to t). If $h^2 = a^2$ then the geodesic has an endpoint at future timelike infinity but does not cross the wormhole.

This is illustrated in Figures 2.18 and 2.19 where paths are shown in the equatorial plane in a $t =$ constant slice of the spacetime.

Proof: The equation of motion in the radial direction (parameterised by t) is

$$\begin{aligned} \dot{r}^2 &= 1 - \frac{h^2}{r^2 + a^2} \\ \implies r^2 &\geq h^2 - a^2 \end{aligned} \tag{2.4.13}$$

So we see that if $h^2 > a^2$, the geodesic does not cross the wormhole throat at $r = 0$ and

is restricted to the $r > 0$ universe. If $h^2 = a^2$ then $\dot{r} \to 0$ as $r \to 0$ and the retarded time co-ordinate diverges. The geodesic has an endpoint at future timelike infinity i^+. If $h^2 < a^2$, we have $\dot{r} \neq 0$. The geodesic passes through $r = 0$ and has future endpoint on $\mathscr{I}_2^+$. $\square$

We are now in a position to consider exactly which points in $\mathscr{I}_1^-$ and $\mathscr{I}_2^+$ can be timelike connected.

Proposition 2.4.4. Let $p \in \mathscr{I}_1^-$ and $q \in \mathscr{I}_2^+$ and choose co-ordinates such that these points lie in the equatorial plane with $\phi = 0$ at p and $\phi = \phi_q$, $u = u_q$ at q. Let $u_{(h)}$ denote the value of the retarded time co-ordinate $u = t - |r|$ at the future endpoint of a null geodesic from p in the equatorial plane with angular momentum $h = (r^2 + a^2)\dot{\phi}$ (where $\dot{}$ denotes differentiation with respect to t).

- Suppose $u_q \leq u_{(0)}$. Then p cannot be timelike connected to q.
- Suppose $u_q > u_{(0)}$. Then p can be timelike connected to q if and only if $\phi_q \in [-\frac{2h_q}{a}K\left(\frac{h_q}{a}\right), \frac{2h_q}{a}K\left(\frac{h_q}{a}\right)]$, where $K(k)$ denotes the complete elliptic integral of the first kind[3] and h_q denotes the angular momentum of a null geodesic from p to q.

In particular, all points with u co-ordinate $u_q > u_{(h_*)}$ can be reached by a timelike curve from p, where h_* is the unique value in $(0, a)$ satisfying $\frac{2h_*}{a}K\left(\frac{h_*}{a}\right) = \pi$ (see Figure 2.20).

Proof: By Lemma 2.2.1, in order to timelike connect p and q it suffices to restrict to curves which lie in the equatorial plane.

By inspection of the Penrose diagram (Figure 2.21) and consideration of a radial null geodesic (i.e. a null geodesic with $h = 0$), we can see immediately that no points on $\mathscr{I}_2^+$ with u co-ordinate $u_q \leq u_{(0)}$ can be reached by a timelike curve from p.

Now consider $q \in \mathscr{I}_2^+$ with u co-ordinate $u_q > u_{(0)}$ and assume without loss of generality that the ϕ co-ordinate at q is $\phi_q \in [0, \pi]$ (otherwise reverse the sign of h in what follows).

[3]The complete elliptic integral of the first kind is defined as $K(k) = \int_1^\infty \frac{dt}{\sqrt{(1-t^2)(1-k^2t^2)}}$ for $|k| < 1$.

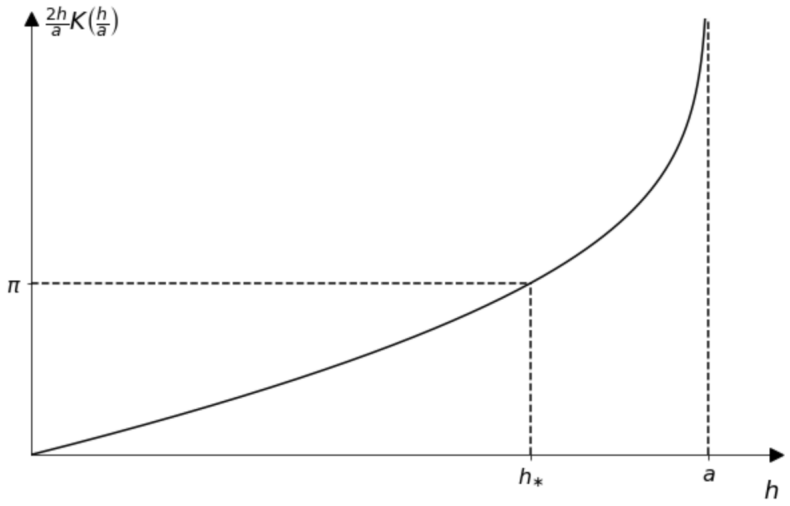

Figure 2.20: The change in the ϕ co-ordinate along a null geodesic with angular momentum $h \in (0, a)$ (so the geodesic crosses the throat) is given by $\Delta\phi = 2hK(h/a)/a$. The angular momentum $h = h_*$ corresponds to $\Delta\phi = \pi$ and as $h \to a$ we see that $\Delta\phi \to \infty$.

Once again consider a null geodesic from p lying in the equatorial plane. Suppose this geodesic has angular momentum $h \in (0, a)$ and hence, by Lemma 2.4.3, crosses the wormhole throat. The change in the ϕ co-ordinate along this geodesic, denoted $\Delta\phi$, is given by

$$\begin{aligned} \Delta\phi &= \int_{-\infty}^{\infty} \frac{h dr}{(r^2+a^2)^{1/2}\,(r^2+a^2-h^2)^{1/2}} \\ &= \frac{2h}{a} K\left(\frac{h}{a}\right) \end{aligned} \tag{2.4.14}$$

So $\Delta\phi$ is a strictly increasing continuous function of $\frac{h}{a}$ for $0 \leq h < a$, with $\Delta\phi = 0$ at $h = 0$ and $\Delta\phi \to \infty$ as $h \to a$ (see Figure 2.20). The change in the retarded time co-ordinate u along this geodesic, denoted Δu, is given by

$$\Delta u = 2\int_0^{\infty} \left(1 - \sqrt{1 - \frac{h^2}{r^2+a^2}}\right) dr \tag{2.4.15}$$

So Δu is an increasing continuous function of h for $0 \leq h < a$, with $\Delta u = 0$ at $h = 0$ and $\Delta u \to \infty$ as $h \to a$. This tells us in particular that the u co-ordinate of p is equal to $u_{(0)}$.

Since $u_q > u_{(0)}$, we can apply the inverse function theorem to (2.4.15) to write $u_q = u_{(h_q)}$

for some unique $h_q \in (0, a)$. If $0 \leq \phi_q < \frac{2h_q}{a} K\left(\frac{h_q}{a}\right)$, then we can reach the point q with a timelike curve from p as follows:

- Follow the null geodesic from p in the equatorial plane with angular momentum h_q until we reach $\phi = \phi_q$ (which we do before reaching $\mathscr{I}_2^+$ since $\Delta\phi = \frac{2h_q}{a} K\left(\frac{h_q}{a}\right)$ along the full null geodesic).

- Complete the path to $q \in \mathscr{I}_2^+$ with the timelike curve which follows the same path as the null geodesic in the first step except with $\dot{\phi} = 0$.

This curve can then be smoothed to form a path from p to q which is timelike everywhere (Proposition 2.2.2). Wee see that all points with u co-ordinate $u_q > u_{(h_*)}$ can be reached by a timelike curve from p, where h_* is the unique value in $(0, a)$ satisfying $\frac{2h_*}{a} K\left(\frac{h_*}{a}\right) = \pi$.

Now suppose $u_q \in (u_{(0)}, u_{(h_*)}]$ and $\phi_q \geq \frac{2h_q}{a} K\left(\frac{h_q}{a}\right)$. Suppose that a timelike curve from p to q exists. Since the interior of the causal diamond $J^+(p) \cap J^-(q)$ is non-empty and globally hyperbolic, there exists a causal geodesic from p to q (Theorem 2.3.6). If this geodesic were null then the change in ϕ along it would be $\frac{2h_q}{a} K\left(\frac{h_q}{a}\right)$ (up to sign). The change in ϕ along a timelike geodesic with the same endpoints would therefore be strictly less than $\frac{2h_q}{a} K\left(\frac{h_q}{a}\right)$. We conclude that there is no timelike curve between p and q. $\square$

2.5 Unique Continuation of the Linear Wave Equation

The Penrose property, or more specifically the property of null geodesic endpoints proved by Penrose for positive mass Schwarzschild in $3+1$ dimensions (see [59] or the proof of Theorem 2.3.2), can help with understanding the problem of unique continuation from null infinity of the linear wave equation. In [2], the authors consider the linear wave equation

$$\Box_g \varphi + a^\mu \partial_\mu \varphi + V\varphi = 0 \tag{2.5.1}$$

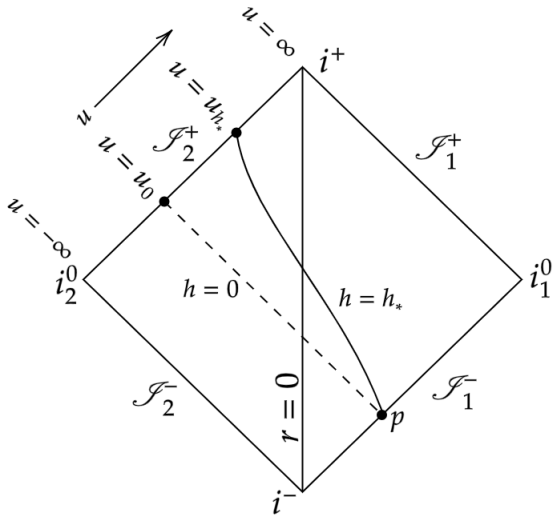

Figure 2.21: The dotted line shows a radial ($h = 0$) null geodesic from p passing through the wormhole throat and finishing at u co-ordinate $u_{(0)}$. The point $p \in \mathscr{I}_1^-$ cannot be timelike connected to any points across the wormhole on $\mathscr{I}_2^+$ which have $u \leq u_{(0)}$. The solid line shows a null geodesic from p with angular momentum h_*. It reaches $\mathscr{I}_2^+$ at u co-ordinate $u_{(h_*)}$ and the angular change along it is exactly π. The point p can be timelike connected to all points on $\mathscr{I}_2^+$ which have $u > u_{(h_*)}$. For points with $u_{(0)} < u \leq u_{(h_*)}$, the result depends on the angular separation from p (see Proposition 2.4.4).

where $\Box_g$ is the Laplace-Beltrami operator for the metric g and the functions a^μ, V satisfy certain fall-off conditions. They investigate conditions on the solution at null infinity which ensure that it can be uniquely continued into some region of the interior spacetime.

Two separate classes of spacetimes are considered in [2]. The first is Minkowski spacetime in $d+1$ dimensions ($d \geq 2$) along with perturbations to the metric which leave the ADM mass unchanged. The second class is Schwarzschild spacetime in $3+1$ dimensions along with perturbations. Again these perturbations are sub-leading in the sense that they do not change the ADM mass of the spacetime. Note that this set-up is consistent with the results [59], summarised in section 2.3.2, that we cannot think of Schwarzschild spacetime in 3+1 dimensions as arising from a perturbation of Minkowski due to differences in causal structure near i^0.

Following [2], we define the following subsets of null infinity

$$\mathscr{I}^+_{u_0} = \{v = \infty,\ u \leq u_0\},\ \mathscr{I}^-_{v_0} = \{u = -\infty,\ v \geq -v_0\} \tag{2.5.2}$$

for any $u_0, v_0 \in \mathbb{R}$, where the retarded and advanced time co-ordinates u and v are given by equation (2.2.3) for perturbations of the Minkowski metric and equation (2.3.8) for perturbations of the Schwarzschild metric. For some $u_0, v_0 \in \mathbb{R}$, we will be interested in uniquely continuing the solution to equation (2.5.1) from $\mathscr{I}^+_{u_0} \cup \mathscr{I}^-_{v_0}$ into a region

$$\mathcal{D}^{(u_0,v_0)}_{\omega} := \left\{0 < \frac{1}{(v+v_0)(u_0-u)} < \omega\right\} \tag{2.5.3}$$

where $\omega > 0$.

It is shown in [2] that for certain perturbations of the Minkowski metric, if the solution is specified on subsets $\mathscr{I}^+_{\epsilon} \subset \mathscr{I}^+$ and $\mathscr{I}^-_{\epsilon} \subset \mathscr{I}^-$ for any $\epsilon > 0$, then this solution can be uniquely continued into the interior spacetime . In particular, if we demand that φ and its first derivatives vanish to infinite order (as defined in [2]) on $\mathscr{I}^+_{\epsilon} \cup \mathscr{I}^-_{\epsilon}$ (for $\epsilon > 0$), then φ must vanish on some open domain in the interior spacetime which contains $\mathscr{I}^+_{\epsilon} \cup \mathscr{I}^-_{\epsilon}$ on its boundary, i.e. $\varphi = 0$ on $\mathcal{D}^{(\epsilon,\epsilon)}_{\omega}$ for some $\omega > 0$.

Now consider perturbations of the Schwarzschild metric in $3+1$ dimensions . We define the sets $\mathscr{I}^+_{u_0}$, $\mathscr{I}^-_{v_0}$ and $\mathcal{D}^{(u_0,v_0)}_{\omega}$ as in (2.5.2) and (2.5.3), with the retarded and advanced time co-ordinates now defined by (2.3.8).

Suppose we demand that the solution, φ, and its first derivatives vanish to infinite order on $\mathscr{I}^+_{u_0} \cup \mathscr{I}^-_{v_0}$ for some u_0, $v_0 \in \mathbb{R}$. Then in [2] it is shown that φ must also vanish on $\mathcal{D}^{(u_0,v_0)}_{\omega}$ for some $\omega > 0$.

In contrast to the case of the perturbed Minkowski metric, we require conditions on φ and its first derivatives only on arbitrarily small sub-regions of $\mathscr{I}^+ \cup \mathscr{I}^-$ surrounding i^0 (since we are allowing $u_0, v_0 < 0$). This agrees with what we would have expected given the results obtained in previous sections. This is because initial data for hyperbolic partial

differential equations hyperbolic propagates along characteristic curves. In this problem, the characteristic curves are the null curves of the metric g. Suppose that, having fixed φ and its first derivatives to vanish sufficiently quickly on some intervals $\mathscr{I}^+_{u_0} \cup \mathscr{I}^-_{v_0}$, we are unable to extend the solution uniquely into a region $\mathcal{D}^{(u_0,v_0)}_\omega$ for any $\omega > 0$. Then for arbitrarily small $\omega > 0$, there must exist null curves which propagate from outside either of these intervals into $\mathcal{D}^{(u_0,v_0)}_\omega$. Equivalently, the following condition must fail to hold:

Definition 2.5.1 (Null Geodesic Endpoint Condition)**.** An asymptotically flat spacetime satisfies the null geodesic endpoint condition if, given any u_0, $v_0 \in \mathbb{R}$, there exists $\omega > 0$ such that any inextendible null geodesic entering $\mathcal{D}^{(u_0,v_0)}_\omega$ must have at least one endpoint in $\mathscr{I}^-_{v_0}$ or $\mathscr{I}^+_{u_0}$.

This is essentially the property which, in [59] (see also the proof of Theorem 2.3.2), Penrose shows holds for positive mass Schwarzschild spacetime in 3+1 dimensions. Indeed for a null geodesic in this spacetime with fixed past endpoint not contained in $\mathscr{I}^-_{v_0}$, the requirement of entering $\mathcal{D}^{(u_0,v_0)}_\omega$ for arbitrarily small ω is equivalent to letting $R \to \infty$. Previously, we considered null geodesics which were symmetric about $t = 0$ and we observed that both endpoints approached i^0 as we let $R \to \infty$ (where R denotes the minimal value of r along the curve). By translating in t, we can choose to keep the past endpoint fixed as $R \to \infty$. We see that this still results in the future endpoint sliding along $\mathscr{I}^+$ towards i^0 and eventually entering $\mathscr{I}^+_{u_0}$ (see Figure 2.22).

For Minkowski spacetime, the null geodesic endpoint condition does not hold. We can, for example, fix the endpoints to lie at $u = 0$ and $v = 0$ while choosing R to be arbitrarily large. Hence for any $u_0, v_0 < 0$, the null geodesic enters $\mathcal{D}^{(u_0,v_0)}_\omega$ for ω arbitrarily small (see Figure 2.23). This is exactly why it is necessary to impose conditions on the solution on $\mathscr{I}^+_\epsilon \cup \mathscr{I}^-_\epsilon$ for some $\epsilon > 0$ in order to achieve the unique continuation result. The solution will vanish in regions $\mathcal{D}^{(\epsilon,\epsilon)}_\omega$ which cannot be entered by any inextendible null geodesic with both endpoints outside $\mathscr{I}^+_\epsilon \cup \mathscr{I}^-_\epsilon$.

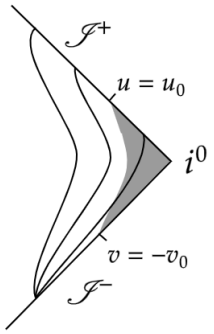

Figure 2.22: In Schwarzschild spacetime, requiring a null geodesic with past endpoint not in $\mathscr{I}^-_{v_0}$ to enter $\mathcal{D}^{(u_0,v_0)}_\omega$ (shaded region) for arbitrarily small $\omega > 0$ forces the future endpoint to lie arbitrarily close to i^0.

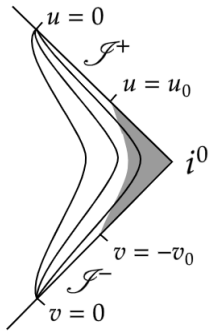

Figure 2.23: For any $u_0, v_0 < 0$, null geodesics in Minkowski spacetime with past and future endpoints lying outside $\mathscr{I}^-_{v_0}$ and $\mathscr{I}^+_{u_0}$ (e.g. at $v = 0$ and $u = 0$) can enter $\mathcal{D}^{(u_0,v_0)}_\omega$ (shaded region) for any $\omega > 0$.

2.6 General Static, Spherically Symmetric Spacetimes

We saw in section 2.3.4 that Penrose's method of proof does not extend to positive mass Schwarzschild in higher dimensions. This is because the null geodesic endpoint condition is no longer satisfied[4]. Indeed, if a null geodesic is chosen to be symmetric about $t = 0$, then at its past and future endpoints we have $v \to 0^-$ and $u \to 0^+$ respectively as $R \to 0$. As noted in [2], this is why it is necessary to impose conditions on φ on $\mathscr{I}^+_\epsilon \cup \mathscr{I}^-_\epsilon$ for some $\epsilon > 0$ (as in Minkowski) in order to obtain a unique continuation result.

As we have seen, to prove that the Penrose property holds for some spacetime we could try to use the same construction as Penrose in [59] (see also the proof of Theorem 2.3.2). As discussed in the previous section, if the metric is stationary then showing that non-radial null geodesic endpoints approach i^0 as we let $R \to \infty$ is equivalent to proving that the null geodesic endpoint condition holds. If we now restrict our attention further and consider only static, spherically symmetric spacetimes in $d + 1$ dimensions ($d \geq 3$) then the other result we require for the Penrose construction is that $|\Delta\phi| \geq \pi$ along all non-radial null geodesics restricted to sufficiently large r.

[4]This is also the reason the positive mass theorem of [61] does not extend to higher dimensions (see discussion in Chapter 4).

A general static, spherically symmetric metric is characterised by two functions, $A(r)$ and $B(r)$, and in $d+1$ dimensions can be written as

$$ds^2 = A(r)^2 dt^2 - B(r)^2 dr^2 - r^2 d\omega_{d-1}^2 \tag{2.6.1}$$

where we assume that the function $A(r)$ is non-zero.

Since both the Penrose property and the null geodesic endpoint condition are conformally invariant, we are only interested in the conformal class of this metric. This allows us to remove one of these functional degrees of freedom. If we conformally re-scale the metric by a factor $A(r)^{-2}$, define a new radial co-ordinate $\tilde{r} = \frac{r}{A(r)}$ and then define the function $C(\tilde{r}) = \frac{B(r(\tilde{r}))}{A(r(\tilde{r}))}\frac{dr}{d\tilde{r}}$, it suffices to consider a metric of the form (dropping tildes)[5]:

$$ds^2 = dt^2 - C(r)^2 dr^2 - r^2 d\omega_{d-1}^2 \tag{2.6.2}$$

Using Lemma 2.2.1, we can restrict attention to the equatorial plane spanned by co-ordinates (t, r, ϕ), on which the induced metric is

$$ds^2 = dt^2 - C(r)^2 dr^2 - r^2 d\phi^2 \tag{2.6.3}$$

Consistent with asymptotic flatness, we assume we can expand $C(r)$ as:

$$C(r) = 1 + \frac{C_{d-2}}{r^{d-2}} + O\left(\frac{1}{r^{d-1}}\right). \tag{2.6.4}$$

A calculation similar to the one carried out in the proof of Theorem 2.3.2 shows that the null geodesic endpoint condition is satisfied if and only if $C_{d-2} > 0$ and $d = 3$. This is precisely the condition required to get the logarithmic divergence observed by Penrose in [59]. On the other hand, the angular condition - that $|\Delta\phi| \geq \pi$ along non-radial null geodesics restricted

[5]This requires us to invert the function $\tilde{r}(r)$ at large r. This is possible if we assume, consistent with asymptotic flatness, that $A(r)$ can be expanded as a Taylor series in $1/r$ (as we assume for $C(r)$ in equation (2.6.4)). This ensures that $\tilde{r}(r)$ is a monotonic function at large r, and hence is invertible by the inverse function theorem. Recall that we can restrict attention to large r if necessary since the Penrose property is a property near i^0.

to sufficiently large r - is satisfied if and only if $C(r) > 1$ for r sufficiently large. We therefore observe that this is a weaker condition than the null geodesic endpoint condition and hence that Penrose's construction works if and only if $d = 3$ and $C_1 > 0$.

To determine if the Penrose property is satisfied for a metric of the form (2.6.2) we can apply the same arguments as were used in previous sections for the Schwarzschild spacetime. We have seen above that if $d = 3$ and $C_1 > 0$ then the Penrose property is satisfied. If $d = 3$ and $C_1 < 0$ or $d > 3$ and $C_{d-2} > 0$, then the comparison arguments outlined in Sections 2.3.3 and 2.3.4 can be used to show that the Penrose property is not satisfied. If $C_{d-2} < 0$ and $d > 3$, we can use the same arguments as Section 2.3.5 to again show that the Penrose property is not satisfied. The only remaining case is $C_{d-2} = 0$ ($d \geq 3$).

This case is straightforward because we have

$$C(r) \geq 1 - \frac{C'}{r^{d-1}} > 0 \tag{2.6.5}$$

for some constant $C' > 0$ and r sufficiently large. This inequality tells us that if a curve at large r is timelike with respect to the metric (2.6.3), then it would still be timelike if we replaced $C(r)$ with $1 - \frac{C'}{r^{d-1}}$. By Lemma 2.2.1, it follows that if the Penrose property holds in our spacetime then it must also hold in the spacetime of dimension $d + 2$ with metric

$$ds^2 = dt^2 - \left(1 - \frac{C'}{r^{d-1}}\right)^2 dr^2 - r^2 d\omega_d^2. \tag{2.6.6}$$

But we have seen above that these higher dimensional, static, spherically symmetric spacetimes do not satisfy the Penrose property, so we conclude that this property is also not satisfied in our spacetime. We summarise our results in the following theorem.

Theorem 2.6.1. If (M, g) is a static, spherically symmetric spacetime in $d + 1$ dimensions ($d \geq 3$), then the metric is conformal to

$$\tilde{ds}^2 = dt^2 - C(r)^2 dr^2 - r^2 d\omega_{d-1}^2 \tag{2.6.7}$$

and we have

$$\boxed{\text{Penrose property} \iff [d = 3 \text{ and } C_1 > 0] \iff \text{Null Geodesic Endpoint Condition}}$$

where we assume that the function $C(r)$ can be written as

$$C(r) = 1 + \frac{C_{d-2}}{r^{d-2}} + O\left(\frac{1}{r^{d-1}}\right). \tag{2.6.8}$$

Chapter3

Generalisations of the Penrose Property

In the previous Chapter the focus was on the Penrose property in asymptotically flat spacetimes. Since the two versions of the Penrose property (Definitions 2.1.5 and 2.1.6) are equivalent in such spacetimes, there was no need to differentiate between them. In this Chapter we will consider how these two properties can be studied in spacetimes which are not asymptotically flat. We will begin with spacetimes which have a non-zero cosmological constant, before moving on to look at product spacetimes of the form $(M, g) = (M', g') \times (M'', g'')$, where (M', g') is an asymptotically flat Lorentzian manifold and (M'', g'') is a compact Riemannian manifold. We will consider how to adapt (if necessary) Definitions 2.1.5 and 2.1.6 to these scenarios and whether or not they remain equivalent. As in the previous Chapter we will primarily rely on examples to understand the various versions of the Penrose property.

3.1 Summary of Results

The following theorem summarises the relationship between the finite version of the Penrose property (Definition 2.1.6) and the appropriate boundary version (Definition 2.1.5 for

spacetimes with $\Lambda \geq 0$ or Definition 3.3.2 if $\Lambda < 0$):

Theorem 3.1.1. In the presence of a cosmological constant, the finite version of the Penrose property is related to the appropriate boundary version according to the following table.

	$\Lambda = 0$	$\Lambda > 0$	$\Lambda < 0$
Finite Version $\iff$ Appropriate Boundary Version?	✓	✓	✗

Our results in Schwarzschild spacetime with different values of the cosmological constant Λ are summarised by the following theorem.

Theorem 3.1.2. The appropriate boundary version of the Penrose property is satisfied in Schwarzschild spacetime with cosmological constant Λ according to the following table.

	$\Lambda = 0$			$\Lambda > 0$			$\Lambda < 0$		
Spacetime Dimension	$m > 0$	$m = 0$	$m < 0$	$m > 0$	$m = 0$	$m < 0$	$m > 0$	$m = 0$	$m < 0$
3	✓	✗	✗	-	✗	-	-	✗	-
4	✓	✗	✗	✓	✗	✗	✗	✗	✓
≥ 5	✗	✗	✗	✓	✗	✗	✗	✗	✓

where a dash indicates that this spacetime has not been considered here.

In Section 3.4 we will show that no additional complications are introduced if we consider the Penrose property in a spacetime which is the product of an asymptotically flat Lorentzian manifold and a compact Riemannian manifold. In particular, we will discuss how to compactify such a spacetime, before showing that both versions of the Penrose property remain equivalent. We will also prove the following theorem.

Theorem 3.1.3. The product spacetime $(M, g) = (M', g') \times (M'', g'')$, where (M', g') is an asymptotically flat Lorentzian manifold and (M'', g'') is a compact Riemannian manifold, satisfies the non-timelike boundary version of the Penrose property if and only if this property is satisfied in (M', g').

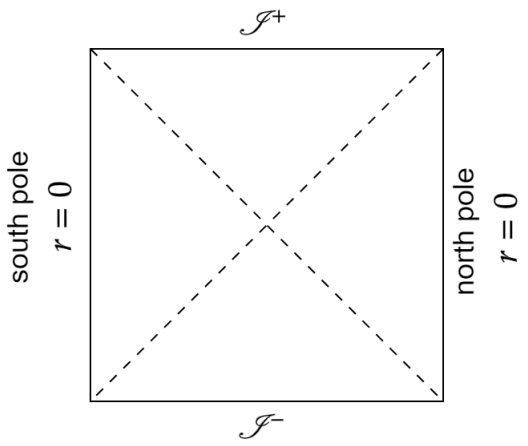

Figure 3.1: Penrose diagram of de Sitter spacetime. This spacetime is topologically $\mathbb{R} \times S^d$, so each point on this diagram (with the exception of the north and south poles) represents a manifold which is topologically S^{d-1}. The dotted lines represent cosmological horizons.

3.2 Asymptotically De Sitter Spacetimes

3.2.1 De Sitter Spacetime

De Sitter spacetime in $d+1$ dimensions is isometric to the submanifold of $\text{Mink}_{d+1,1}$ defined by

$$-t^2 + \sum_{i=1}^{d+1} x_i^2 = l^2 \tag{3.2.1}$$

where $(t, x_1, ..., x_{d+1})$ are a standard Cartesian co-ordinate system on $\mathbb{R}^{d+1,1}$ and the radius of curvature, l, is a positive constant which is related to the cosmological constant by

$$\Lambda = \frac{d(d-1)}{2l^2} \tag{3.2.2}$$

It is topologically $\mathbb{R} \times S^d$ and the metric expressed in static co-ordinates is

$$ds^2 = \left(1 - \frac{r^2}{l^2}\right) dt^2 - \left(1 - \frac{r^2}{l^2}\right)^{-1} dr^2 - r^2 d\omega_{d-1}^2 \tag{3.2.3}$$

The Penrose diagram is shown in Figure 3.1. Note that the hypersurfaces $\mathscr{I}^{\pm}$ are spacelike. This means that when studying the Penrose property in asymptotically de Sitter spacetimes we cannot restrict attention to curves near the conformal boundary. Consequently, and in contrast to the asymptotically flat case, this property is not a property of the metric asymptotics. In fact it is now a global property of spacetime. This suggests that obtaining a more general result is likely to be more complicated.

Theorem 3.2.1. Compactified de Sitter spacetime does not satisfy the non-timelike boundary version of the Penrose property. Moreover, for any $p \in \mathscr{I}^-$, the only point on $\mathscr{I}^+$ which cannot be reached from p by a smooth timelike curve is the antipodal point.

Proof: If we choose co-ordinates such that $p \in \mathscr{I}^-$ lies at the south pole then it is clear from Figure 3.1 that this point is not timelike connected to the north pole on $\mathscr{I}^+$.

Now suppose $q \in \mathscr{I}^+$ does not lie at the north pole. The following construction is illustrated in Figure 3.2. Consider the null geodesic from p whose projection onto the S^d part of the spacetime is a great circle intersecting the projection of q. We denote by q' the point in the full spacetime at which this intersection happens (so the projection of q' onto S^d is the same as the projection of q). We follow this geodesic from p to q' before switching to a timelike path ending at q whose projection onto S^d is a single point. By Proposition 2.2.2, we can modify our path in the full de Sitter spacetime so as to obtain a smooth timelike curve from p to q. $\square$

This result is similar to Proposition 2.2.3 which said that in Minkowski spacetime of any dimension, the only points on $\mathscr{I}^-$ and $\mathscr{I}^+$ which cannot be timelike connected are certain pairs of antipodal points.

It is also straightforward to see that the finite version of the Penrose property is not satisfied in de Sitter spacetime.

Theorem 3.2.2. The finite version of the Penrose property is not satisfied in de Sitter spacetime in $(d+1)$ dimensions for any $d \geq 1$.

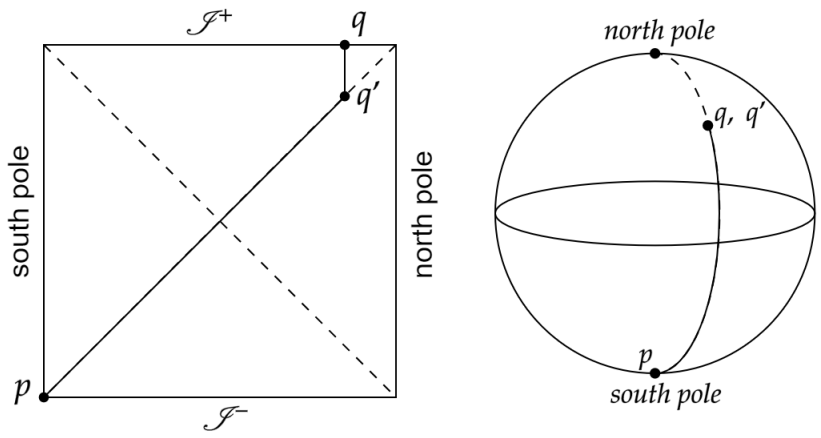

Figure 3.2: We choose the null geodesic from the south pole on $\mathscr{I}^-$ to the north pole on $\mathscr{I}^+$ which passes through the point, q', with the same co-ordinates on S^d as q. This null geodesic is a great circle when projected onto S^d. We then follow a timelike path from q to q' which remains at a constant position on S^d.

Proof: Consider two timelike curves, one remaining at the north pole and the other at the south pole. It is clear from Figure 3.1 that these curves cannot be timelike connected. □

We can also see the failure of the two versions of the Penrose property in de Sitter spacetime by recalling its definition as a submanifold of Minkowski spacetime of one dimension higher. This argument is based on the one given in Theorem 2.1.8 to show that Minkowski spacetime does not satisfy the Penrose property.

Consider the hyperbola in $\text{Mink}_{d+1,1}$ defined by

$$\begin{aligned} x_2 = x_3 = ... = x_{d+1} = 0 \\ -t^2 + x_1^2 = l^2 \end{aligned} \tag{3.2.4}$$

Note that this hyperbola satisfies equation (3.2.1) and hence its branches define endless timelike curves in de Sitter spacetime. These curves are everywhere spacelike separated, so we see that the finite version of the Penrose property fails. Moreover, they become null as we approach their endpoints. We conclude that these endpoints lie on $\mathscr{I}^{\pm}$ in compactified de Sitter spacetime and the past endpoint of one branch cannot be timelike connected to the future endpoint of the other. This means that the non-timelike boundary version of the

Penrose property also fails.

In the remainder of this section we will be interested in spacetimes which are *asymptotically de Sitter* (Definition 2.1.3).

Theorem 3.2.3. For asymptotically de Sitter spacetimes, the finite and non-timelike boundary versions of the Penrose property are equivalent.

Proof: The proof of this is identical to the proof in the asymptotically flat case (Theorem 2.1.7). □

Theorem 3.2.1 also leads to the following analogue of Theorem (2.1.9). In light of the above result, we will refer to both properties together as "the Penrose property" when referring to asymptotically de Sitter spacetimes.

Theorem 3.2.4. Let $(\overline{M}, \overline{g})$ be the conformal compactification of an asymptotically de Sitter spacetime which satisfies the Penrose property and let $\mathscr{I} = \mathscr{I}^- \cup \mathscr{I}^+$ denote its conformal boundary at infinity. Then there is no compactification of de Sitter spacetime which has $\mathscr{I}$ as its conformal boundary at infinity and $\overline{g} \leq \overline{g}_{dS}$ on $J^-(\mathscr{I}^+) \cap J^+(\mathscr{I}^-)$.

Proof: Suppose such a compactification of de Sitter spacetime exists and let $\lambda \in J^-(\mathscr{I}^+) \cap J^+(\mathscr{I}^-)$ be a $\overline{g}$–timelike curve between antipodal points on $\mathscr{I}^-$ and $\mathscr{I}^+$. Then the inequality $\overline{g} \leq \overline{g}_{dS}$ implies that λ is timelike with respect to the compactified de Sitter metric $\overline{g}_{dS}$. This contradicts Theorem 3.2.1. □

3.2.2 Schwarzschild-de Sitter

From Theorem 3.2.4, we see that in order to rule out theories of quantum gravity defined with respect to some background de Sitter spacetime (as was done in Chapter 2, following [59], for theories defined with respect to a background Minkowski spacetime) it is sufficient to find a physically relevant spacetime which satisfies the Penrose property. Inspired by [59], we begin by considering the Schwarzschild-de Sitter spacetime.

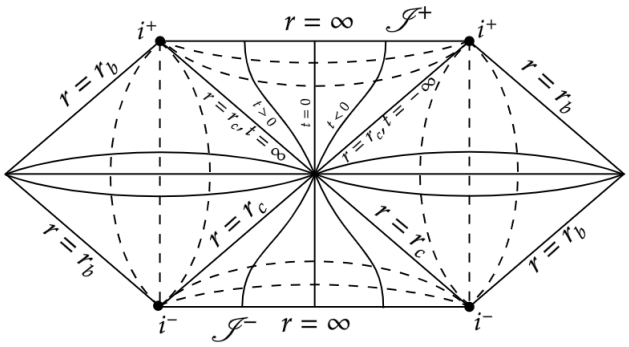

Figure 3.3: Portion of the Penrose diagram for the exterior ($r > r_b$) region of the Schwarzschild-de Sitter spacetime in the case where there are cosmological and event horizons which do not coincide. For $r_b < r < r_c$, constant t surfaces are spacelike while constant r surfaces are timelike. When $r > r_c$, constant r surfaces are spacelike and constant t surfaces are timelike. See [8] for more details.

The Schwarzschild-de Sitter metric in $d+1$ dimensions is given by [27]

$$ds^2 = V(r)dt^2 - \frac{dr^2}{V(r)} - r^2 d\omega_{d-1}^2 \tag{3.2.5}$$

where

$$V(r) = 1 - \frac{\mu}{r^{d-2}} - \frac{r^2}{l^2} \tag{3.2.6}$$

We have once again introduced a *mass parameter*, μ, which in this case is related by

$$\mu = \frac{16\pi m}{(d-1)A_{S^{d-1}}} \tag{3.2.7}$$

to the leading order term, m, in the Abbott-Deser mass [1] calculated just inside the cosmological horizon for a black hole with event horizon at $r_b << l$. The parameter l is related to the cosmological constant by (3.2.2).

We begin by considering the positive mass case $\mu > 0$ and assume that the spacetime is "sub-extremal", so $V(r)$ has two positive roots at $r_c \geq r_b > 0$. In this case there is a cosmological horizon at $r = r_c$ and a black hole horizon at $r = r_b$. The Penrose diagram for the region $r > r_b$ is as shown in Figure 3.3 (assuming $r_c > r_b > 0$).

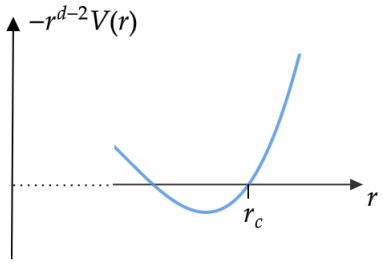

Figure 3.4: A portion of the function $-r^{d-2}V(r) = \mu - r^{d-2} + r^d/l^2$ is plotted (assuming $\mu > 0$). If μ is increased slightly then r_c, the value of r at the largest root of $r^{d-2}V(r)$, will decrease.

Theorem 3.2.5. The Penrose property is satisfied by the Schwarzschild-de Sitter spacetime with positive mass parameter $\mu > 0$ in $d+1$ dimensions, for all $d \geq 3$.

Proof: For $r > r_c$ we have $V(r) < 0$. Suppose we follow a null curve of constant t in the equatorial plane $\theta_1 = ... = \theta_{d-2} = \pi/2$. Let $\Delta\phi > 0$ denote the change in the co-latitude ϕ along the section of this curve from $r = r_c$ to $r = \infty$. We have

$$\begin{aligned} -\frac{dr^2}{V(r)} &= r^2 d\phi^2 \\ \implies \Delta\phi &= \int_{r_c}^{\infty} \frac{dr}{r\sqrt{\frac{r^2}{l^2} + \frac{\mu}{r^{d-2}} - 1}} \\ &= \int_1^{\infty} \frac{dy}{y\sqrt{\frac{r_c^2}{l^2}\left(y^2 - \frac{1}{y^{d-2}}\right) + \frac{1}{y^{d-2}} - 1}} \end{aligned} \tag{3.2.8}$$

where we have made the substitution $y = r/r_c$ and used the fact that r_c satisfies $V(r_c) = 0$. It will be convenient to consider $\Delta\phi$ as a function of μ. An illustration of the graph of

$$-r^{d-2}V(r) = \mu - r^{d-2} + r^d/l^2 \tag{3.2.9}$$

is shown in Figure 3.4. Increasing μ slightly will shift this graph upwards, which in turn will decrease r_c (the largest root of this graph). This tells us that

$$\frac{\partial r_c^2}{\partial \mu} < 0 \tag{3.2.10}$$

We also see that

$$\begin{aligned}
\frac{\partial \Delta\phi}{\partial r_c^2} &= -\int_1^\infty \frac{\left(y^2 - \frac{1}{y^{d-2}}\right) dy}{2l^2 y \left(\frac{r_c^2}{l^2}\left(y^2 - \frac{1}{y^{d-2}}\right) + \frac{1}{y^{d-2}} - 1\right)^{3/2}} \\
&< 0 \\
\implies \frac{\partial \Delta\phi}{\partial \mu} &= \frac{\partial \Delta\phi}{\partial r_c^2}\frac{\partial r_c^2}{\partial \mu} \\
&> 0 \\
\implies \Delta\phi &> \Delta\phi|_{\mu=0} \\
&= \int_l^\infty \frac{dr}{r\sqrt{\frac{r^2}{l^2} - 1}} \\
&= \frac{\pi}{2}
\end{aligned} \tag{3.2.11}$$

Using this fact we can construct a timelike path between any two points in $\mathscr{I}^-$ and $\mathscr{I}^+$ using the procedure described below and illustrated in Figure 3.5.

Choose co-ordinates such that p and q both lie in the equatorial plane and $\phi = 0$ at p, $\phi = \phi_q \in [0, \pi]$ at q. Let $t = t_p$ at p and $t = t_q$ at q. Starting at p, we follow a path in the equatorial plane with $t = t_p$ until we reach $r = r_c$. We choose the first part of this path to be null, with ϕ varying until we reach $\phi = \phi_q/2$ (the above calculation shows that this occurs before we reach $r = r_c$). After this, we choose ϕ to remain constant until we reach $r = r_c$, so this part of the path will be timelike. At this point on the Penrose diagram, all $t =$ constant surfaces intersect. This means we can switch to a similar path in the equatorial plane with $t = t_q$ until we reach $r = \infty$. Again we choose this path to be null initially, with ϕ varying until we reach $\phi = \phi_q$. After this we set ϕ constant, so the path is once again timelike and finishes at q. Applying Proposition 2.2.2, this path can then be smoothed to form a timelike curve from p to q. □

This result should be compared to Theorem 2.3.2 and Proposition 2.3.4 (summarised in Theorem 2.3.7), where it was found that the positive mass asymptotically flat Schwarzschild spacetime satisfies the Penrose property in $3 + 1$ dimensions but not in higher dimensions.

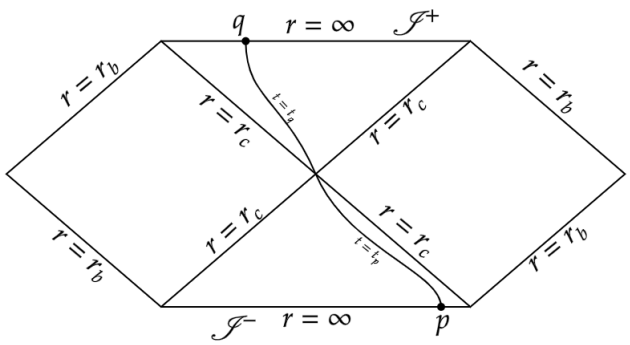

Figure 3.5: The projection onto the $r - t$ plane of a timelike path from p to q is shown We follow two separate curves of constant t. These curves join at $r = r_c$ and can be smoothed to form a path from p to q which is timelike everywhere.

As in the asymptotically flat case, the Penrose property fails in negative mass Schwarzschild-de Sitter spacetime.

Theorem 3.2.6. The Penrose property does not hold in Schwarzschild-de Sitter spacetime with mass parameter $\mu \leq 0$ in $d + 1$ dimensions for any $d \geq 3$.

Proof: If $\mu = 0$ then this is de Sitter spacetime which was covered in Theorem 3.2.1.

Let $\mu < 0$. Suppose p and q can be connected by a timelike curve γ as shown in Figure 3.6 and choose co-ordinates so that these points lie in the equatorial plane. Let w, w' denote the points on γ at which $r = r_h$, where this is the unique root of $V(r)$ (note that w and w' may be the same point). Since the interiors of the sets $J^+(p) \cap J^-(w)$, $J^+(w) \cap J^-(w')$ and $J^+(w') \cap J^-(q)$ (shown as the shaded regions in Figure 3.6) are non-empty and globally hyperbolic, Theorem 2.3.6 tells us we can replace γ with separate causal geodesics from p to w, from w to w' and from w' to q.

Solving the geodesic equations, we find that along a causal geodesic in the equatorial plane from $r = r_h$ to $r = \infty$, we have (choosing ϕ increasing without loss of generality)

$$\Delta\phi = \int_{r_h}^{\infty} \frac{h \mathrm{d}r}{r^2 \left(E^2 - V(r)\left(\frac{h^2}{r^2} + L^2\right)\right)^{1/2}} \tag{3.2.12}$$

where $E = -V(r)\dot{t}$, $h = r^2\dot{\phi}$ and $L^2 = \left(\frac{ds}{d\tau}\right)^2$ are constants and $\dot{}$ denotes differentiation with

respect to an affine parameter s. It is clear that $\Delta\phi$ is maximised by setting $E = L = 0$ (note that $V(r) < 0$ for $r > r_h$). This corresponds to a null geodesic along a line $t =$ constant. These curves were considered in the proof of Theorem 3.2.5 and here we will denote the change in ϕ along such a curve by $\Delta\phi_{max}$. We see from equation (3.2.11) that for $\mu < 0$ we have

$$\begin{aligned} &\frac{\partial \Delta\phi_{max}}{\partial \mu} < 0 \\ \implies \Delta\phi &\leq \Delta\phi_{max} \\ &< \Delta\phi_{max}|_{\mu=0} \\ &= \frac{\pi}{2} \end{aligned} \tag{3.2.13}$$

So $2\Delta\phi_{max}$ is an upper bound for the change in ϕ along the curve γ excluding the portion between w and w'. This upper bound is strictly less than π and crucially does not depend on the positions of p and q (a fact which follows from the invariance of the metric under $t-$translations). It is clear that as p and q slide along $\mathscr{I}^-$ and $\mathscr{I}^+$ respectively towards opposite corners of the Penrose diagram (Figure 3.6), the geodesic between w and w' approaches a radial geodesic and hence the change in ϕ along it tends to 0. It follows that if p and q are chosen to be sufficiently close to opposite corners in the Penrose diagram then the change in ϕ along γ must be strictly less than π. If we also choose p and q to be antipodal then we conclude that they cannot be timelike connected. □

We see that, in contrast to the $\Lambda = 0$ case, for each $p \in \mathscr{I}$ there is now an open set of points on $\mathscr{I}$ which do no lie in the timelike future of p. We also observe that if the finite version of the Penrose property is extended to include curves which do not escape to the asymptotic region (and for consistency extend the non-timelike boundary version of the Penrose property to include their endpoints at $i^{\pm}$) then Theorem 3.2.5 would no longer be true. In particular, we would be able to choose endless timelike curves remaining in the two causally disconnected regions between the event and cosmological horizons (see Figure 3.3). The past endpoint at i^- of either of these curves would be timelike disconnected from the future endpoint at i^+ of the other. The complication here arises because the conformal

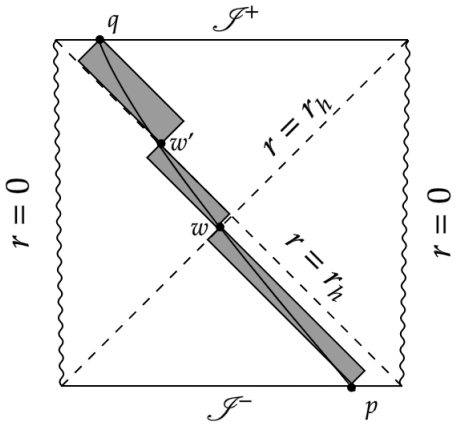

Figure 3.6: Penrose diagram for the Schwarzschild-de Sitter spacetime with negative mass. This figure shows the construction used in the proof of Theorem 3.2.6.

boundary is a spacelike hypersurface. As a result it is possible for the non-timelike boundary version of the Penrose property as stated in Definition 2.1.5 to hold and yet for i^- and i^+ not to be timelike connected.

The results of this section provide justification for our choice to exclude timelike curves which fail to reach the asymptotic region. Recall that Penrose's original motivation for studying the Penrose property was to make comparisons between the spacetime of interest and an appropriate "background" spacetime. In the case of [59] (see also Chapter 2) this background was Minkowski spacetime, while in this section the relevant background is de Sitter. Our conventions give us a property which is strong enough that when we find a physically relevant spacetime which satisfies it, Theorem 3.2.4 ensures that this is enough to rule out any "$SO(d+1,1)$ covariant" construction of quantum gravity based on a background de Sitter spacetime. In light of Theorem 3.2.5, we remark that the positive mass Schwarzschild-de Sitter spacetime provides such an example. If we were to include the points $i^{\pm}$ in the definition of the non-timelike boundary version of the Penrose property (and include curves which do not escape to the asymptotic region in the finite version) then this property would not be satisfied by the positive mass Schwarzschild de-Sitter spacetime and we would be unable to use Theorem 3.2.4 to rule out such a quantum gravity construction.

3.3 Anti-de Sitter Spacetimes

3.3.1 Defining the Penrose Property

In this section we will consider spacetimes which are *asymptotically anti-de Sitter* (Definition 2.1.4).

The conformal boundary at infinity, denoted $\mathscr{I}$, is timelike and hence cannot be separated into "past" and "future" components. As a result it is not obvious what the analogue of the non-timelike boundary version of the Penrose property should be.

To address this, we begin by considering pure anti-de Sitter spacetime in $d+1$ dimensions. This spacetime is isometric to the submanifold of $\text{Mink}_{d,2}$ defined by

$$-t^2 - x_1^2 + \sum_{i=2}^{d+1} x_i^2 = -l^2 \tag{3.3.1}$$

where $(t, x_1, ..., x_{d+1})$ are a standard Cartesian co-ordinate system on $\mathbb{R}^{d+1,1}$ and the radius of curvature, l, is a positive constant which is related to the cosmological constant by

$$\Lambda = -\frac{d(d-1)}{2l^2} \tag{3.3.2}$$

The metric in static co-ordinates is given by

$$ds^2 = V(r)dt^2 - \frac{dr^2}{V(r)} - r^2 d\omega_{d-1}^2 \tag{3.3.3}$$

where $V(r) = 1 + r^2/l^2$.

In order to formulate an appropriate analogue of the non-timelike boundary version of the Penrose property, we begin with a result from [47]. Given $p \in \mathscr{I}$, it will be useful to distinguish between the set of points in $\mathscr{I}$ which can be reached by future pointing causal

curves from p which either remain on $\mathscr{I}$ or which have only their endpoints on $\mathscr{I}$. We define the following sets

$$\begin{aligned} A(p) &= \{q \in \mathscr{I} : \exists \text{ future directed causal curve } \gamma \text{ from } p \text{ to } q \text{ such that } \gamma \setminus \{p,q\} \subset \text{int}(\overline{M})\} \\ B(p) &= \{q \in \mathscr{I} : \exists \text{ future directed causal curve } \gamma \text{ from } p \text{ to } q \text{ such that } \gamma \subset \mathscr{I}\} \end{aligned} \tag{3.3.4}$$

where the interior of a set X, denoted $\text{int}(X)$, is defined to be the union of all open subsets of X. We will also write $A_0(p)$ to denote the set $A(p)$ defined with respect to the compactified AdS metric. Note that no such notation is required for the set $B(p)$, since the metric on the conformal boundary at infinity of an asymptotically AdS spacetime agrees with that of pure AdS.

We will also make use of the fact that the timelike future of a point is an open set, and hence

$$\begin{aligned} \text{int}(A(p)) = \{q \in \mathscr{I} : \exists \text{ a future directed timelike curve } \gamma \text{ from } p \text{ to } q \text{ such that} \\ \gamma \setminus \{p,q\} \subset \text{int}(\overline{M})\}. \end{aligned} \tag{3.3.5}$$

In order to define an appropriate boundary version of the Penrose property, the following result will be useful.

Theorem 3.3.1 (Horowitz, Itzhaki [47])**.** *$A_0(p) = B(p)$ in Anti-de Sitter spacetime in $d+1$ dimensions, for any $d \geq 2$.*

Proof: We write the metric in Poincaré co-ordinates

$$ds^2 = \frac{l^2}{z^2}(dt^2 - dz^2 - \sum_{i=1}^{d-1}(dx^i)^2) \tag{3.3.6}$$

where $0 \leq z < \infty$, with $z = 0$ corresponding to points on the conformal boundary. The disadvantage of these co-ordinates is that they only cover part of the spacetime (the "Poincaré patch"). The advantage is that they show the AdS metric to be conformally flat. Conformally

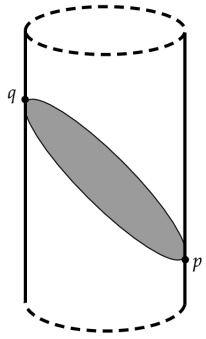

Figure 3.7: Diagram showing a portion of conformal anti-de Sitter spacetime with its timelike conformal boundary. The shaded region is the boundary of the future lightcone of a point p on this conformal boundary. All future pointing null geodesics from p (including those restricted to the boundary) have the same future endpoint at q.

compactified AdS has metric

$$\overline{ds}^2 = dt^2 - dz^2 - \sum_{i=1}^{d-1}(dx^i)^2 \tag{3.3.7}$$

Consider the boundary of the future lightcone from a point p on the conformal boundary. This is a null hypersurface (Figure 3.7), on which we can choose a sequence of curves approaching the conformal boundary so that, parameterising these curves by an affine parameter s, the sequence of co-ordinate functions $z(s) \to 0$ uniformly. We see from (3.3.7) that this means $\dot{t}^2 - \sum_{i=1}^{d-1}(\dot{x}^i)^2 \to 0$ uniformly along this sequence (where $\dot{}$ denotes differentiation with respect to s), and hence the limit curve on the conformal boundary at infinity (given by $z = 0$) is null.

This tells us that, for any $p \in \mathscr{I}$, the intersection between $\mathscr{I}$ and $\partial J^+(p)$ is a null curve[1]. We conclude that $A_0(p) = B(p)$. $\square$

With this result in mind, we define a boundary version of the Penrose property in asymptotically AdS spacetimes as follows.

Definition 3.3.2 (Penrose property - timelike boundary version)**.** Let (M, g) be an

[1]This is in contrast with the intersection between a null plane and a timelike cylinder in Minkowski spacetime which gives a spacelike curve.

asymptotically AdS spacetime with conformal compactification $(\overline{M}, \overline{g})$. Then (M, g) satisfies the *timelike boundary version of the Penrose property* if $B(p) \subset \text{int}(A(p))$ for any $p \in \mathscr{I}$.

This definition is similar to the one used for asymptotically flat spacetimes in the following sense. First note that it is not satisfied in AdS spacetime, however from Theorem 3.3.1 we see that it is "almost" satisfied. Similarly, the non-timelike boundary version of the Penrose property "almost" holds in Minkowski spacetime, where only antipodal points on $\mathscr{I}^-$ and $\mathscr{I}^+$ lying sufficiently close to i^0 cannot be timelike connected. The only null curve between such points is the one which lies entirely on the conformal boundary and passes through i^0. This is shown in Figure 2.1. The non-timelike boundary version of the Penrose property applied to an asymptotically flat spacetime (Definition 2.1.5) asks whether the spacetime curvature near i^0 allows us to do better and connect these points (along with all other pairs of points on $\mathscr{I}^-$ and $\mathscr{I}^+$) using a timelike curve through the interior of the spacetime (see the discussion in section 2.1). Similarly, our definition of the timelike boundary version of the Penrose property asks if the spacetime curvature allows us to use timelike curves through the interior to connect points which can only be connected by null curves on the conformal boundary.

We stress that, as in the asymptotically flat case, this property is a property of spacetimes near the conformal boundary. In particular, suppose we could find a timelike curve through the interior spacetime from p to q, for some $q \in B(p)$. Then we can also find such a curve from p to w for any $w \in B(q)$. This is done by smoothing the timelike curve from p to q and the boundary causal curve from q to w in such a way as to get a timelike curve through the interior with the same endpoints. But by choosing q arbitrarily close to p, any timelike curve between them must remain arbitrarily close to the boundary and its existence is determined by the asymptotic properties of the metric. This is in contrast to the behaviour observed in the asymptotically de Sitter case, where it was necessary to consider curves which leave the asymptotic region.

We now state the result of Gao and Wald which shows that the timelike boundary version of the Penrose property fails in spacetimes which focus null geodesics entering the bulk.

Theorem 3.3.3 (Gao, Wald [39], Theorem 2). Let (M, g) be a spacetime with conformal compactification $(\overline{M}, \overline{g})$ such that

1. Every complete null geodesic in (M, g) contains a pair of conjugate points[2];
2. $\overline{M}$ is strongly causal;
3. For any $p, q \in \overline{M}$, $J^+(p) \cap J^-(q)$ is compact;
4. $\mathscr{I}$ is a timelike hypersurface in $\overline{M}$.

Then $\partial A(p) \subset B(p)$, so in particular the timelike boundary version of the Penrose property (Definition 3.3.2) fails.

Note that AdS spacetime does not satisfy the conditions of this theorem, so there is no contradiction with Theorem 3.3.1. In particular, radial null geodesics do not contain conjugate points.

Sketch of Proof (following [39]): We begin by showing that $A(p)$ ($p \in \mathscr{I}$) is open. Suppose $r \in A(p)$ and let λ be a causal curve from p to r which otherwise does not intersect $\mathscr{I}$. If λ is not a null geodesic then there exists a timelike curve in M with the same endpoints (Proposition 2.2.2). If λ is a null geodesic then it contains a pair of conjugate points (assumption 1) and can be similarly deformed to a timelike curve through M without changing its endpoints. This shows that $r \in I^+(p)$, an open set. We conclude that some neighbourhood of r is also contained in $A(p)$ and hence that $A(p)$ is open.

Now suppose $p, q \in \mathscr{I}$ and $q \in \partial A(p)$. This tells us that $q \notin I^+(p)$, otherwise an open neighbourhood of q would be contained in $A(p)$. By taking the limit of a sequence of timelike curves from p with endpoints approaching q (and using the facts that $J^+(p) \cap J^-(q)$ is compact, $\overline{M}$ is strongly causal and $\mathscr{I}$ is timelike) we can construct a causal curve, γ, from p to q (see [39] for details of this construction). Suppose a segment of γ enters the interior of the

[2]To guarantee this, we could impose the null generic condition and the null energy condition, although this latter condition could be replaced by a weaker condition due to Borde, see Theorem 4.5.1.

spacetime. Then, since $A(p')$ is open for any $p' \in \mathscr{I}$, this segment can be deformed to become timelike (without changing its endpoints). The entire curve γ can then be deformed to give a timelike curve from p to q (Proposition 2.2.2). This is a contradiction, so we conclude that γ lies entirely in $\mathscr{I}$ and hence $q \in B(p)$. $\square$

As explained in [39], Theorem 3.3.3 says that null geodesics through spacetimes satisfying the conditions of the theorem are "delayed" relative to null geodesics in pure AdS. To make this comparison we use null geodesics on the conformal boundary as a reference. This is actually the same effect as is observed in positive mass asymptotically flat spacetimes and is the reason that the Penrose property can be shown to fail in higher dimensional positive mass Schwarzschild (see Proposition 2.3.4 and the discussion in Chapter 2).

From Theorem 3.3.1, we immediately get the following analogue of Theorem 2.1.9.

Theorem 3.3.4. Let $(\overline{M}, \overline{g})$ be the conformal compactification of an asymptotically anti-de Sitter spacetime which satisfies the timelike boundary version of the Penrose property and let $\mathscr{I}$ denote its conformal boundary at infinity. Then, given any $p \in \partial\mathscr{I}$, there is no compactification of AdS spacetime which has $\mathscr{I}$ as its conformal boundary at infinity and $\overline{g} \leq \overline{g}_{AdS}$ on some neighbourhood of $p \in \overline{M}$.

Proof: Suppose such a compactification exists and let $p \in \partial\mathscr{I}$ be a point with neighbourhood $U \subset \overline{M}$ on which $\overline{g} \leq \overline{g}_{AdS}$ holds. Let $q \in B(p)$. So there exists a curve $\lambda \subset \mathscr{I}$ from p to q which is causal with respect to $\overline{g}$. Since $(\overline{M}, \overline{g})$ satisfies the timelike version of the Penrose property, given any $p' \in \lambda$ there exists a $\overline{g}$–causal curve through the interior spacetime from p to p'. By choosing p' sufficiently close to p, this curve must lie entirely in U. The condition $\overline{g} \leq \overline{g}_{AdS}$ implies that this curve is causal with respect to the metric $\overline{g}_{AdS}$. We therefore have a piecewise $\overline{g}_{AdS}$-causal curve from p to q which lies in the interior from p to p' and on the boundary from p' to q. Since $\mathscr{I}$ is totally geodesic as a submanifold of $\overline{M}$, this curve is not a null geodesic, so can be smoothed to give a $\overline{g}_{AdS}$ timelike curve from p to q which otherwise lies entirely in the interior spacetime (this follows Proposition 2.2.2 and the methods used to prove [58, Proposition 2.23]). It follows that $q \in \mathrm{int}(A_0(p))$. We conclude that $B(p) \subset \mathrm{int}(A_0(p))$ and hence $B(p) \neq A_0(p)$, since both of these sets are closed. This

contradicts Theorem 3.3.1. □

3.3.2 Schwarzschild-Anti de Sitter

As an example, and to compare with the results of Sections 2.3 and 3.2.2, we consider the Schwarzschild-anti de Sitter spacetime. In $d+1$ dimensions, the metric for this spacetime is

$$ds^2 = V(r)dt^2 - \frac{dr^2}{V(r)} - r^2 d\omega_{d-1}^2 \tag{3.3.8}$$

where

$$V(r) = 1 - \frac{\mu}{r^{d-2}} + \frac{r^2}{l^2}. \tag{3.3.9}$$

and we have introduced a *mass parameter*, μ, which is related to the mass of the AdS ground state [73], m, by

$$\mu = \frac{16\pi m}{(d-1)A_{S^{d-1}}}. \tag{3.3.10}$$

The parameter l is related to the cosmological constant by (3.3.2).

The Penrose diagram for the positive mass Schwarzschild-AdS spacetime is shown in Figure 3.8. This figure also shows how the finite version of the Penrose property can be seen to fail in this spacetime.

Theorem 3.3.5. The Schwarzschild-AdS spacetime in $d+1$ dimensions ($d \geq 3$) satisfies the timelike boundary version of the Penrose property if and only if the mass parameter $\mu < 0$.

Note that the Schwarzschild-AdS spacetime does not satisfy the conditions of Theorem 3.3.3 so is not covered by this result. In particular, if $\mu < 0$ then there is a naked singularity and condition 3 is not satisfied. If $\mu > 0$ then the endless null geodesic along the horizon does not contain any conjugate points (indeed the null generic conditions fails along this geodesic). As mentioned in Section 3.3.1, if $\mu = 0$ then no radial null geodesic contains conjugate points.

Proof: We begin by considering the case where $\mu < 0$ and we aim to show that $B(p) \subset \text{int}(A(p))$. In this case $V(r) > 0$ for all $r > 0$, so the singularity at $r = 0$ is naked.

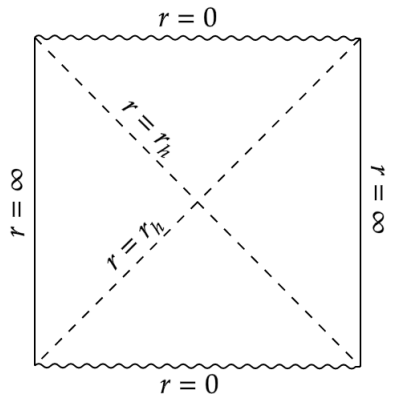

Figure 3.8: Penrose diagram for the positive mass Schwarzschild-AdS spacetime. This spacetime contains a spacelike singularity at $r = 0$, an event horizon at $r = r_h$ (where $V(r_h) = 0$) and a timelike conformal boundary at infinity.

We first compactify the Schwarzschild-AdS metric using the same procedure as was used in the asymptotically flat case in 2.3.2, where we define the tortoise co-ordinate, r_*, by

$$\begin{aligned} dr_* &= \frac{dr}{V(r)} \\ &= \frac{1}{1+\frac{r^2}{l^2}}\left(1+O(r^{-d})\right)dr \\ \implies r_* &= l\tan^{-1}(r/l) + O(r^{-(d-1)}) \end{aligned} \tag{3.3.11}$$

We see that all terms involving μ are sub-leading, and in particular tend to 0 as $r \to \infty$. From this it is clear that the co-ordinates used to compactify Schwarzschild-AdS spacetime (equation (3.3.8)) agree at $r = \infty$ with those used to compactify pure anti-de Sitter. This allows us to use a spacetime comparison argument similar to those used in Sections 2.3.3 and 2.3.4[3].

[3]The agreement of compactified co-ordinates on the conformal boundary is crucial for making spacetime comparisons such as the one used in this proof. The failure of this is precisely why a naïve comparison argument fails to show that the Penrose property does not hold in positive mass Schwarzschild spacetime in $3+1$ dimensions. In this situation we have $ds^2 \leq ds^2_{Mink}$, however when we compactify both metrics as in Sections 2.2 and 2.3.2, the compactified co-ordinates diverge away from each other as we approach null infinity. This means that all timelike curves in compactified Schwarzschild correspond to curves between past and future timelike infinity in compactified Minkowski (where we identify co-ordinates (T, χ, θ, ϕ) on the compact manifolds). As a result, we cannot use the failure of the Penrose property in Minkowski spacetime to deduce that it also fails in $3+1$ dimensional positive mass Schwarzschild. It is precisely this incompatibility in the causal structure at infinity when compared to that of Minkowski which the Penrose property aims to detect.

In what follows we use the subscript 0 to denote pure AdS spacetime (i.e. Schwarzschild-AdS with $\mu = 0$) with the same radius of curvature, l, as the Schwarzschild-AdS spacetime we are considering. We have

$$\begin{aligned} & V(r) > V_0(r) \\ \implies & ds^2 > ds_0^2 \\ \implies & \overline{ds}^2 > \frac{\Omega_0^2}{\Omega^2}\overline{ds}_0^2 \end{aligned} \tag{3.3.12}$$

where Ω^2 and Ω_0^2 are the conformal compactification factors for the Schwarzschild-AdS and pure AdS spacetimes respectively. Recall that these factors are strictly positive on the interior spacetime and that the two metrics agree on the boundary. As a result, for any $p \in \mathscr{I}$, the set $B(p)$ is the same for both metrics.

Now suppose p, $q \in \mathscr{I}$ and $q \in B(p) = A_0(p)$. This means that p and q are connected by a curve which lies in the interior spacetime (other than its endpoints) and is causal with respect to the conformal AdS metric. From inequality (3.3.12), we see that this curve is timelike with respect to the conformal negative mass Schwarzschild-AdS metric. We conclude that $q \in \text{int}(A(p))$.

If $\mu > 0$ then a similar argument shows that the timelike boundary version of the Penrose property does not hold. Note that in this case $V(r)$ has exactly one positive root (corresponding to the position of the event horizon). However, since we are interested in timelike connecting points on the conformal boundary, we can restrict attention to regions where r is large and hence $V(r) > 0$ (see the comment in Section 3.3 explaining why the timelike boundary version of the Penrose property is a property of spacetimes near their timelike boundary). Inequality (3.3.12) is reversed, so we have

$$\overline{ds}^2 < \frac{\Omega_0^2}{\Omega^2}\overline{ds}_0^2. \tag{3.3.13}$$

Now suppose p, $q \in \mathscr{I}$ and $q \in \partial B(p)$. Suppose $q \in \text{int}(A(p))$, so p and q are connected by a curve through the interior spacetime which is timelike with respect to the conformal

Schwarzschild-AdS metric. Inequality (3.3.13) implies that this curve is also timelike with respect to the conformal AdS metric, so $q \in \text{int}(A_0(p))$ and hence $q \in \text{int}(B(p))$ by Theorem 3.3.1. This is a contradiction. □

It seems that for asymptotically AdS spacetimes, the timelike boundary version of the Penrose property is characteristic of spacetimes with negative mass. This agrees with Theorem 3.3.3, which associates the failure of this property with spacetimes which focus null geodesics, a property we associate with global positivity of mass via the positive mass theorem (see discussion of this in Chapter 4). If we regard the negative mass AdS-Schwarzschild spacetime as unphysical (perhaps due to the presence of a naked singularity), then Theorem 3.3.5 means that we are unable to use Theorem 3.3.4 to rule out a "$SO(d, 2)$ covariant" construction of quantum gravity defined with respect to a background anti-de Sitter spacetime. This is relevant for the AdS-CFT conjecture [50].

Finally, we observe that the finite version of the Penrose property (Definition 2.1.6) does not generalise to an interesting property in asymptotically AdS spacetimes.

Theorem 3.3.6. For asymptotically anti-de Sitter spacetimes, the timelike boundary version of the Penrose property is not equivalent to the finite version of the property, which fails trivially.

Proof: Since the conformal boundary of an asymptotically AdS spacetime is timelike, we can find two open sets on this boundary which are not timelike connected. We then choose two causal curves (endless in the uncompactified spacetime) one with both endpoints in the first of these open sets and the other with both endpoints in the second. Since the open sets are not timelike connected it follows that neither are these two curves. We see that the finite version of the Penrose property fails for any asymptotically AdS spacetime. This is illustrated in Figure 3.9.

From Theorems 3.3.1 and 3.3.5, we see that there are examples of asymptotically AdS spacetimes which do and do not satisfy the timelike boundary version of the Penrose property, so we conclude that this property is not equivalent to the finite version. □

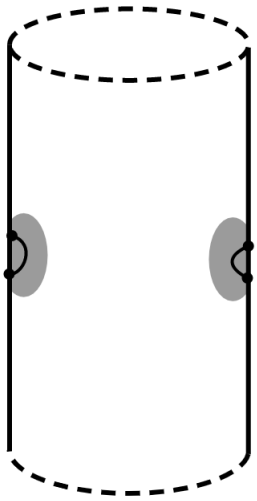

Figure 3.9: This figure shows how in an asymptotically AdS spacetime we can choose two timelike curves (endless in the uncompactified spacetime) with endpoints in open sets on the timelike boundary which are not timelike connected.

3.4 Product Spacetimes

In this section we consider spacetimes of the form $(M, g) = (M', g') \times (M'', g'')$, where (M', g') is an asymptotically flat Lorentzian manifold and (M'', g'') is a compact Riemannian manifold. Before proceeding we must consider how to compactify such spacetimes. Since (M', g') is asymptotically flat, we can conformally embed M into the warped product manifold $\tilde{M} = \tilde{M}' \times_{\Omega'} M''$ endowed with the metric

$$\overline{g} := \Omega'^2 g = \overline{g}' - \Omega'^2 g'' \tag{3.4.1}$$

where $\overline{g}' = \Omega'^2 g'$.[4]

Since $\Omega' = 0$ on $\partial\overline{M'}$, the metric $\overline{g}$ degenerates to $\overline{g}'$ on $\partial\overline{M'} \times M''$. For this reason, we define

$$\begin{aligned} \partial\overline{M} &= \left(\left(\partial\overline{M}' \cup i^- \cup i^+\right) \times M''\right) / \sim \\ &\cong \partial\overline{M}' \end{aligned} \tag{3.4.2}$$

[4]Recall that we are using the 'mostly minus' signature $(+, -, ..., -)$.

where the equivalence relation $\sim$ is defined by

$$(x, y_1) \sim (x, y_2) \text{ for any } x \in \partial\overline{M}', \; y_1, y_2 \in M''. \tag{3.4.3}$$

We then define $\overline{M} := (\text{int}(\overline{M}') \times M'') \cup \partial\overline{M}$ and refer to $(\overline{M}, \overline{g})$ as the conformal compactification of (M, g). The addition of $\partial\overline{M}$ causally completes M (endless causal curves in M have endpoints on $\partial\overline{M}$). Despite this, $\overline{M}$ is not a manifold with boundary, since $\partial\overline{M}$ is not co-dimension 1 in $\overline{M}$. However, it still makes sense to consider the non-timelike boundary version of the Penrose property for such product spacetimes, where the set $\partial\overline{M}$ inherits the splitting of $\partial\overline{M}'$ into "past" and "future" components, denoted $\mathscr{I}^-$ and $\mathscr{I}^+$ respectively.

Theorem 3.1.3: The product spacetime $(M, g) = (M', g') \times (M'', g'')$, where (M', g') is an asymptotically flat Lorentzian manifold and (M'', g'') is a compact Riemannian manifold, satisfies the non-timelike boundary version of the Penrose property if and only if this property is satisfied in (M', g').

Proof: If (M, g) satisfies the Penrose property then so does (M', g'), since timelike curves in (M, g) remain timelike after projection onto (M', g'). If (M', g') satisfies the Penrose property then so does (M, g), since we can identify $p \in \mathscr{I}^-$ and $q \in \mathscr{I}^+$ with points on null infinity in $\partial\overline{M}'$ and timelike connect them in (M, g) using a curve following a timelike path in (M', g') which has zero length in (M'', g''). $\square$

In fact, the finite version of the Penrose property in (M, g) is also equivalent to this same property in (M', g').

Theorem 3.4.1. The product spacetime $(M, g) = (M', g') \times (M'', g'')$, where (M', g') is an asymptotically flat Lorentzian manifold and (M'', g'') is a compact Riemannian manifold, satisfies the finite version of the Penrose property if and only if this property is satisfied in (M', g').

Proof: It is clear that if (M, g) satisfies the finite version of the Penrose property then so does (M', g'): we simply project all timelike curves in (M, g) to timelike curves in (M', g').

Now suppose (M', g') satisfies the finite version of the Penrose property and let $\gamma_1 = \gamma_1' \times \gamma_1''$ and $\gamma_2 = \gamma_2' \times \gamma_2''$ be endless timelike curves in (M, g). Then there exists $(p', p'') \in \gamma_1$, $(q', q'') \in \gamma_2$ such that p' and q' can be connected in (M', g') by a timelike curve γ'.

Define the curve $\gamma \subset M$ as follows. In M' we define it to follow the same path as γ' from p' to q' and then the same path as γ_2' into the infinite future. In M'', we define this curve to have zero length and remain at p''. Using Proposition 2.2.2, we then smooth γ to obtain a curve which is timelike in (M, g) with past endpoint at (p', p'') and future endpoint in the compactified spacetime $(\overline{M}, \overline{g})$ which agrees with that of γ_2 (recall that M'' does not contribute to the boundary of $\overline{M}$). The curves γ and γ_2 therefore have the same timelike past, so in particular (p', p'') lies in the timelike past of γ_2. Hence there must exist a point $w \in \gamma_2$ such that (p', p'') lies in the timelike past of w, as required. □

We saw in Theorem 2.1.7 that the two versions of the Penrose property (Definitions 2.1.5 and 2.1.6) are equivalent in asymptotically flat spacetimes. From Theorems 3.1.3 and 3.4.1 we therefore see that they are also equivalent in the type of product spacetimes considered in this section.

We conclude this Chapter by considering the example of the black string spacetime.

Example 3.4.2 (The Black String)**.** The finite black string metric, defined on $\left(\mathbb{R}^{d,1} \setminus \{0\}\right) \times S^1$, is given by [34]

$$ds^2 = V(r)dt^2 - \frac{dr^2}{V(r)} - r^2 d\omega_{d-1}^2 - dz^2 \tag{3.4.4}$$

where

$$V(r) = 1 - \frac{\mu}{r^{d-2}} \tag{3.4.5}$$

and the mass parameter, μ, is related to the ADM mass, m, by (2.3.20). We also have $z \sim z + L$ for some constant $L \in (0, \infty)$.

The Penrose diagram for this spacetime (Figure 3.10) is the same as the Penrose diagram for Schwarzschild except each interior point now represents a manifold which is topologically

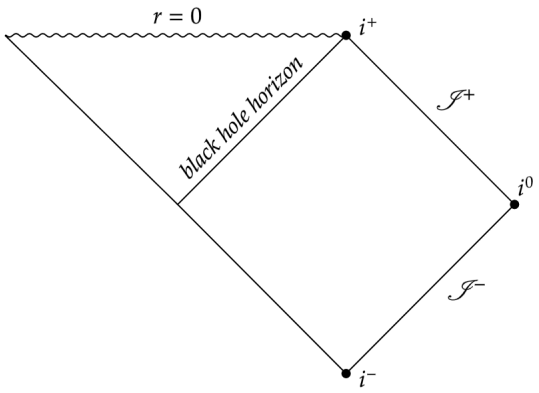

Figure 3.10: The Penrose diagram for the black string spacetime (shown here in the case $\mu > 0$) is the same as for Schwarzschild except each interior point now represents a manifold which is topologically $S^{d-1} \times S^1$ rather than S^{d-1}.

$S^{d-1} \times S^1$ rather than S^{d-1}. Note that endless null geodesics through $\overline{M}$ can now project to curves in $\overline{M}'$ which have endpoints at timelike infinity. For example, consider the null geodesic in $\overline{M}$ with $r, \phi, \theta_1, ..., \theta_{d-2}$ constant (where $\phi, \theta_1, ..., \theta_{d-2}$ are the usual spherical polar co-ordinates on S^{d-1}) and $\frac{dz}{dt} = \sqrt{V(r)}$. Note that the z co-ordinate along this null geodesic does not approach a constant value in the infinite past or future.

Along with Theorem 2.3.7, Theorems 3.1.3 and 3.4.1 tell us that the two equivalent versions of the Penrose property are satisfied by the finite black string spacetime according to the table below:

Spacetime dimension of Schwarzschild part	$m > 0$	$m \leq 0$
3	✓	✗
4	✓	✗
≥ 5	✗	✗

It is straightforward to extend Theorem 2.1.9 to instead refer to a background spacetime of

$$\text{Mink}_{d,1} \times (M'', g'') \tag{3.4.6}$$

where (M'', g'') is a compact Riemannian manifold. Example 3.4.2 provides evidence against

a self-consistent quantum gravity construction for $d = 3$ (but not for $d \geq 4$) based on this background spacetime.

Chapter4

Positivity of Mass in Higher Dimensions

4.1 The Argument of Penrose, Sorkin and Woolgar

In [61], the authors claim that the positive mass theorem can be proved solely using arguments relating to the causal structure of spacetime[1]. These arguments have the advantage of relying specifically on properties of spacetime which one would expect to be characteristic of positive mass, in particular the focusing and retarding of null geodesics which pass near the source (and the corresponding relative time advancement of geodesics passing far from the source). Conversely, null geodesics which pass far from a negative mass source will be delayed relative

[1]It should be noted that this paper was never published. After discussions with people familiar with the argument and after studying it carefully myself, I believe that this was likely due to a lack of precision rather than the methodology itself being flawed. In particular, there are issues regarding the time delay estimates in Section III. I have made every effort to be precise about the arguments used to obtain the time delay estimate Lemma 4.3.3. Specifically, I have explicitly used Minkowski retarded and advanced time co-ordinates to define a time of flight, rather than a Hamilton-Jacobi function. According to [26] this was the source of the problems with the argument as given in [61]. One issue which could lead to confusion is regarding the paths of null geodesics. In [61], the time delay in equation (III.1.5) is calculated for a curve following the path of a Minkowski null ray and it is argued that corrections to this will be sub-leading. I have avoided making any such assumption. In fact, despite the spacetime being asymptotically flat, in positive mass Schwarzschild in 3+1 dimensions, null geodesics arbitrarily far from the mass source eventually diverge infinitely far from Minkowski geodesics. This is discussed in more detail in Section 2.3.2. In fact, Lemma 4.3.1 proves that this does not happen for a certain class of spacetimes in higher dimensions. This is then used in Lemma 4.3.3 to derive a time delay estimate in a more precise way.

to those which pass nearby. This is used to argue that a certain class of negative mass spacetimes must contain a null line as defined by Galloway [38]:

Definition 4.1.1. A null line is an inextendible achronal null geodesic.

Importantly for us, since they are achronal, null lines cannot contain conjugate points.

On the other hand, under certain conditions (see for example Theorem 4.5.1 in Section 4.5) it is possible to show that such a null line cannot exist. This allows us to prove a positive mass theorem among spacetimes satisfying these conditions (Corollary 4.5.2). If the Einstein equations are assumed to hold, conditions on the Riemann tensor can equivalently be stated as conditions on the stress-energy tensor and hence can be thought of as requirements on the matter content of spacetime.

The argument given in [61] concerns $3+1$ dimensional spacetimes only and relies on the fact that, as we let their distance of closest approach tend to infinity, null geodesics in a negative mass spacetime become infinitely delayed relative to those passing nearer to the source. This divergence is precisely the opposite of the null geodesic endpoint condition (Definition 2.5.1) which was observed to hold in $3+1$ dimensional positive mass Schwarzschild and used to prove Theorem 2.3.2. As discussed in Sections 2.3.3 and 2.3.4 for the specific example of the Schwarzschild metric, it appears that this effect becomes vanishingly small in higher dimensions, owing to the faster decay at infinity of the leading order non-Minkowski terms in the metric. Indeed, [61] contains a brief discussion of this point and notes that it prevents the argument given from immediately generalising to higher dimensions.

However, in [23] the result is generalised to include higher dimensions (albeit for a more restrictive class of metrics than those considered in [61]). The assumptions made in this Chapter are weaker than those of [23]. In particular we will require the metric to be *uniformly Schwarzschildean* (Definition 4.2.2) as in [26] rather than the more restrictive assumption that it is *strongly uniformly Schwarzschildean* [23]. We will also drop the assumption made

in [23, Theorem 1.1] that the spacetime is weakly asymptotically regular[2]). On the other hand, our proof will apply only to higher dimensions. We will also be unable to obtain a rigidity result in the $m = 0$ case. We hope that this method of proof will be enlightening as it is closer in spirit to the methods employed in [61], namely the construction of a null line as a *fastest causal curve* (Section 4.4) between two antipodal generators of past and future null infinity.

The theorem we will prove is the following (see later sections for definitions of various terms):

Theorem 4.1.2. Let (M, g) be a uniformly Schwarzschildean spacetime in $d + 1$ dimensions ($d \geq 4$) with ADM mass $m < 0$ and suppose $\mathcal{D} \cup \mathscr{I}$ is a globally hyperbolic subset of $\overline{M}$. Then (M, g) contains a null line.

For $3 + 1$ dimensional spacetimes the argument in [61], which we now outline, proceeds by constructing a *fastest causal curve* between a generator, Λ^-, of $\mathscr{I}^-$ and the antipodal generator, Λ^+ on $\mathscr{I}^+$. One causal curve is said to be *faster* than another if it departs $\mathscr{I}^-$ no earlier and arrives at $\mathscr{I}^+$ no later. A fastest causal curve (if it exists) is defined to be such that no other causal curve is faster.

In order to specify the generator Λ^+ we specify some radial, outgoing, future pointing, Minkowski-null direction[3] k^a. We then define Λ^+ to be the intersection of $\mathscr{I}^+$ with the set of null geodesics whose tangent vector asymptotes towards this direction at future null infinity. We similarly define Λ^- as the intersection of $\mathscr{I}^-$ with the set of null geodesics with tangent vector which asymptotes to $-k^a$ at past null infinity. In this Chapter we will restrict attention to a quasi-Cartesian frame (Definition 4.2.1) and choose co-ordinates $(x_0, x_1, ..., x_d)$ such that k^a has components $k^\mu = (1, 0, ..., 0, 1)$ in this frame.

The key lemma in [61] is Lemma III.2.1. This gives an estimate of the *time of flight* along a curve which has endpoints on $\Lambda^\pm$ and is the union of two null geodesics joined at a point

[2]A spacetime is weakly asymptotically regular if every null line starting in the domain of outer communications either crosses an event horizon or reaches arbitrarily large values of r in the asymptotically flat regions.

[3]We follow Penrose's "abstract index notation" where Latin indices label the rank of a tensor, while Greek indices denote the components of a tensor in some co-ordinate basis.

with $x_d = 0$[4]. The time of flight is defined to be the retarded time of arrival on Λ^+ minus the advanced time of departure from Λ^- (where these are defined using the Hamilton-Jacobi functions describing null geodesics with endpoints on $\mathscr{I}^+$ and $\mathscr{I}^-$ respectively. This quantity is shown to behave asymptotically like

$$4P \cdot k \log(b/B) \tag{4.1.1}$$

where P^a is the ADM 4-momentum of the spacetime [3], b is the value of $r := \sqrt{\sum_{i=1}^{d} x_i^2}$ (defined using quasi-Cartesian co-ordinates) at the point where the null geodesics join, and B is a positive constant.

Suppose for a contradiction that $P \cdot k < 0$, i.e. the 4-momentum of the spacetime is not future causal. The aim is to show that there must then exist a fastest causal curve from Λ^- to Λ^+ which enters the interior of the spacetime. If this is the case then this curve must lie on the boundary of the causal future of some point $p \in \Lambda^-$ and hence must be a null geodesic [70, Corollary after Theorem 8.1.2] without conjugate points [44, Proposition 4.5.12].

The construction begins by finding points $p \in \Lambda^-$, $q \in \Lambda^+$ such that there is no causal curve which departs Λ^- later than p and arrives at Λ^+ earlier than q. These will be the endpoints of the fastest causal curve, γ, to be constructed. We then consider a sequence of causal curves, $(\gamma_i)_{i=0}^{\infty}$, with endpoints on $\Lambda^{\pm}$ tending towards p and q and with γ_i faster than γ_j for $i > j$. The curve γ is defined to be the limit of this sequence of causal curves, where we use the fact that in a globally hyperbolic set, the space of causal curves between two compact sets is compact [67, Theorem 23].

We have argued that γ does not contain any conjugate points. It remains to check that γ does in fact enter the interior of the spacetime and hence defines a null line. The curves $(\gamma_i)_{i=0}^{\infty}$ can be modified (possibly making them faster) so that they consist of two null geodesics joined at a point with $x_d = 0$, $r = b_i$. This means that the estimate (4.1.1) now applies. If we were to have $b_i \longrightarrow \infty$ as $i \longrightarrow \infty$ then this estimate tells us that the time of flight

[4]Note that our choice of co-ordinates such that $k^\mu = (1, 0, ..., 0, 1)$ ensures our curve must pass through such a point.

along γ_i would also diverge to $+\infty$ as $i \longrightarrow \infty$. In particular, the sequence $(\gamma_i)_{i=0}^{\infty}$ would eventually become slower than γ_0. This contradicts the definition of the sequence, so we conclude that b_i must not diverge along the sequence and hence, possibly restricting to a subsequence, all of the γ_i must enter the compact set $\mathcal{K} := (J^+(p_0) \cap J^-(q_0)) \setminus \mathcal{U}_R$, where $\mathcal{U}_R := \{x \in J^+(p_0) \cap J^-(q_0) : r(x) > R\}$ (see Section 4.2 for definitions). Once again, using the compactness result of [67], we conclude that γ must also enter this set, and hence must enter the interior of the spacetime. We therefore conclude that γ is a null line.

This argument does not generalise to higher dimensions because the time of flight along curves restricted to arbitrarily large values of r no longer diverges. Instead, the time of flight estimate (4.1.1) is replaced by Lemma 4.3.3. This lemma says that the time of flight along a curve from Λ^- to Λ^+ which consists of two null geodesics tends to 0 as we let $R \longrightarrow \infty$, where R is such that $r > R$ along the curve.

However, Lemma 4.3.3, combined with ideas from Chapter 2, turn out to be sufficient to construct a null line in higher dimensional negative mass spacetimes (with some slightly modified assumptions).

Using a comparison argument, similar to those used to prove Propositions 2.3.3 and 2.3.4, involving a Minkowski metric defined on a neighbourhood of conformal infinity, we will show how the presence of negative mass allows us to construct a Minkowski-null curve from Λ^- to Λ^+ which is timelike with respect to the physical metric g. To do this, we show that if retarded and advanced time co-ordinates are defined as in equation (2.2.3), then the time of flight along a Minkowski null geodesic is exactly zero. Next we observe that for negative mass spacetimes, the Minkowski null cones at sufficiently large r are contained inside the g-null cones. Hence an η-null geodesic restricted to sufficiently large values of r must be timelike with respect to the metric g. Then since the timelike future of any point is an open set, it must be possible to modify this curve slightly to obtain a g-timelike curve, γ_0, between Λ^- and Λ^+ which has time of flight strictly less than zero. This allows us to use a similar construction as was used in $3+1$ dimensions based on a sequence of faster and faster causal curves $(\gamma)_{i=0}^{\infty}$ from Λ^- to Λ^+. If $b_i \longrightarrow \infty$ along this sequence, then by Lemma 4.3.3 the time

of flight will tend to 0 and in particular will eventually become larger than the time of flight of γ_0. As in 3+1 dimensions, we conclude that the limit of the sequence $(\gamma)_{i=0}^{\infty}$ is a null line which enters the interior of the spacetime.

4.2 Definitions and Assumptions

In order to carry out the comparison with Minkowski spacetime mentioned in the previous section, it will be necessary to impose stronger conditions than those used in [61]. These conditions will be more similar to the ones used in [23, 26]. In this section we outline the various assumptions made.

For the purposes of Theorem 4.1.2, requiring the metric to be $C^{1,1}$ will be sufficient, although in order to obtain a focusing result in Section 4.5 it may be necessary to make stronger assumptions. For example, in Theorem 4.5.1 we assume that the quantity $R_{ab}T^aT^b$ is finite and continuous, where T^a is tangent to a null geodesic. To ensure this, it would be sufficient to assume that the metric is C^2.

Definition 4.2.1. A spacetime (M, g) admits *quasi-Cartesian co-ordinates* if there are co-ordinates, defined on some subset of M diffeomorphic to $\mathbb{R} \times \mathbb{R}^d \setminus B$ (where B denotes a closed ball in $\mathbb{R}^d$), with respect to which the components of the metric, g, take the form

$$g_{\mu\nu} = \eta_{\mu\nu} + h_{\mu\nu} \tag{4.2.1}$$

where

$$\begin{aligned} h_{\mu\nu} &= O\left(r^{-\alpha}\right) \\ \partial_\rho h_{\mu\nu} &= O\left(r^{-(\alpha+1)}\right) \end{aligned} \tag{4.2.2}$$

for some $\alpha > 1$.

Note that Schwarzschild spacetime in $3+1$ dimensions does not satisfy these conditions since in this case we have $h_{\mu\nu} = O(r^{-1})$ and $\partial_\rho h_{\mu\nu} = O(r^{-2})$. As a result, this spacetime is not

covered by the results of this Chapter. However, the conditions stated above are satisfied by Schwarzschild in higher dimensions.

Requiring our spacetime to admit quasi-Cartesian co-ordinates will allow us to prove Lemma 4.3.3, however in order to construct a null line we will need to consider a more restrictive class of metrics. We follow [26] and make the definition below.

Definition 4.2.2. For $m \in \mathbb{R}$, we say that a metric g on $\mathbb{R} \times \left(\mathbb{R}^d \setminus B\right)$, where B is a ball of radius R with $R^{d-2} > \mu$, is *uniformly Schwarzschildean* if, in the co-ordinates of (2.3.6) (or equivalently in the co-ordinates of equation (1) of [26]),

$$\begin{aligned} g - g_m &= o\left(|m| r^{-(d-2)}\right) \\ \partial_i (g - g_m)_{jk} &= o\left(|m| r^{-(d-1)}\right) \end{aligned} \tag{4.2.3}$$

where g_m denotes the Schwarzschild metric of mass m. In the above, o refers to $r \to \infty$, uniformly in t and angular variables, with m fixed.

As in [26] we will abuse notation and allow $m = 0$ in this definition, by which we mean the metric is flat for $r > R$, for some $R \in \mathbb{R}_{\geq 0}$.[5]

Note that requiring a spacetime to be uniformly Schwarzschildean is a less restrictive condition than is used in [23], where the spacetime is assumed to be *strongly uniformly Schwarzschildean*.

As in [14], we also assume that $\overline{M}$ can be extended slightly past conformal infinity so that it is indeed a manifold. This is required in order to satisfy the conditions of Theorem 23 in [67], which in turn is used in the proof of Theorem 4.1.2.

We will also require the following result regarding the completeness of $\mathscr{I}^{\pm}$.

Proposition 4.2.3. [44, Proposition 6.9.4] In a $(d+1)$-dimensional asymptotically flat spacetime, $\mathscr{I}^+$ and $\mathscr{I}^-$ are topologically $\mathbb{R} \times S^{d-1}$.

[5] This case will not be important for us since we will be unable to comment on the $m = 0$ case.

4.3 Time of Flight Estimate in Higher Dimensions

In this section we will derive a higher dimensional analogue of [61, Lemma III.2.1] which gives an estimate for the time of flight of causal curves near infinity with endpoints on $\Lambda^{\pm}$. In [61] it was found that the time of flight diverged logarithmically as we considered curves restricted to increasingly large values of r. We will show that in higher dimensions, the time of flight tends to 0 as the impact parameter approaches infinity. The absence of a divergence is the reason the 3+1 dimensional argument given in [61] does not generalised to higher dimensions.

We will show that higher dimensional spacetimes admitting quasi-Cartesian co-ordinates can be compactified using the same procedure (and same retarded and advanced time co-ordinates) as Minkowski spacetime. As a result, the time of flight along curves with endpoints on $\mathscr{I}^{\pm}$ can be calculated as the difference between the Minkowski retarded and advanced time co-ordinates, $u = t - r$ and $v = t + r$, evaluated at future and past null infinity respectively. This method avoids the need to consider Hamilton-Jacobi functions $S^{\pm}$, as is done in [23] and [61].

Recall that Minkowski spacetime can be compactified as in Section 2.2 and the conformal boundary at infinity can be split into two parts as follows:

$$\begin{aligned} \mathscr{I}^{+} &:= \{u \in \mathbb{R}, v = \infty\} \\ \mathscr{I}^{-} &:= \{u = -\infty, v \in \mathbb{R}\}. \end{aligned} \tag{4.3.1}$$

The points i^{+}, i^{-} and i^{0} are given by

$$\begin{aligned} i^{+} &:= \{u = \infty, v = \infty\} \\ i^{-} &:= \{u = -\infty, v = -\infty\} \\ i^{0} &:= \{u = -\infty, v = \infty\} \end{aligned} \tag{4.3.2}$$

This is illustrated in Figure 2.4.

If the same procedure (with the same u and v) is carried out for Schwarzschild spacetime of

mass m in 3+1 dimensions, the result is a spacetime where null geodesics which do not cross the event horizon have endpoints at $i^{\pm}$ if $m > 0$ (they are infinitely delayed), or are located entirely at i^0 if $m < 0$ (they are infinitely advanced). Instead, the standard procedure for the conformal compactification of Schwarzschild (as outlined in Section 2.3.2) involves defining retarded and advanced time co-ordinates by

$$\begin{aligned} u_s &= t - r_* \\ v_s &= t + r_* \end{aligned} \tag{4.3.3}$$

where

$$\begin{aligned} \frac{dr_*}{dr} &= \frac{1}{V(r)} \\ \implies r_* &= \begin{cases} r + 2m\log(r/2m - 1) & \text{if } d = 3 \\ r + O(r^{3-d}) & \text{if } d \geq 4. \end{cases} \end{aligned} \tag{4.3.4}$$

The subscript 's' has been inserted to distinguish these Schwarzschild retarded and advanced time co-ordinates from the ones defined in (2.2.3) for Minkowski spacetime.

In 3+1 dimensions, r_* diverges from r logarithmically. This is the reason we do not obtain a good compactification using Minkowski retarded and advanced time co-ordinates (in the sense that null geodesics escaping to the asymptotic region do not have endpoints on the surfaces $\mathscr{I}^{\pm}$ as defined in (4.3.1)). We see that in higher dimensions, u_s and v_s agree with the Minkowski u and v at $r = \infty$. Consequently, we could alternatively have used these Minkowski retarded and advanced time co-ordinates to compactify Schwarzschild in higher dimensions, since the structure of the conformal boundary at infinity would be the same in both cases. The following lemma (similar to [20, Proposition B.1]) shows that this is a general feature of higher dimensional spacetimes admitting quasi-Cartesian co-ordinates.

Lemma 4.3.1. Let (M, g) be a spacetime in $d + 1$ dimensions ($d \geq 4$) which admits quasi-Cartesian co-ordinates. Let γ be a future endless g-null geodesic segment with co-ordinates $x^{\mu}(s)$, where $s \geq 0$ is an affine parameter (increasing to the future). Suppose $r \longrightarrow \infty$ as $s \longrightarrow \infty$, so we have $r \geq R$ along γ for some R which, by a simple shift in s, can

be chosen to be arbitrarily large. Then $\dot{x}^\mu(s)$ tends to a finite limit as $s \longrightarrow \infty$, denoted $\dot{x}^\mu_\infty$, (where $\dot{}$ denotes differentiation with respect to s). Moreover, for R sufficiently large, there exists a constant C such that

$$|x^\mu(s) - \dot{x}^\mu_\infty s - x^\mu(0)| \leq \frac{C}{R^{\alpha-1}} \tag{4.3.5}$$

for any $s \geq 0$ and any index μ. In particular, Minkowski retarded time $u := t - r$ tends to a finite limit as $s \longrightarrow \infty$.

Similarly, if γ is instead past endless and the affine parameter s is chosen so that $s \leq 0$ and $r \geq R$ along γ, then $\dot{x}^\mu(s)$ tends to a finite limit, denoted $\dot{x}^\mu_{-\infty}$, as $s \longrightarrow -\infty$. Moreover, for R sufficiently large, there exists a constant C' such that

$$|x^\mu(s) - \dot{x}^\mu_{-\infty} s - x^\mu(0)| \leq \frac{C'}{R^{\alpha-1}} \tag{4.3.6}$$

holds for any $s \leq 0$ and any index μ. In particular, Minkowski advanced time $v := t + r$ tends to a finite limit as $s \longrightarrow -\infty$.

Crucially, the right hand sides of (4.3.5) and (4.3.6) tend to 0 as $R \to \infty$ (since $\alpha > 1$).

Proof: Let R be such that $r \geq R$ for all $s \geq 0$. Since $r \longrightarrow \infty$ as $s \longrightarrow \infty$, by shifting the origin of s we are free to make R arbitrarily large and enforce $\frac{dr^2}{ds}|_{s=0} \geq 0$. Next, re-scale s so that $\frac{dx^i}{ds}\frac{dx^i}{ds}|_{s=0} = 1$. Let $s_1 > 0$ be maximal such that $\frac{3}{4} < \frac{dx^i}{ds}\frac{dx^i}{ds} < \frac{5}{4}$ for all $0 \leq s < s_1$. From the geodesic equations, we have

$$\frac{d^2r^2}{ds^2} = 2\left(\frac{dx^i}{ds}\frac{dx^i}{ds} + x^i\Gamma^i_{\mu\nu}\frac{dx^\mu}{ds}\frac{dx^\nu}{ds}\right) \tag{4.3.7}$$

Since γ is null, for R sufficiently large and $0 \leq s < s_1$ we have $|dt/ds| < 2$ and hence $|dx^\mu/ds|$ is bounded for $\mu = 0, 1, ..., d$. Since (M, g) admits quasi-Cartesian co-ordinates, we also have

$$\left|\Gamma^\mu_{\nu\rho}\right| \leq C_1 r^{-\alpha-1} \tag{4.3.8}$$

for some constant C_1.

Substituting this into equation (4.3.7), we have

$$\frac{d^2r^2}{ds^2} \geq 2 \times \left(\frac{3}{4} - C_2 r^{-\alpha}\right) \tag{4.3.9}$$

for some constant C_2. Hence for $0 \leq s < s_1$ and $r \geq R$ (increasing R if necessary), we have

$$\begin{aligned} & \frac{d^2r^2}{ds^2} > 1 \\ \implies & r^2(s) \geq r^2(0) + s\left.\frac{dr^2}{ds}\right|_{s=0} + \frac{s^2}{2} \\ & \geq R^2 + \frac{s^2}{2} \\ & > C_3(R+s)^2 \end{aligned} \tag{4.3.10}$$

for some constant $C_3 > 0$. To derive the final inequality above, we note that if C_3 is chosen to be sufficiently small then this inequality holds for $s = 0$ and the equation

$$\left(\frac{1}{2} - C_3\right)s^2 - 2C_3Rs + (1 - C_3)R^2 = 0, \tag{4.3.11}$$

viewed as a quadratic in s, has no real solutions.

From this it follows that, for $0 < s \leq s_1$ and any index μ, we have

$$\begin{aligned} & \left|\int_0^s \frac{d^2x^\mu}{ds'^2}ds'\right| \leq \int_0^s \left|\frac{d^2x^\mu}{ds'^2}\right| ds' \\ \implies & \left|\frac{dx^\mu}{ds'}(s) - \frac{dx^\mu}{ds'}(0)\right| \leq \int_0^s \left|\Gamma^\mu_{\nu\rho}\frac{dx^\nu}{ds'}\frac{dx^\rho}{ds'}\right| ds' \\ & \leq C_4 \int_0^s r^{-\alpha-1}ds' \\ & < C_5 \int_0^s (R+s')^{-\alpha-1}ds' \\ & \leq \frac{C_5}{\alpha}R^{-\alpha} \\ \implies & \left|\sum_{i=1}^d \frac{dx^i}{ds}\frac{dx^i}{ds}(s_1) - 1\right| \leq C_6 R^{-\alpha} \end{aligned} \tag{4.3.12}$$

where C_4, C_5 and $C_6 > 0$ are constants. To obtain the final inequality we have used the fact that if $\mathbf{x}, \mathbf{y} \in (\mathbb{R}^d, \delta)$, where δ denotes the Euclidean metric, with $|\mathbf{x}| \leq K$ and $|\mathbf{y}| = 1$, then we have

$$\begin{aligned} \left|\mathbf{x}^2 - \mathbf{y}^2\right| &= |(\mathbf{x}+\mathbf{y}) \cdot (\mathbf{x}-\mathbf{y})| \\ &\leq |\mathbf{x}+\mathbf{y}|\,|\mathbf{x}-\mathbf{y}| \\ &\leq (1+K)\,|\mathbf{x}-\mathbf{y}|\,. \end{aligned} \tag{4.3.13}$$

If instead of integrating from 0 to s in (4.3.12) we instead integrate between s_2 and $s_3 > s_2$, we find that

$$\left|\frac{dx^\mu}{ds}(s_3) - \frac{dx^\mu}{ds}(s_2)\right| \leq \frac{C_5}{\alpha}(R+s_2)^{-\alpha} \text{ for all } s_3 > s_2 \tag{4.3.14}$$

The right hand side of this inequality tends to 0 as $s_2 \longrightarrow \infty$, so we conclude that $\dot{x}^\mu(s)$ tends to a finite limit as $s \longrightarrow \infty$ (where $\dot{}$ denotes differentiation with respect to s). We denote this limit by $\dot{x}^\mu_\infty$.

Then for any $s \geq 0$ and any index μ, we have:

$$\begin{aligned} \left|\int_0^s \frac{dx^\mu}{ds'} - \dot{x}^\mu_\infty ds'\right| &\leq \int_0^s \left|\frac{dx^\mu}{ds'} - \dot{x}^\mu_\infty\right| ds' \\ \implies |x^\mu(s) - \dot{x}^\mu_\infty s - x^\mu(0)| &\leq \int_0^s \frac{C_5}{\alpha(R+s')^\alpha} ds' \\ &\leq \frac{C}{R^{\alpha-1}} \end{aligned} \tag{4.3.15}$$

where $C = \frac{C_5}{\alpha(\alpha-1)} > 0$ is a constant.

Asymptotic flatness implies that $\eta_{\mu\nu}\dot{x}^\mu_\infty \dot{x}^\nu_\infty = 0$ and hence that the curve $x^\mu_{Mink}(s) := x(0)^\mu + \dot{x}^\mu_\infty s$ defines a Minkowski null geodesic along which u tends to a finite value as $s \longrightarrow \infty$. We conclude that u must also tend to a finite limit along γ as $s \longrightarrow \infty$.

If γ is instead a past endless null geodesic segment then similar arguments can be used to show that $\dot{x}^\mu(s)$ tends to a finite limit as $s \longrightarrow -\infty$ and to derive (4.3.6). One can then

deduce that $v := t + r$ tends to a finite limit as $s \longrightarrow -\infty$. $\square$

Lemma 4.3.1 tells us that if we compactify a higher dimensional spacetime which admits quasi-Cartesian co-ordinates using the same procedure as used for Minkowski (including the same retarded and advanced time co-ordinates), then null geodesics escaping to the asymptotic region in the infinite future (respectively past) will have endpoints on the null hypersurface $\mathscr{I}^+$ (respectively $\mathscr{I}^-$) as defined in (4.3.1). This can be summarised in the following corollary.

Corollary 4.3.2. Let (M, g) be a spacetime in $d + 1$ dimensions ($d \geq 4$) which admits quasi-Cartesian co-ordinates. Then (M, g) is asymptotically flat and furthermore the compactification map φ in Definition 2.1.1 can be taken to be the same as for Minkowski spacetime.

The above results allow us to define the time of flight, $u_\infty - v_\infty$, for higher dimensional spacetimes admitting quasi-Cartesian co-ordinates, as in Definition 2.4.1. Here u_∞ denotes the value of $u = t - r$ at the future endpoint of the curve and v_∞ denotes the value of $v = t + r$ at its past endpoint. Lemma 4.3.1 tells us that the time of flight is finite along null geodesics which escape to the asymptotic region in both the future and the past (so in particular do not enter black or white holes). In [61], the time of flight is defined to be $S^+ - S^-$, where the Hamilton-Jacobi functions S^+ and S^- are finite on future and past null infinity respectively. According to [23], the proof of existence of the optical functions $S^\pm$ is the missing step of the argument in [61]. The procedure used here means that it is not necessary for us to define such functions.

We now prove an estimate for the time of flight along certain curves in higher dimensional spacetimes which admit quasi-Cartesian co-ordinates.

Lemma 4.3.3. (**Time of Flight Estimate**) Let (M, g) be a spacetime in $d + 1$ dimensions ($d \geq 4$) which admits quasi-Cartesian co-ordinates and let γ be a causal curve which connects Λ^- to Λ^+ and is comprised of two null geodesic segments. Suppose γ lies entirely in the

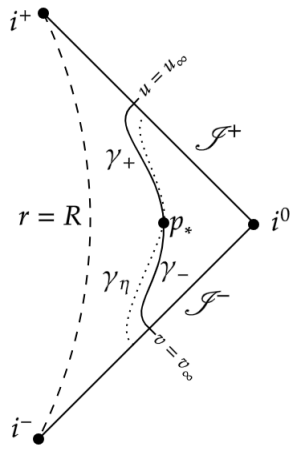

Figure 4.1: Lemma 4.3.3 shows that if γ_- is a g-null geodesic from Λ^- to p_* and γ_+ is a g-null geodesic from p_* to Λ^+, with both restricted to the region $r > R$, then the time of flight along $\gamma_- \cup \gamma_+$ approaches 0 as $R \longrightarrow \infty$. The lemma is proved by comparing this time of flight to the time of flight along a Minkowski null geodesic, γ_η, through p_*, along which the time of flight is 0.

region $r > R$. Then, for R sufficiently large, the time of flight along γ satisfies

$$|u_\infty - v_\infty| \leq \frac{A}{R^{\alpha-1}} \tag{4.3.16}$$

for some constant A.

Proof: Let p_* denote the point at which the two null geodesic segments are joined. Let γ_+ denote the null geodesic from p_* to Λ^+ and let γ_- denote the null geodesic from Λ^- to p_*. Let γ_η denote the curve through p_* with co-ordinates

$$x^\mu_\eta(s) = x^\mu_{p_*} + sk^\mu \tag{4.3.17}$$

where $k^\mu = (1, 0, ..., 0, 1)$ is the Minkowski-null direction used to define $\Lambda^\pm$ (see Section 4.1).

Choose the affine parameter s so that $\frac{dx^i}{ds}\frac{dx^i}{ds}|_{s=0} = 1$ (as in the proof of Lemma 4.3.1). We will use inequality (4.3.5), which tells us that for R sufficiently large, the time of flight along γ is close to the time of flight along γ_η, which we now calculate.

Let $u_{\gamma_\eta,\infty}$ denote the u co-ordinate at the future endpoint of γ_η; b denote the impact parameter

of γ_η; and t_b denote the value of the t co-ordinate on γ_η when $r = b$. Suppose $s = s_b$ when $t = t_b$ and $r = b$. Along γ_η we have $\dot{t} = 1$ and hence

$$t(s) = t_b + s - s_b \tag{4.3.18}$$

Furthermore, $x^d = 0$ at $r = b$, so we have

$$\begin{aligned} & r(s) = \sqrt{b^2 + (s - s_b)^2} \\ \implies & u(s) := t(s) - r(s) \\ & = t_b + s - s_b - \sqrt{b^2 + (s - s_b)^2} \\ \implies & u_{\gamma_\eta,\infty} := \lim_{s \longrightarrow \infty} u(s) \\ & = t_b \end{aligned} \tag{4.3.19}$$

Similarly, the advanced time co-ordinate at the past endpoint of γ_η is $v_{\gamma_\eta,\infty} = t_b$. Hence the time of flight along γ_η is

$$u_{\gamma_\eta,\infty} - v_{\gamma_\eta,\infty} = 0 \tag{4.3.20}$$

Consequently, it follows from Lemma (4.3.1) that the time of flight along γ satisfies

$$\begin{aligned} |u_\infty - v_\infty| &\leq |u_\infty - u_{\gamma_\eta,\infty}| + |u_{\gamma_\eta,\infty} - v_{\gamma_\eta,\infty}| + |v_{\gamma_\eta,\infty} - v_\infty| \\ &\leq \frac{A}{R^{\alpha-1}} \end{aligned} \tag{4.3.21}$$

for some constant $A > 0$. $\square$

Note that the above argument relied on the fact that defining the time of flight along γ using Minkowski retarded null and advanced time co-ordinates gives a finite result (Lemma 4.3.1). For Schwarzschild in $3 + 1$ dimensions, this time of flight is $\pm\infty$ for $m \gtrless 0$. As a result, although the metric is asymptotically flat, we cannot conclude that this time of flight approaches 0 if γ is restricted to arbitrarily large r.

4.4 Constructing a Fastest Causal Curve

As discussed in Section 4.1, our proof of the positive mass theorem will involve constructing a causal curve from Λ^- to Λ^+ which has negative time of flight. To do this we use a comparison argument based on Minkowski spacetime, similar to the ones used in Chapter 2. This argument relates to the compactified spacetimes.

Lemma 4.4.1. Let (M, g) be a uniformly Schwarzschildean spacetime in $d+1$ dimensions ($d \geq 4$) with ADM mass $m < 0$. Then there exists an endless timelike curve from Λ^- to Λ^+ which has negative time of flight.

Note that a uniformly Schwarzschildean spacetime in higher dimensions necessarily admits quasi-Cartesian co-ordinates. This means that the results of the previous section apply. In particular, we define the time of flight along curves with endpoints on $\mathscr{I}^-$ and $\mathscr{I}^+$ using Definition 2.4.1, with $u = t - r$ and $v = t + r$.

Proof: The metric is uniformly Schwarzschildean, so the line element can be written in some neighbourhood of conformal infinity as

$$ds^2 = ds^2_{Mink} - \frac{\mu}{r^{d-2}}\left(dt^2 + dr^2\right) + o\left(r^{-(d-2)}\right) \tag{4.4.1}$$

where by $o\left(r^{-(d-2)}\right)$ we mean that this term is equal to $g'_{\mu\nu}dx^\mu dx^\nu$ for some $g'_{\mu\nu} = o\left(r^{-(d-2)}\right)$.

Since these co-ordinates are defined on some region diffeomorphic to $\mathbb{R} \times \left(\mathbb{R}^d \setminus B\right)$, we are able to identify curves in this region with curves in Minkowski spacetime (we simply identify the quasi-Cartesian co-ordinates with some Cartesian co-ordinate system in Minkowski). Furthermore, since the spacetime (M, g) can be compactified to $(\overline{M}, \overline{g})$ using the same procedure as Minkowski, we can also identify curves in a neighbourhood of $\mathscr{I}$ in $(\overline{M}, \overline{g})$ with curves in compactified Minkowski (we simply identify the compactified co-ordinates).

It is clear from (4.4.1) that for sufficiently large r the term proportional to μ will dominate the other non-Minkowski terms. This means that if $\mu < 0$ (or equivalently $m < 0$), then there

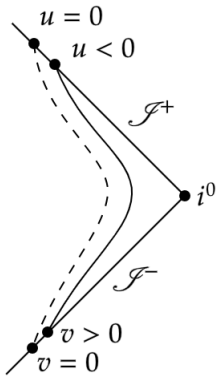

Figure 4.2: The Minkowski null geodesic between Λ^- and Λ^+ with endpoints at $u = 0$ and $v = 0$ respectively is shown as a dotted line. If the metric g is uniformly Schwarzschildean with negative mass and the impact parameter is sufficiently large then this path can be modified so that it still connects Λ^- to Λ^+ but is g-timelike and has strictly negative time of flight. This modification is shown as an unbroken line.

exists some R_0 such that

$$ds^2 > ds^2_{Mink} \tag{4.4.2}$$

along any Minkowski causal curve at $r > R_0$.

Consider a Minkowski null geodesic with past endpoint at $v = 0$ on Λ^-, future endpoint at $u = 0$ on Λ^+ and impact parameter $b > R_0$ (recall that Minkowski null geodesics connect antipodal points on $\mathscr{I}^\pm$). This curve is restricted to the region where $r > R_0$ and hence inequality (4.4.2) guarantees that, after identifying compactified co-ordinates, it defines a g-timelike curve in $(\overline{M}, \overline{g})$.

Now since $I^\pm(p)$ are open sets for any point $p \in \overline{M}$, we must be able to modify this curve slightly so that it remains g–timelike but has past endpoint at $v > 0$ on Λ^- and future endpoint at $u < 0$ on Λ^+ (see Figure 4.2). This ensures that the curve has negative time of flight. □

This curve will be the starting point for our sequence of faster and faster causal curves used in the proof of Theorem 4.1.2 to construct a fastest causal curve from Λ^- to Λ^+. We will

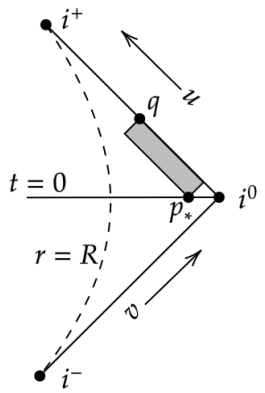

Figure 4.3: The causal diamond $J^+(p_*) \cap J^-(q)$ (taken with respect to the Minkowski metric) is contained in the shaded region bound by curves of constant u or v. These curves are straight lines at 45° in the Penrose diagram. Given some $R > 0$, if we choose the point p_* sufficiently close to i^0 (i.e. to have sufficiently large r co-ordinate), then causal curves from p_* to q cannot enter the region $r \leq R$.

also use the time of flight estimate, Lemma 4.3.3, in this construction. However in order to do so it is necessary to prove the following lemma.

Lemma 4.4.2. Let (M, g) be a $d+1$ dimensional uniformly Schwarzschildean spacetime ($d \geq 4$) and let $R > 0$. Let p_* be a point with $t = 0$ and let $q \in \mathscr{I}^+$. Then there exists a constant R' such that if p_* has r co-ordinate $r_{p_*} > R'$, then any g-null geodesic from p_* to q is confined to the region $r > R$.

Recall that the Minkowski metric in $d+1$ dimensions is

$$ds^2 = dt^2 - dr^2 - r^2 d\omega_{d-1}^2 \tag{4.4.3}$$

It follows that along Minkowski causal curves, we have

$$\begin{gathered} \dot{t}^2 - \dot{r}^2 \geq 0 \\ \implies \dot{v} = 0 \text{ or } \frac{du}{dv} = \frac{\dot{t} - \dot{r}}{\dot{t} + \dot{r}} \geq 0 \end{gathered} \tag{4.4.4}$$

where $\dot{}$ denotes differentiation with respect to an affine parameter s. Using this, Figure 4.3 illustrates how Lemma 4.4.2 is true in Minkowski spacetime.

The need to prove this lemma is the downside of compactifying using retarded and advanced time co-ordinates $u = t - r$ and $v = t - r$. It is possible that g–causal curves from p_* have $\frac{du}{dv} < 0$ and hence escape the shaded region shown in Figure 4.4. The proof below relies on results obtained in the proof of Lemma 4.3.1. These are used to show that g-null geodesics and η-null geodesics emanating from the same point remain close in a neighbourhood of i^0 (see Figure 4.4).

Proof: Let γ be a g–null geodesic from p_* to q and let s be an affine parameter along γ (increasing to the future) such that $\frac{dx^i}{ds}\frac{dx^i}{ds}|_{s=0} = 1$ and $\frac{dr^2}{ds}|_{s=0} \geq 0$. Let s_0 denote the value of s at p_*.

From Figure 4.3 we see that, for fixed R, in order for a curve from p_* to q (with r sufficiently large at p_*) to enter the region $r < R$, it must leave the shaded region and hence have $\frac{du}{dv} < 0$ at some point.

We first consider the case where $\dot{u} < 0 < \dot{v}$ along some portion of γ. It is possible, if γ reaches small values of r, that we may have $\dot{t} \leq 0$ at some point. However since the metric is asymptotically flat, there exists $\delta > 0$ such that $\dot{t} > \delta > 0$ for sufficiently large r. We therefore have $\dot{v} = \dot{t} + \dot{r} > 2\dot{t} > 2\delta$.

It follows that for $r > R_0$ (with R_0 sufficiently large) we have

$$\begin{aligned} 0 > (\dot{t} - \dot{r})(\dot{t} + \dot{r}) &\geq \eta_{\mu\nu}\dot{x}^\mu\dot{x}^\nu \\ &\geq (\eta_{\mu\nu} - g_{\mu\nu})\dot{x}^\mu\dot{x}^\nu \\ &\geq -A'r^{-(d-2)} \\ \implies 0 > \frac{du}{dv} = \frac{\dot{t} - \dot{r}}{\dot{t} + \dot{r}} &> -B'r^{-(d-2)} \end{aligned} \tag{4.4.5}$$

for some constants $A', B' > 0$. We have also used the fact that, by Lemma 4.3.1, $\dot{x}^\mu$ tends to a finite limit along γ and hence $|\dot{x}^\mu|$ remains bounded for each index μ.

Choose c such that the u co-ordinate of q satisfies $u_q < c$ and consider a segment of γ in the

region $\{u < c\} \cap \{r > R_0\} \cap \{t \geq 0\}$. We have

$$\begin{aligned} & 0 \leq t < r + c \\ \implies & 0 \leq v < 2r + c. \end{aligned} \tag{4.4.6}$$

From this we have

$$\begin{aligned} \left| \frac{1+v^2}{1+u^2} \frac{du}{dv} \right| &\leq \left(1 + (2r+c)^2\right) \frac{B'}{r^{d-2}} \\ &\longrightarrow 0 \text{ as } r \longrightarrow \infty \end{aligned} \tag{4.4.7}$$

Let $\epsilon > 0$. From the above, we see that if R_0 is sufficiently large, we have

$$1 - \epsilon \leq \frac{dT}{d\chi} = \frac{1 + \frac{1+v^2}{1+u^2}\frac{du}{dv}}{1 - \frac{1+v^2}{1+u^2}\frac{du}{dv}} \leq 1 \tag{4.4.8}$$

in the region $\{u < c\} \cap \{r > R_0\} \cap \{t \geq 0\}$, where T and χ are defined in (2.2.5).

Now consider the case where $\dot{v} < 0 < \dot{u}$ along a portion of γ. We have $\dot{u} = \dot{t} - \dot{r} > 2\dot{t} > 2\delta$ for r sufficiently large. Analogously to (4.4.5), it follows that for $r > R_0$ (with R_0 sufficiently large) we have

$$0 > \frac{du}{dv} = \frac{\dot{t} - \dot{r}}{\dot{t} + \dot{r}} > -B'' r^{-(d-2)} \tag{4.4.9}$$

for some constant $B'' > 0$.

We also have

$$\begin{aligned} \left| \frac{1+u^2}{1+v^2} \frac{dv}{du} \right| &\leq \frac{B''}{r^{d-2}} \\ &\longrightarrow 0 \text{ as } r \longrightarrow \infty. \end{aligned} \tag{4.4.10}$$

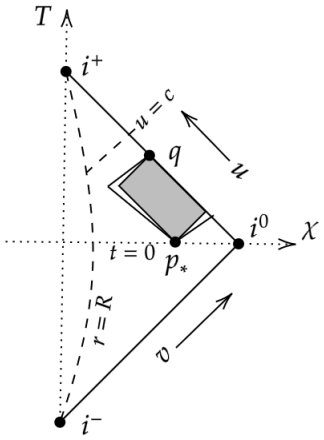

Figure 4.4: The shaded region shows $J^+(p_*) \cap J^-(q)$ calculated with respect to the Minkowski metric. This region is bound by curves with $\left|\frac{dT}{d\chi}\right| = 1$. For any c and any $\epsilon > 0$, g-causal curves in $\{u < c\} \cap \{r > R_0\} \cap \{t \geq 0\}$, with R_0 sufficiently large, have $\left|\frac{dT}{d\chi}\right| \geq 1 - \epsilon$.

Hence for any $\epsilon > 0$, if R_0 is sufficiently large we have

$$-1 \leq \frac{dT}{d\chi} = \frac{\frac{1+u^2}{1+v^2}\frac{dv}{du} + 1}{\frac{1+u^2}{1+v^2}\frac{dv}{du} - 1} \leq -1 + \epsilon \tag{4.4.11}$$

in the region $\{u < c\} \cap \{r > R_0\} \cap \{t \geq 0\}$.

Putting these results together, we find that for any c and any $\epsilon > 0$, there exists some $R_0 > 0$ such that causal curves in the region $\{u < c\} \cap \{r > R_0\} \cap \{t \geq 0\}$ have

$$\left|\frac{dT}{d\chi}\right| \geq 1 - \epsilon. \tag{4.4.12}$$

From this we conclude that g-causal curves in this region are confined to a wedge in the Penrose diagram bound by straight lines with gradients which, by choosing R_0 sufficiently large, can be chosen arbitrarily close to ± 1. It follows that for any $R > 0$, there exists some R' such that if p_* has r co-ordinate $r_{p_*} > R'$ then any g-causal curve from p_* to q does not enter the region $r \leq R$. This is illustrated in Figure 4.4. $\square$

Theorem 4.1.2 Let (M, g) be a uniformly Schwarzschildean spacetime in $d + 1$ dimensions ($d \geq 4$) with ADM mass $m < 0$ and suppose $\mathcal{D} \cup \mathscr{I}$ is a globally hyperbolic subset of $\overline{M}$.

Then (M, g) contains a null line.

Proof: Using Lemma 4.4.1, we construct a causal curve from Λ^- to Λ^+ which has negative time of flight. Denote this curve by γ_0 and label its past and future endpoints p_0 and q_0 respectively.

Following [61], we introduce a partial ordering $\leq$ on $((J^+(p_0) \cap \Lambda^-) \cup i^0) \times ((J^-(q_0) \cap \Lambda^+) \cup i^0)$. We say that $(p', q') \leq (p'', q'')$ if $p' \in J^+(p'')$ and $q' \in J^-(q'')$. Define the set F to contain all pairs of points in $(J^+(p_0) \cap \Lambda^-) \times (J^-(q_0) \cap \Lambda^+)$ which can be connected by a causal curve through $\mathcal{D}$ and choose (p, q) to be any element of the closure of this set which is minimal with respect to the partial ordering $\leq$ (so a priori one or both of these points could lie at i^0).

We can then define sequences of points $\{p_i\}_{i=0}^{\infty}$ along Λ^- and $\{q_i\}_{i=0}^{\infty}$ along Λ^+ such that

- $(p_i, q_i) \leq (p_j, q_j)$ for $i > j$
- p_i and q_i are connected by a causal curve γ_i
- $p_i \longrightarrow p$ and $q_i \longrightarrow q$ as $i \longrightarrow \infty$

The first condition here ensures that the time of flight along γ_i is less than or equal to the time of flight along γ_j for $j < i$.

We first check that the sequence of curves $\{\gamma_i\}_{i=0}^{\infty}$ does not escape to infinity. By this we mean that there exists some $R > 0$ such that, possibly restricting to a subsequence, every curve γ_i enters the region $\{r < R\}$.

The curve γ_i can be replaced by a (possibly faster) curve γ_i' from Λ^- to Λ^+ which is the union of two null geodesics joined at $p_{*,i}$, the point at which γ_i intersects the hypersurface $t = 0$.

Let R_i denote the r co-ordinate at $p_{*,i}$. Suppose that $R_i \longrightarrow \infty$ as $i \longrightarrow \infty$. Then for any $R > 0$, by Lemma 4.4.2 (and restricting to a subsequence if necessary) the sequence of curves $\{\gamma_i\}_{i=0}^{\infty}$ is eventually contained in the region $r > R$.

Then Lemma 4.3.3 implies that the time of flight along γ_i' satisfies

$$|u_{\gamma_i',\infty} - v_{\gamma_i',\infty}| \leq \frac{A}{R^{d-3}} \tag{4.4.13}$$

for some constant A, where we note that a uniformly Schwarzschildean spacetime admits quasi-Cartesian co-ordinates with $\alpha = d - 2$.

From this we see that, for R sufficiently large, the time of flight along the γ_i' (and hence also the time of flight along γ_i) will eventually become strictly greater than the time of flight along γ_0 (which was chosen to be strictly negative). But this contradicts the definition of the sequence $(\gamma_i)_{i=0}^{\infty}$ as consisting of faster and faster causal curves. We therefore conclude that, restricting to a subsequence if necessary, each of the causal curves γ_i enters the set $\mathcal{K} := (J^+(p_0) \cap J^-(q_0)) \setminus \mathcal{U}_R$, where $\mathcal{U}_R := \{x \in J^+(p_0) \cap J^-(q_0) : r(x) > R\}$.

But $\mathcal{U}_R$ is an open set in $J^+(p_0) \cap J^-(q_0)$ and, since $\mathcal{D}$ is globally hyperbolic, $J^+(p_0) \cap J^-(q_0)$ is compact. It follows that $\mathcal{K}$ is a compact set. Hence, defining γ to be the limit of the sequence $\{\gamma_i\}_{i=0}^{\infty}$ in the Vietoris topology (Appendix A), we see that γ must also enter $\mathcal{K}$. In particular this means that γ enters the interior of the spacetime. Furthermore, since each of the γ_i are causal, so too is the limit curve γ.

So γ is a fastest causal curve from Λ^- to Λ^+ which enters the interior of the spacetime. Such a curve necessarily lies on the boundary of the future null cone from p and hence must be a null geodesic ([70] Corollary after Theorem 8.1.2) without conjugate points ([44] Proposition 4.5.12). We conclude that γ is a null line. □

4.5 A Focusing Theorem in Higher Dimensions

Theorem 4.1.2 shows that certain higher dimensional, negative mass spacetimes contain a null line. This means that such spacetimes would be ruled out if we also impose conditions which forbid the existence of a null line.

We will require conditions which ensure that endless null geodesics encounter sufficient regions of positive focusing to guarantee that conjugate points will occur. This focusing of geodesics is consistent with the sort of behaviour we would expect to be caused by regions of positive mass (assuming the Einstein equations hold). In this sense, Corollary 4.5.2 below agrees with our prior understanding of positivity of mass.

In [61], the conditions imposed are those stated in Borde's Focusing Theorem [11] (where we require these to hold for every complete causal geodesic). This theorem requires the quantity $R_{ab}T^aT^b$ to be finite and continuous, where T^a is tangent to the null geodesic under consideration. To guarantee this, it is sufficient to assume that the metric is C^2.

Theorem 4.5.1. (**Borde [11, Focusing Theorem 2]**) Let g be a C^2 metric and let γ be a complete, affinely parameterised, causal geodesic with tangent T^a such that $T_{[a}R_{b]cd[e}T_{f]}T^cT^d \neq 0$ at some point on γ. Suppose that for any $\epsilon > 0$ and any $t_1 < t_2$, there exist $\delta > 0$ and intervals I_1 and I_2 of length $\geq \delta$ with endpoints $< t_1$ and $> t_2$ respectively such that

$$\int_{t'}^{t''} R_{ab}T^aT^b dt \geq -\epsilon \qquad \forall t' \in I_1, \quad \forall t'' \in I_2 \tag{4.5.1}$$

Then γ contains a pair of conjugate points.

Theorem 4.5.1 was originally stated in $3+1$ dimensions, although the proof does not rely on this and hence the theorem also holds in higher dimensions. For this reason, we may use the conditions of this theorem in our higher dimensional generalisation of the positive mass theorem. As is pointed out in [61], if the Einstein equations are assumed to hold then the conditions of Borde's theorem can equivalently be expressed in terms of the energy-momentum tensor.

Note that the conditions of Borde's theorem are entirely global. Other conditions often used in such focusing theorems relate to local positivity of energy (assuming the Einstein equations hold). These conditions can be violated in a quantum theory, so our approach has the advantage that it may be possible to extend it to the semi-classical regime.

It may be the case that we could impose weaker conditions than those used in Borde's theorem

and still rule out the existence of null lines. For example, Theorem 4.1.2 only required the metric to be $C^{1,1}$, so a focusing result for metrics which fail to be C^2 would provide a more general result. This is mentioned at the end of Section II.2 in [61] and also in [57]. The important thing is that we impose sufficiently strong conditions to ensure that null lines cannot exist. The condition that $T_{[a}R_{b]cd[e}T_{f]}T^cT^d \neq 0$ at some point on every null geodesic is called the *null generic condition* and is satisfied in all but a very special class of spacetimes (in fact, Theorem 4.5.1 only requires this condition to hold on complete null geodesics). In [45] it is argued that it is therefore physically unrealistic to consider spacetimes for which the null generic condition fails. Furthermore, as discussed in [61], even if this condition were to fail in our spacetime, we would expect it to be satisfied by some other spacetime which is "nearby" in a suitable sense and whose 4-momentum differs by an arbitrarily small amount. As a result, assuming the null generic condition to hold does not appear to weaken the positivity of mass result obtained here.

Using Theorems 4.1.2 and 4.5.1, we derive the following corollary, which is our version of the positive mass theorem in higher dimensions.

Corollary 4.5.2. Let (M, g) be a uniformly Schwarzschildean spacetime in $d+1$ dimensions ($d \geq 4$) which satisfies the conditions of Borde's theorem for every complete null geodesic and is such that $\mathcal{D} \cup \mathscr{I}$ is globally hyperbolic as a subset of $\overline{M}$. Then $m \geq 0$.

4.6 Summary

We have proved a version of the positive mass theorem for higher dimensional uniformly Schwarzschildean spacetimes. As mentioned in Section 4.1, the assumptions made about our spacetime are weaker than those of [23]. In particular, we only require the metric to be uniformly Schwarzschildean, whereas in [23] the more restrictive requirement that the metric be *strongly uniformly Schwarzschildean* is made. We also drop the assumption of weak asymptotic regularity. However, as in [23] we fail to prove anything regarding the $m = 0$ case (a similar problem is encountered in [61] in 3+1 dimensions). This is because the method

used in Section 4.4 to construct the initial timelike curve, γ_0, with strictly negative time of flight is no longer guaranteed to work. Its success will be determined by the higher order terms in the metric.

The assumptions made here are also fundamentally different to those used in the proofs by Witten [72] and Schoen and Yau [64–66] (extended to all dimensions up to seven by Eichmair, Huang, Lee and Schoen [33]). The proof given here relies on properties of the spacetime in a neighbourhood of conformal infinity, whereas these other methods impose conditions only on some initial data surface. The "global" proof presented in this Chapter is interesting because it relies more clearly on properties we expect to hold in positive mass spacetimes. In particular, we show that null geodesic focusing is compatible only with spacetimes of non-negative mass. Consequently this proof also acts as evidence that it is consistent to think of the ADM mass defined in higher dimensions as describing the total mass contained in the spacetime. Furthermore, as mentioned above and in [61], by relying solely on global focusing results such as Theorem 4.5.1, this proof avoids imposing non-negativity of energy locally. This leads to the possibility that the methods described here can be generalised to the semi-classical setting, where such local conditions can be violated by quantum matter.

Chapter5

Asymptotic Flatness in Higher Dimensions

In Chapter 2 we noted that the Penrose property in asymptotically flat spacetimes is a property of neighbourhoods of i^0. In this Chapter we will discuss in detail the structure of conformally compactified spacetimes at this point. In particular, we will show that $(d+1)$-dimensional Myers-Perry metrics ($d \geq 4$) admit a conformal completion which includes a point, i^0, at spatial infinity from which $\mathscr{I}^{\pm}$ form the null cone, with a metric which is of $C^{d-3,1}$ differentiability class near this point. Thus, all derivatives of order less than $d-3$ extend continuously to i^0 and $\mathscr{I}$, while the derivatives of the metric of order $d-3$ remain bounded as i^0 is approached, but do not necessarily extend to functions which are continuous at i^0.

We conclude that the conformal structure at spacelike and null infinity is quite similar to that of Minkowski spacetime, except for a loss of differentiability at i^0 which becomes less severe in higher dimensions. We also show that the result is optimal in *even* spacetime dimensions in the following sense: no C^{d-2} completions exist unless the ADM mass vanishes.

Recall that the Riemannian metric obtained from quotienting the spacetime metric of asymptotically flat, stationary, odd-dimensional, electrovacuum metrics by the stationary isometries admits a conformal completion at a point at infinity which is real-analytic [7].

However, this result does not translate in any obvious way to the associated spacetime metric and we do not know whether or not this result is optimal in such dimensions either.

Our observation concerning the differentiability of the conformally rescaled metric has immediate consequences concerning causality near i^0. Recall that the usual results of causality theory, except perhaps the ones explicitly involving geodesics, apply for metrics which are Lipschitz continuous [28, 52], and hence in dimensions $d \geq 4$ for metrics with the Myers-Perry asymptotics by our results here. Some care has to be taken in the borderline case of $d = 4$, since not all statements involving geodesics remain true for $C^{1,1}$ metrics. However, when $d > 4$ the full standard causality theory, including arguments involving geodesics, applies.

The case $d = 3$ requires special attention, since the conformal metric constructed here or in [5, 22] is only Hölder continuous at i^0. Recall that a function f is Hölder continuous if there exist constants $C \geq 0$, $\beta > 0$ such that $|f(x) - f(y)| \leq C|x - y|^\beta$ for all x and y in the domain of f. If f and all its partial derivatives up to and including order k are Hölder continuous with exponent β, then we write $f \in C^{k,\beta}$. It is not obvious whether or our construction can be improved to yield a conformally rescaled metric which is Lipschitz-continuous at i^0. However, the conformal metric is smooth everywhere except at i^0. It is then easily seen that the causal bubbles of [28] do not occur. So, as emphasised in this reference, standard causality theory, except possibly some arguments involving geodesics, also applies in this case.

5.1 Three dimensional spacetimes

As described in Section 2.3.1, three-dimensional spacetimes are special. The requirement that the spacetime be empty at large spacelike distances imposes flatness. If one assumes the existence of a well-behaved spacelike hypersurface, the spatial geometry at large distances is that of a flat cone with a deficit angle. This deficit angle can *a priori* have either sign, but positivity of matter energy implies positivity of this angle. Then the spacetime metric is flat

in the Minkowskian domain of dependence of the angular sector

$$\{z \in \mathbb{C},\ |z| \geq R, \arg z \in [0, \alpha]\} \subset \{t = 0\}\,, \tag{5.1.1}$$

where $R > 0$, $\alpha \in (0, 2\pi)$ (except if there is no matter) and the boundary $\arg z = 0$ should be identified with the boundary $\arg z = \alpha$. The Lorentzian Kelvin transformation (see (5.2.3)) with $r^* = |z|$ leads, after addition of a point $i^0 = \{t = 1/|z| = 0\}$, to a conformal completion where the conformally rescaled metric has a deficit angle of $2\pi - \alpha$ at i^0 on the spacelike hyperplane $\{\tau = 0\}$, and the null conformal boundary at infinity, $\mathscr{I}$, is the light-cone emanating from i^0 with the same deficit angle.

5.2 The Schwarzschild metric

We begin by compactifying the Schwarzschild metric in $d+1$ dimensions. This was done in Section 2.3.2, however in this section we will use a slightly different procedure. In particular we will use compactified co-ordinates which have their origin at i^0. This will make it easier to analyse the differentiability properties of the metric at this point.

We rewrite the $(d+1)$-dimensional Schwarzschild metric (2.3.19) as

$$\begin{aligned} ds^2 &= -\left(1 - \frac{\mu}{r^{d-2}}\right) dt^2 + \frac{dr^2}{1 - \frac{\mu}{r^{d-2}}} + r^2 d\omega_{d-1}^2 \qquad (5.2.1)\\ &= \left(1 - \frac{\mu}{r^{d-2}}\right)\big(- dt^2 + dr_*^2 + r_*^2 d\omega_{d-1}^2 \\ &\qquad + \left(\frac{r^2}{1 - \frac{\mu}{r^{d-2}}} - r_*^2\right) d\omega_{d-1}^2\big)\,. \qquad (5.2.2) \end{aligned}$$

where r_* is related to r by (4.3.4).

If we ignore the final correction term above, then up to a conformal factor this is the Minkowski metric with radial coordinate r_*. Now, the Minkowski part of the metric can be conformally

completed by adding a point, i^0, at spatial infinity as follows. Let

$$\tau = \frac{t}{r_*^2 - t^2}\,, \qquad \rho = \frac{r_*}{r_*^2 - t^2}\,, \tag{5.2.3}$$

where these co-ordinates are defined on the region $\{-r_* < t < r_*\}$, so we have $-\rho < \tau < \rho$. The point i^0 corresponds to $\tau = \rho = 0$. We have

$$-dt^2 + dr_*^2 + r_*^2 d\omega_{d-1}^2 = \frac{1}{\left(\rho^2 - \tau^2\right)^2}\left(-d\tau^2 + d\rho^2 + \rho^2 d\omega_{d-1}^2\right)\,, \tag{5.2.4}$$

which allows us to rewrite (5.2.2) as

$$\begin{aligned} g \equiv \Omega^{-2}\overline{g} \;\; = \;\; & \underbrace{\frac{1 - \frac{\mu}{r^{d-2}}}{\left(\rho^2 - \tau^2\right)^2}}_{=:\Omega^{-2}} \Big(- d\tau^2 + d\rho^2 + \rho^2 d\omega_{d-1}^2 \\ & \underbrace{\qquad + \underbrace{\left(\rho^2 - \tau^2\right)^2 \left(\frac{r^2}{1 - \frac{\mu}{r^{d-2}}} - r_*^2 \right)}_{=:\psi} d\omega_{d-1}^2 \Big)}_{=:\delta\overline{g}}\,. \end{aligned} \tag{5.2.5}$$

The question arises of the regularity at i^0 of the conformal factor Ω, of the function ψ and of the correction term $\delta\overline{g}$. To determine this we invert (5.2.3):

$$t = \frac{\tau}{\rho^2 - \tau^2}\,, \qquad r_* = \frac{\rho}{\rho^2 - \tau^2}\,. \tag{5.2.6}$$

We consider first the somewhat simpler case of $d \geq 4$, since in this case r asymptotes to r_* and there are no logarithmic terms. We find that there exist smooth functions $f\,,\, f_*\,,\, h\,,\, h_* : \mathbb{R} \to \mathbb{R}$, with $f\,(0) = f_*\,(0) = h\,(0) = h_*\,(0) = 0$, such that for large r, and

assuming that all coordinates as well as the mass parameter are unitless, we have

$$\begin{aligned}
r_* &= r\left(1-\frac{\mu}{(d-3)\,r^{d-2}}\left(1+f\left(r^{2-d}\right)\right)\right),\\
r &= r_*\left(1+\frac{\mu}{(d-3)\,r_*^{d-2}}\left(1+f_*\left(r_*^{2-d}\right)\right)\right),\\
\frac{r^2}{1-\frac{\mu}{r^{d-2}}}-r_*^2 &= \frac{(d-1)\,\mu}{(d-3)\,r^{d-4}}\left(1+h\left(r^{2-d}\right)\right)\\
&= \frac{(d-1)\,\mu}{(d-3)\,r_*^{d-4}}\left(1+h_*\left(r_*^{2-d}\right)\right)\\
&= \frac{(d-1)\,\mu}{(d-3)}\left(\rho\left(1-\frac{\tau^2}{\rho^2}\right)\right)^{d-4}\left(1+h_*\left(\left(\frac{\rho}{\rho^2-\tau^2}\right)^{2-d}\right)\right),\\
\rho^{-2}\psi &= \frac{(d-1)\,\mu}{(d-3)}\rho^{d-2}\left(1-\frac{\tau^2}{\rho^2}\right)^{d-2}\times\\
&\quad \left(1+h_*\left(\rho^{d-2}\left(1-\frac{\tau^2}{\rho^2}\right)^{d-2}\right)\right),\\
\delta\overline{g}\equiv\psi d\omega_{d-1}^2 &= \psi\rho^{-2}\left(\left(dx^1\right)^2+\ldots+\left(dx^n\right)^2-d\rho^2\right)\\
&= \psi\rho^{-2}\left(\left(dx^1\right)^2+\ldots+\left(dx^n\right)^2-\rho^{-2}\left(x^1dx^1+\ldots+x^ndx^n\right)^2\right),
\end{aligned}\tag{5.2.7}$$

where (x,y,z) are the usual Cartesian coordinates on $\mathbb{R}^3$, with $\rho^2=x^2+y^2+z^2$.

Now, in the coordinates above, the original Schwarzschild metric is defined only in the region $-\rho<\tau<\rho$. Hence it is convenient to extend the function τ^2/ρ^2 beyond $\tau=\pm\rho$ by any smooth function which is constant for, say, $|\tau|\geq 2\rho$. Then both $\delta\overline{g}$ and $\overline{g}$, so extended, are continuous in a neighbourhood of $\{\rho=0\}$ for all $d\geq 4$.

Next, the function $\lambda:=\psi\rho^{-2}$ appearing in (5.2.7) has the property that for all multi-indices $\alpha\in\mathbb{N}^{d+1}$ we have, for small ρ,

$$\rho^{\alpha_0+\ldots+\alpha_d}\partial_0^{\alpha_0}\cdots\partial_d^{\alpha_d}\lambda=O\left(\rho^{d-2}\right). \tag{5.2.8}$$

A similar property holds for the functions $\lambda x^ix^j/\rho^2$:

$$\rho^{\alpha_0+\ldots+\alpha_d}\partial_0^{\alpha_0}\cdots\partial_d^{\alpha_d}\left(\lambda\frac{x^ix^j}{\rho^2}\right)=O\left(\rho^{d-2}\right). \tag{5.2.9}$$

It follows that $\lambda \in C^{d-3,1}$ for $d \geq 4$, which shows that $\overline{g}$ is of differentiability class $C^{d-3,1}$ near i^0.

We note that if the spatial dimension is even, both the conformal factor Ω and the metric induced on the slices $\tau = 0$, as constructed above, are smooth, even analytic. This is a special case of [7], where analyticity at i^0 is established on static slices for all metrics which are static and vacuum (or indeed electrovacuum) at large distances in even spatial dimension $d \geq 6$. Analyticity is also established there in dimension four if one assumes in addition the non-vanishing of the ADM mass.

For completeness we apply the method above to the $d = 3$ case. This was previously analysed in [5, Appendix C] from a somewhat different perspective, with two completions better behaved than the one here, constructed in [22].

$$
\begin{aligned}
r_* &= r + \mu \ln\left(\frac{r}{\mu} - 1\right) , \\
r &= r_* - \mu \ln\left(\frac{r_*}{\mu}\right) + \frac{\mu^2\left(\ln\left(\frac{r_*}{\mu}\right) + 1\right)}{r_*} + O\left(\frac{\ln^2 r_*}{r_*^2}\right) , \\
\frac{r^2}{1 - \frac{\mu}{r}} - r_*^2 &= -2\mu r_* \ln\left(\frac{r_*}{\mu}\right) + \mu r_* + O\left(\ln^2\left(\frac{r_*}{\mu}\right)\right) \\
&= -\frac{2\mu\rho}{\rho^2 - \tau^2} \ln\left(\frac{\rho}{\rho^2 - \tau^2}\right) + \mu \frac{\rho}{\rho^2 - \tau^2} + O\left(\ln^2\left(\frac{\rho}{\rho^2 - \tau^2}\right)\right) , \\
\psi &= -2\mu\rho\left(\rho^2 - \tau^2\right) \ln\left(\frac{\rho}{\rho^2 - \tau^2}\right) + \mu\rho\left(\rho^2 - \tau^2\right) , \\
&\quad + O\left(\left(\rho^2 - \tau^2\right)^2 \ln^2\left(\frac{\rho}{\rho^2 - \tau^2}\right)\right) \\
\rho^{-2}\psi &= 2\mu\rho\left(1 - \frac{\tau^2}{\rho^2}\right)\left(\ln\left(1 - \frac{\tau^2}{\rho^2}\right) + \ln(\rho) - \mu\rho\right) \\
&\quad + O\left(\rho^2\left(1 - \frac{\tau^2}{\rho^2}\right)^2 \ln^2\left(\frac{\rho}{\rho^2 - \tau^2}\right)\right) , \qquad (5.2.10) \\
\delta\overline{g} \equiv \psi d\omega_2^2 &= \psi\rho^{-2}\left(dx^2 + dy^2 + dz^2 - d\rho^2\right) . \qquad (5.2.11)
\end{aligned}
$$

Note that for any $\beta \in (0,1)$ the function $\left(1 - \frac{\tau^2}{\rho^2}\right) \ln\left(1 - \frac{\tau^2}{\rho^2}\right)$ extends in $C^{0,\beta}$ across the light-cone $\tau = \pm\rho$, but is not Lipschitz. Similarly $\rho \ln \rho$ is $C^{0,\beta}$ but not $C^{0,1}$. It follows that, in the coordinates above, $\overline{g}$ can be extended across $\tau = \pm\rho$ to a metric satisfying $\overline{g} \in C^{0,\beta}$

for any $\beta \in (0,1)$, but $\overline{g} \notin C^{0,1}$. The constructions in [22, Section III] in spatial dimension $d = 3$ provide a completion of the Schwarzschild metric at i^0 *either* without the $\rho \log \rho$ terms *or* without the $\left(1 - \frac{\tau^2}{\rho^2}\right) \log \left(1 - \frac{\tau^2}{\rho^2}\right)$ terms. It is not known whether such terms can be removed altogether to obtain a $C^{0,1}$ metric.

An analysis similar to the above shows that the conformal factor in (5.2.5), namely

$$\Omega = \frac{\rho^2 - \tau^2}{\sqrt{1 - \frac{\mu}{r}}}\,, \tag{5.2.12}$$

consists of a smooth function $\rho^2 - \tau^2$ multiplied by a function which is $C^{1,\beta}$ across the light-cone for all $\beta \in [0,1)$, but is not $C^{1,1}$ there.

We can remove this problematic function by absorbing a factor of $1 - \frac{\mu}{r}$ into $\overline{g}$. This does not change the differentiability properties of $\overline{g}$, and the resulting conformal factor, $\rho^2 - \tau^2$, is a smooth function on the conformally completed manifold.

5.3 Myers-Perry metrics

In Kerr-Schild coordinates the Myers-Perry metrics [54] take the form

$$g_{\mu\nu} = \eta_{\mu\nu} + h k_\mu k_\nu\,, \tag{5.3.1}$$

where h is a function to be defined later and k_μ is a null co-vector for the $(d+1)$-dimensional Minkowski metric η, and hence also for the full metric:

$$g^{\mu\nu} = \eta^{\mu\nu} - h k^\mu k^\nu\,, \quad \eta^{\mu\nu} k_\mu k_\nu = g^{\mu\nu} k_\mu k_\nu = 0\,, \quad k^\nu = \eta^{\mu\nu} k_\mu = g^{\mu\nu} k_\mu \tag{5.3.2}$$

In the calculations to follow we assume $d \geq 3$, and note that $d = 3$ is the Kerr metric in Kerr-Schild coordiantes.

In order to handle even and odd dimensions simultaneously, we introduce a parameter

$$\epsilon = \begin{cases} 0, & d = 2n \text{ is even;} \\ 1, & d = 2n+1 \text{ is odd,} \end{cases} \tag{5.3.3}$$

and write

$$\begin{aligned} (x^\mu) &\equiv (x^0, x^i) = (t, x_1, y_1, \ldots, x_n, y_n, \epsilon z) \\ &= (t, r_1\cos(\varphi_1), r_1\sin(\varphi_1), \ldots, r_n\cos(\varphi_n), r_n\sin(\varphi_n), r_{n+1}) \ , \end{aligned} \tag{5.3.4}$$

with the Minkowski metric taking the form

$$\eta = -dt^2 + \sum_{i=1}^{n}(dx_i^2 + dy_i^2) + \epsilon dz^2 = -dt^2 + \sum_{i=1}^{n}(dr_i^2 + r_i^2 d\varphi_i^2) + dr_{n+1}^2 \, . \tag{5.3.5}$$

Note that with the definitions above, $r_{n+1} \equiv 0$ in even space dimensions $d = 2n$, so $dr_{n+1} \equiv 0$.

In these coordinates, the co-vector field k is

$$\begin{aligned} k_\alpha dx^\alpha &= dt + \sum_{i=1}^{n} \frac{\hat{r}(x_i dx_i + y_i dy_i) + a_i(x_i dy_i - y_i dx_i)}{\hat{r}^2 + a_i^2} + \epsilon \frac{z dz}{\hat{r}} \\ &= dt + \sum_{i=1}^{n+1} \frac{\hat{r} r_i dr_i + a_i r_i^2 d\varphi_i}{\hat{r}^2 + a_i^2} \end{aligned} \tag{5.3.6}$$

where $a_i \in \mathbb{R}$ are constants with $a_{n+1} = 0$ and we have defined the function $\hat{r}$ implicitly by the condition that k is null:

$$\sum_{i=1}^{n} \frac{x_i^2 + y_i^2}{\hat{r}^2 + a_i^2} + \epsilon \frac{z^2}{\hat{r}^2} = 1 \quad \Longleftrightarrow \quad \sum_{i=1}^{n+1} \frac{r_i^2}{\hat{r}^2 + a_i^2} = 1 \, . \tag{5.3.7}$$

The function h in (5.3.2) is defined to be

$$h = \frac{\mu \hat{r}^{2-\epsilon}}{\Pi F} \tag{5.3.8}$$

where

$$F = 1 - \sum_{i=1}^{n} \frac{a_i^2(x_i^2 + y_i^2)}{(\hat{r}^2 + a_i^2)^2}\,, \tag{5.3.9}$$

$$\Pi = \prod_{i=1}^{n} (\hat{r}^2 + a_i^2)\,. \tag{5.3.10}$$

Letting

$$r^2 := \sum_{i=1}^{n+1} r_i^2 \equiv \sum_{i=1}^{n} (x_i^2 + y_i^2) + \epsilon z^2\,, \tag{5.3.11}$$

one finds the following asymptotic expansions for large r

$$\hat{r}^2 = r^2 - \sum_{i=1}^{n} \frac{a_i^2 r_i^2}{r^2} + O(r^{-2}) = r^2 \left(1 + O(r^{-2})\right)\,, \tag{5.3.12}$$

$$F = 1 + O(r^{-2})\,, \tag{5.3.13}$$

$$\Pi = r^{d-\epsilon} \left(1 + O(r^{-2})\right)\,, \tag{5.3.14}$$

$$h = \frac{\mu}{r^{d-2}} \left(1 + O(r^{-2})\right) \tag{5.3.15}$$

$$\begin{aligned} g = \eta + \frac{\mu}{r^{d-2}} \Big(& dt^2 + 2dt \sum_{i=1}^{n+1} \frac{r r_i dr_i + a_i r_i^2 d\varphi_i}{r^2} \\ & + \sum_{i,j=1}^{n+1} \frac{(r r_i dr_i + a_i r_i^2 d\varphi_i)\left(r r_j dr_j + a_j r_j^2 d\varphi_j\right)}{r^4} \\ & + g'_{\mu\nu} dx^\mu dx^\nu \Big)\,. \end{aligned} \tag{5.3.16}$$

where $g'_{\mu\nu} = O(r^{-2})$ for all indices $\mu, \nu \in \{0, 1, ..., d\}$

We see from the final equation above that the metric is asymptotically flat at spatial infinity [70], with well defined energy, but the mixed time-space metric functions decay slower by one power of r than is usually expected. This can be remedied by a fine-tuning of the coordinates, although this will not be necessary for our purposes.

We can carry out a variant of the calculations of Section 5.2 as follows. We write the metric

as in (5.3.2) and perform a Kelvin transformation as in (5.2.3), with r_* replaced by r,

$$t = \frac{\tau}{\rho^2 - \tau^2}\,, \qquad r = \frac{\rho}{\rho^2 - \tau^2}\,, \tag{5.3.17}$$

to obtain:

$$\begin{aligned} g &= \eta + h\, k \otimes k \\ &= \underbrace{\frac{1}{(\rho^2-\tau^2)^2}}_{=:\Omega^{-2}} \left(\underbrace{-d\tau^2 + d\rho^2 + \rho^2 d\Omega^2_{d-1}}_{\eta} + (\rho^2-\tau^2)^2 h\, k \otimes k \right) . \end{aligned} \tag{5.3.18}$$

To understand the properties of $\Omega^2 g$ at $i^0 := \{\rho = \tau = 0\}$ we need to analyse the function h and the covector field

$$\tilde{k} := (\rho^2 - \tau^2) k\,. \tag{5.3.19}$$

For this we return to (5.3.7) which, after setting

$$r_i := r\, m_i \,(i = 1, ..., n+1)\,, \qquad x := 1/r\,, \qquad \hat{x} := 1/\hat{r} \tag{5.3.20}$$

(thus $\sum_{i=1}^{n+1} m_i^2 = 1$), can be rewritten as

$$\underbrace{\hat{x} \sqrt{\sum_{i=1}^{n+1} \frac{m_i^2}{1 + a_i^2 \hat{x}^2}}}_{=:f_1(\hat{x}^2, m_i)} = x\,. \tag{5.3.21}$$

The function $0 < f_1 \leq 1$ is real analytic, with $f_1(0, m_i) = 1$, and one can easily check that $\hat{x} \mapsto \hat{x} f_1(\hat{x}^2, m_i)$ is strictly increasing. Hence for any given collection $(m_i)_{i=1}^{n+1}$, by the (analytic) inverse function theorem for real-valued functions defined on subsets of $\mathbb{R}$, there exists a real-analytic function $s \mapsto f_2(s, m_i) > 0$ solving (5.3.21):

$$\hat{x} = x f_2(x^2, m_i)\,, \text{ with } f_2(0, m_i) = 1\,. \tag{5.3.22}$$

In terms of the coordinates (τ, ρ), this reads

$$\hat{r} = \frac{1}{\rho\left(1-\frac{\tau^2}{\rho^2}\right) f_2\left(\rho^2(1-\frac{\tau^2}{\rho^2})^2, m_i\right)} =: \frac{f_3(\tau^2, \rho^2, m_i)}{\rho\left(1-\frac{\tau^2}{\rho^2}\right)}\,, \text{ with } f_3(0,0,m_i) = 1\,. \tag{5.3.23}$$

As in the Schwarzchild case we are only interested in the region $|\tau/\rho| \leq 1$. It is therefore convenient to extend the function $1 - \tau^2/\rho^2$ beyond this region to a smooth function which is constant for $|\tau/\rho| \geq 2$. The function f_3 is then a smooth function of its arguments on the set

$$\mathcal{O} := \{\tau^2 + \rho^2 < \delta\} \times \{(m_i) \in S^{d+\epsilon-1}\}\,, \tag{5.3.24}$$

for some $\delta > 0$. It also follows that the functions r^{-2}, $\hat{r}^{-2}$, $r/\hat{r}$ and $\hat{r}/r$ are smooth on $\mathcal{O}$, with $r/\hat{r}|_{i^0} = 1$.

One now checks that there exist functions $f_.$, all smooth on $\mathcal{O}$, such that:

$$
\begin{aligned}
F &= 1-\sum_{i=1}^{n}\frac{a_i^2 r^2 m_i^2}{(\hat{r}^2+a_i^2)^2} = 1-\rho^2 f_4\,, && (5.3.25)\\
\Pi^{-1} &= \prod_{i=1}^{n}(\hat{r}^2+a_i^2)^{-1} = \rho^{d-\epsilon}\left(1-\frac{\tau^2}{\rho^2}\right)^n\left(1+\rho^2 f_5)\right)\,, && (5.3.26)\\
h &= \frac{m\hat{r}^{2-\epsilon}}{\Pi F} = m\rho^{d-2}\left(1-\frac{\tau^2}{\rho^2}\right)^{d-2}\left(1+\rho^2 f_6)\right)\,, && (5.3.27)\\
\tilde{k} &= \rho^2\left(1-\frac{\tau^2}{\rho^2}\right)\left(dt+\sum_{i=1}^{n}\frac{\hat{r}r_i dr_i+a_i r_i^2 d\varphi_i}{\hat{r}^2+a_i^2}+\epsilon\frac{z dz}{\hat{r}}\right)\\
&= \rho^2\left(1-\frac{\tau^2}{\rho^2}\right)\left(dt+\sum_{i=1}^{n+1}\left(m_i d(rm_i)(1+\rho^2 f_{7,i})+a_i m_i^2(1+\rho^2 f_{8,i})d\varphi_i\right)\right)\\
&= \rho^2\left(1-\frac{\tau^2}{\rho^2}\right)\Big(\underbrace{d(t+r)}_{(d\tau-d\rho)(\rho-\tau)^{-2}}+\underbrace{\sum_{i=1}^{n+1}\big(rm_i dm_i}_{=0}\\
&\quad+\underbrace{\rho^2 f_{7,i}m_i d(rm_i)}_{\rho^3 f_{7,i}m_i dm_i/(\rho^2-\tau^2)+\rho^2 f_{7,i}m_i^2 dr}+a_i m_i^2(1+\rho^2 f_{8,i})d\varphi_i\big)\Big)\\
&= \frac{1+\frac{\tau}{\rho}}{1-\frac{\tau}{\rho}}(d\tau-d\rho)+\sum_{i=1}^{n+1}\Big(\rho^3 f_{7,i}m_i dm_i\\
&\quad+\rho^2\left(1-\frac{\tau^2}{\rho^2}\right)\left(\rho^2 f_{7,i}m_i^2 dr+a_i m_i^2(1+\rho^2 f_{8,i})d\varphi_i\right)\Big)\,. && (5.3.28)
\end{aligned}
$$

Using

$$
dr=\rho^{-2}\left(1-\frac{\tau^2}{\rho^2}\right)^{-2}\left(\frac{2\tau}{\rho}d\tau-\left(1+\frac{\tau^2}{\rho^2}\right)d\rho\right)\,, \qquad (5.3.29)
$$

we can rewrite $\tilde{k}$ as

$$
\begin{aligned}
\tilde{k} &= \frac{1+\frac{\tau}{\rho}}{1-\frac{\tau}{\rho}}(d\tau-d\rho)+\sum_{i=1}^{n+1}\left(\rho^3 f_{7,i}m_i dm_i+a_i\rho^2 m_i^2 f_{9,i}d\varphi_i\right)\big)\\
&\quad+\frac{1}{1-\frac{\tau^2}{\rho^2}}\sum_{i=1}^{n+1}f_{7,i}m_i^2\big(2\rho\tau d\tau-\big(\rho^2+\tau^2\big)d\rho\big)\,. && (5.3.30)
\end{aligned}
$$

It follows that $h\,\tilde{k}\otimes\tilde{k}$ takes the form

$$
h\,\tilde{k}\otimes\tilde{k} = m\rho^{d-2}\left(1-\frac{\tau^2}{\rho^2}\right)^{d-4}\psi_{\mu\nu}dy^\mu dy^\nu\,, \qquad (5.3.31)
$$

where $(y^\mu) \equiv (y^0, y^i) := (\tau, \rho m^i)$, and the functions $\psi_{\mu\nu}$ satisfy

$$\rho^{\alpha_0+\ldots+\alpha_d}(\partial_{y^0})^{\alpha_0}\cdots(\partial_{y^n})^{\alpha_d}\psi_{\mu\nu} = O(1) \tag{5.3.32}$$

for all $\alpha \in \mathbb{N}^{d+1}$.

If $d \geq 4$ then this leads, as in the Schwarzschild case, to a conformally extended metric of differentiability class $C^{d-3,1}$. When $d = 3$ the behaviour of this completion at i^0 along spacelike directions is better than in the completion of Section 5.2, but is worse when the light cone is approached.

5.4 The ADM mass as an obstruction to differentiability

So far we have transformed the metric to the form

$$g = \frac{1}{(\rho^2 - \tau^2)^2}\overline{g}\,, \tag{5.4.1}$$

where

$$\overline{g}_{\mu\nu} = \eta_{\mu\nu} + \overline{h}_{\mu\nu}\,, \quad \overline{h}_{\mu\nu} = \begin{cases} O(\rho \ln \rho), & d = 3, \\ O(\rho^{d-2}), & d \geq 4, \end{cases} \tag{5.4.2}$$

and $\rho \equiv |\boldsymbol{y}|$. We want to show that the differentiability conditions obtained so far are optimal in the following sense.

Suppose for a contradiction that in odd spatial dimension d, with $d \geq 3$, there exists a coordinate system $(y^\mu) \equiv (\tau, \boldsymbol{y})$ in which $\overline{h}_{\mu\nu} = O(\rho^{d-2})$ and $\overline{h}_{\mu\nu}$ is of differentiability class C^{d-2}. Consider the metric $\gamma := g_{ij}dx^i dx^j$ induced by g on the zero level-set of τ, where the coordinates x^i are obtained by a Kelvin-inversion from the coordinates y^i:

$$x^i = \frac{y^i}{\rho^2}\,. \tag{5.4.3}$$

We find

$$g_{ij} = \delta_{ij} + \overline{h}_{ij} - 4\frac{\overline{h}_{k(i}x^k x_{j)}}{r^2} + 4\frac{\overline{h}_{k\ell}x^k x^\ell x_i x_j}{r^4}\,, \tag{5.4.4}$$

where for visual convenience we have set $x_i := x^i$. This leads to the following ADM integrand, up to a constant multiplicative factor and the measure on S^{d-1}:

$$\begin{aligned}\sigma &\equiv U_i\frac{x^i}{r}\times r^{d-1} := \left(\frac{\partial g_{ij}}{\partial x^j} - \frac{\partial g_{jj}}{\partial x^i}\right)\frac{x^i}{r}\times r^{d-1}\\ &= \Big(\frac{\partial\overline{h}_{ij}}{\partial x^j} - 4\frac{\frac{\partial\overline{h}_{k(i}}{\partial x_j}x^k x_{j)}}{r^2} + 4\frac{\frac{\partial\overline{h}_{k\ell}}{\partial x_j}x^k x^\ell x_i x_j}{r^4} - \frac{\partial\overline{h}_{jj}}{\partial x^i}\\ &\quad -4\overline{h}_{k(i}\partial_j\left(\frac{x^k x_{j)}}{r^2}\right) + 4\overline{h}_{k\ell}\partial_j\left(\frac{x^k x^\ell x_i x_j}{r^4}\right)\Big)\frac{x^i}{r}\times r^{d-1}\,.\end{aligned} \tag{5.4.5}$$

Suppose that $\overline{h}_{ij}$ is of differentiability class C^{d-2}. Then $\overline{h}_{ij}$ is a homogeneous polynomial of order $d-2$ in $\boldsymbol{y}$ up to $o(\rho^{d-2})$ terms and $\partial\overline{h}_{ij}/\partial y^k$ is a homogeneous polynomial of order $d-3$ in $\boldsymbol{y}$ up to $o(\rho^{d-3})$ terms. Using

$$\frac{\partial\overline{h}_{ij}}{\partial x^k} = \frac{\partial\overline{h}_{ij}}{\partial y^\ell}\frac{(r^2\delta^\ell_k - 2x^\ell x^k)}{r^4} = \frac{\partial\overline{h}_{ij}}{\partial y^\ell}(\rho^2\delta^l_k - y^\ell y^k)\,, \tag{5.4.6}$$

this implies that, up to $o(1)$ terms, the right-hand side of (5.4.5) is a sum of homogeneous polynomials in $\boldsymbol{x}/r$ of order $d+a$, where a is even.

When d is odd this implies immediately that the ADM mass vanishes. While the above calculations apply for all $d \geq 3$, the vanishing of mass is not true if the spatial dimension, d, is even. As pointed out in Section 5.2, in even spatial dimension dimensions the conformal compactification of the Riemannian hypersurfaces of constant t, induced by the spacetime compactification of the Schwarzschild metric described there, leads to a real-analytic conformal metric with a real-analytic conformal factor.

5.4.1 Asymptotic symmetries

Somewhat more generally, one might wish to consider the collection of metrics with asymptotic behaviour captured by (5.4.1) and (5.4.2). A natural question is then to determine the set

of coordinate transformations compatible with a conformal compactification of this form (compare [62]). A detailed analysis of this in four-dimensional spacetimes can be found in [22].

First, there are Lorentz transformations in the coordinates y^μ, which preserve both the conformal factor Ω and the asymptotic behaviour of the metric.

Next, there are coordinate transformations of the form

$$y^\mu \mapsto y^\mu + \xi^\mu(\tau/\rho, y^i/\rho)\rho^{d-1}\,, \tag{5.4.7}$$

with ξ^μ a smooth functions of its arguments. These are higher dimensional generalisations of the usual supertranslations at i^0. There is, however, a key difference: in four spacetime dimensions the Hamiltonian charges associated with the coordinate transformations (5.4.7) are non-zero in general, while in higher dimensions the decay in (5.4.7) is too fast, leading to vanishing Hamiltonian generators.

We note that the four-dimensional *logarithmic ambiguities*,

$$x^\mu \mapsto x^\mu + \eta_{\alpha\beta}(C^\mu x^\alpha - 2C^\alpha x^\mu)x^\beta \ln|\vec{x}|\,, \tag{5.4.8}$$

with constants C^μ (see [22, Theorem 2], compare [4, 9, 21]) are absent in higher dimensions.

Chapter6

Conformal Geodesics

In [69], spiralling of conformal geodesics was ruled out for metrics which are Riemannian and conformally Einstein. The conformal geodesic equations were also integrated for some example geometries and it was observed that the solutions did not spiral. It remained an open problem as to whether spiralling was possible in other geometries. In this Chapter we will prove a general no-spiralling theorem for conformal geodesics in Riemannian signature conformal manifolds. We begin by considering the analogous result for metric geodesics. The standard proof that metric geodesics cannot spiral relies on the existence of a geodesically convex neighbourhood at each point [19, Proposition 4.2]. Such a proof will not work for conformal geodesics since these are not local length minimisers (despite the Lagrangian formulation given in [31]). With this in mind, we begin by constructing a proof of the no-spiralling theorem for metric geodesics which does not rely on length minimisation arguments. This will then form the basis of our proof in the conformal geodesic case.

6.1 The Conformal Geodesic Equations

Conformal geodesics are curves defined on a conformal manifold $(M, [g])$, which we assume to be Riemannian. Given any choice of metric $g \in [g]$, these curves can be defined by the

following set of conformally invariant third order differential equations [69]:

$$\nabla_u a = -\left(|a|^2 + L(u,u)\right) u + L^{\#} u \tag{6.1.1}$$

where u is the unit tangent vector to the curve (i.e $g(u,u) = 1$), $a := \nabla_u u$ is the perpendicular acceleration (i.e $g(u,a) = 0$) and $|a| := \sqrt{g(a,a)}$. The Schouten tensor $L : T_pM \times T_pM \mapsto \mathbb{R}$ is defined by

$$L = \frac{1}{d-2}\left(Ric - \frac{R}{2(d-1)} g\right) \tag{6.1.2}$$

in terms of the Ricci tensor Ric, the Ricci scalar R and the dimension, d, of the manifold. We denote by $L^{\#} : T_pM \mapsto T_pM$ the corresponding endomorphism defined by $g(L^{\#}v, w) = L(v,w)$ for all vector fields v, w.

Conformally transforming the metric to $\hat{g} = \Omega^2 g$, where $\Omega : M \to \mathbb{R}$ is a strictly positive function, results in changes to the Schouten tensor, the Levi–Civita connection, the unit tangent vector and the acceleration vector as follows:

$$\begin{aligned}
\hat{L} &= L - \nabla\Upsilon + \Upsilon \otimes \Upsilon - \frac{1}{2}|\Upsilon|^2 g, \\
\hat{\nabla}_v w &= \nabla_v w + \Upsilon(w)v + \Upsilon(v)w - g(v,w)\Upsilon^{\sharp}, \\
\hat{u} &= \Omega^{-1} u, \\
\hat{a} &= \Omega^{-2}(a - \Upsilon^{\sharp} + \Upsilon(u)u),
\end{aligned}$$

where $\Upsilon \equiv \Omega^{-1} d\Omega$ and $\Upsilon^{\sharp}$ is a vector field defined by $\Upsilon(w) = g(\Upsilon^{\sharp}, w)$. It is now a matter of explicit calculation to verify that the conformal geodesic equations (6.1.1) are conformally invariant.

In the remainder of this Chapter we shall fix a metric, g, in the conformal class and consider (6.1.1) for this choice of metric. We will denote the set of unit vectors in T_pM by $S(T_pM)$, and $S(TM)$ will denote the corresponding unit tangent bundle over M.

Picard's theorem applied to equation (6.1.1) shows that a conformal geodesic is uniquely specified locally by an initial point $p \in M$, an initial unit tangent, u_0, at p and an initial

acceleration, a_0, at p which is perpendicular to u_0 [69, Theorem 1.1]. We will denote the conformal geodesic with these initial conditions and arc length parameter t by $\gamma_{p,u_0,a_0}(t)$.

Definition 6.1.1. A curve, γ, with arc length parameter $t \in [0, \infty)$, spirals towards a point $p_* \in M$ if for any neighbourhood N containing p_*, there exists some T such that $\gamma(t) \in N$ for all $t > T$.

We demand that the conformal geodesic has a well defined unit tangent vector and thus exclude the trivial case where it consists only of a single point.

Throughout this Chapter we will refer to balls in (M, g) and in various tangent spaces. We make the following definitions

$$B(q, r) := \{q' \in M : d(q, q') < r\}, \ \bar{B}(q, r) := \{q' \in M : d(q, q') \leq r\} \tag{6.1.3}$$

where $d : M \times M \to \mathbb{R}_{\geq 0}$ denotes the Riemannian distance function induced by the metric g.

We will also refer to balls in the tangent space $T_{u_0}(T_pM)$, where $u_0 \in S(T_pM)$. These are defined by identifying $T_{u_0}(T_pM)$ with T_pM and using the Riemannian distance function induced by the metric g on the vector space T_pM.

6.1.1 Outline of Proof for Metric Geodesics

Theorem 6.1.2. Let (M, g) be a Riemannian manifold. Then geodesics on (M, g) cannot spiral.

Sketch of proof (without using length minimisation arguments):

- **Step 1:** Define the exponential map and geodesic ball at $p \in M$ and establish that all metric geodesics through p reach the boundary of this geodesic ball.

  The exponential map, $\exp_p$, at a point $p \in M$ [58, Definition 1.10] is a diffeomorphism

from some neighbourhood of $V \subset T_pM$ containing 0 to a neighbourhood $V' \subset M$ containing p. A *geodesic ball* is any open ball centred on p and contained in V'. The exponential map at p allows us to construct a co-ordinate system on any geodesic ball and geodesic segments foliate the geodesic ball with the point p removed. For the purposes of this proof, the important property of the geodesic ball is that all metric geodesics through p must reach its boundary.

- **Step 2:** Show that for any compact $U \subset M$ there exists $\epsilon > 0$ such that for all $p \in U$, $B(p, \epsilon)$ is a geodesic ball.

  We define a function on M which maps each point $p \in M$ to the supremum of the set $\{r \in \mathbb{R}_{\geq 0} : B(p, r) \text{ is a geodesic ball}\}$ (capped at 1 to avoid any complications involving infinite sizes). Since the exponential map defined at any $p \in M$ is a local bijection, this function is always strictly positive. It can also be shown that this function is continuous. The result follows from the fact that this continuous function restricted to the compact set U is bounded from below by some $\epsilon > 0$.

- **Step 3:** Use the fact that metric geodesics intersect the boundary of the geodesic ball to deduce that they cannot spiral.

  Suppose the metric geodesic γ spirals towards some $p_* \in M$. Then for any $R < d(p_*, \gamma(0))$ there is a unique $T > 0$ such that $d(p_*, \gamma(T)) = R$ and $d(p_*, \gamma(t)) < R$ for all $t > T$. Denote the point $\gamma(T)$ by p. This is the point at which γ enters $B(p_*, R)$ for the final time.

  Let $U \subset M$ containing p_* be compact. Choose $R = \epsilon/2$ (where ϵ is as in Step 2) and find the corresponding p (reducing ϵ if necessary so that $R < d(p_*, \gamma(0))$. By reducing ϵ further if necessary, we can assume that $p \in U$. Then, by the results of Step 2, $B(p, \epsilon)$ is a geodesic ball. From Step 1 we know that γ must leave this geodesic ball at some later parameter value. In doing so, it must once again reach a distance of at least $R = \epsilon/2$ from p_*. This is a contradiction, since we assumed that $d(p_*, \gamma(t)) < R$ for all $t > T$. This argument is illustrated in Figure 6.1. □

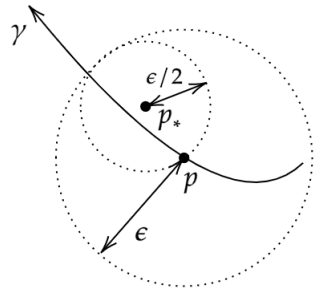

Figure 6.1: We find $T \in \mathbb{R}$ and $\epsilon > 0$ such that there is a geodesic ball of radius ϵ centred at $p := \gamma(T)$, where $d(p_*, \gamma(T)) = \epsilon/2$ and $d(p_*, \gamma(t)) < \epsilon/2$ for all $t > T$. However, we have also shown that γ must leave this geodesic ball and hence reach a distance of $\epsilon/2$ from p_* at some $t > T$. This is our contradiction. We show geodesic balls as circles for ease of illustration.

6.1.2 Outline of Proof for Conformal Geodesics

The exponential map at $p \in M$ was useful because it allowed us to identify a subset of M which was foliated by segments of metric geodesics through p. Inspired by this, we will define an exponential map which allows us to see how conformal geodesics foliate some subset of M.

Despite some additional complexities in the conformal geodesic case, we are able to prove a no-spiralling theorem by following three steps analogous to those used in the proof of Theorem 6.1.2. These three steps correspond to the three main sections of this Chapter.

Theorem 6.1.3. Let $(M, [g])$ be a conformal manifold with C^4 conformal metric. Then conformal geodesics on $(M, [g])$ cannot spiral.

Outline of Proof (see Section 6.4 for the complete proof using results derived in Sections 6.2 and 6.3):

- **Step 1:** Define an exponential map adapted to conformal geodesics and identify a domain and range on which it is a homeomorphism.

  In Section 6.2, we define a conformal geodesic analogue of the exponential map at some $(p, u_0) \in S(TM)$. Unlike for metric geodesics, there is no subset of the

domain of this exponential map on which it is a homeomorphism onto some ball centred at p. Instead, in Section 6.2.3 we find that it is a homeomorphism onto some set which we call a *heart* at p. We say that this heart has *direction* u_0. Crucially, in Section 6.2.4 we show that conformal geodesics with unit tangent u_0 at p re-intersect the boundary of a certain heart, H_{p,u_0}, at p with direction u_0. This is analogous to the fact that metric geodesics through some point re-intersect the boundary of a geodesic ball centred at that point.

Result of Step 1 (Theorem 6.2.7): Let $(p, u_0) \in S(TM)$. Then any conformal geodesic with unit tangent u_0 at p re-intersects the boundary of the heart H_{p,u_0}.

- **Step 2:** Define a notion of size for a heart and show that given any compact $U \subset M$, there exists $\epsilon > 0$ such that there is a heart at p with direction u_0 which has size at least ϵ, for any $p \in U$ and any $u_0 \in S(T_pM)$.

  In the metric geodesic case we considered geodesic balls in M since these had an obvious size associated to them. In the conformal geodesic setting we consider certain half balls in $T_{u_0}(T_pM)$ which are mapped to hearts in M. The size of a heart is defined by considering the radii of balls in M which have u_0 tangent to their boundary and are contained inside this heart. Note that this size has units of length, regardless of the dimension of the conformal manifold. We show that as we vary p and u_0 (as well as the radius of the domain ball[1]) in $T_{u_0}(T_pM)$ we are able to find a lower bound for this size which is strictly positive and varies continuously with p and u_0 (provided the conformal metric is C^4). The result follows from the fact that a continuous function on a compact set is bounded and attains its bound.

  Result of Step 2 (Theorem 6.3.3): Let $(M, [g])$ be a conformal manifold with C^4

[1]This is important since we need to rule out making the heart have zero size by simply choosing the domain to be trivial. To avoid this, we choose the domain to be the ball in $T_{u_0}(T_pM)$ with u_0 perpendicular to its boundary and radius equal to

$$\frac{1}{2} \times \sup\{r : \text{the exponential map is a homeomorphism on the ball of radius } r \text{ with } u_0 \text{ perpendicular to its boundary}\}.$$

conformal metric and let U be a compact subset of M. Then there exists some $\epsilon > 0$ such that for any $(p, u_0) \in S(TU)$ there is a heart, H_{p,u_0}, at p with direction u_0 which has size at least ϵ.

- **Step 3:** Using the fact that a conformal geodesic with unit tangent u_0 at p must re-intersect the boundary of H_{p,u_0}, deduce that conformal geodesics cannot spiral.

  Suppose γ is a conformal geodesic which spirals towards some $p_* \in M$. We consider a metric geodesic ball centred on p_* (i.e. a set $B(p_*, r)$ for some r) which is entered by γ for the final time at some point p where γ has unit tangent u_0 (i.e. γ enters the ball at p and never re-intersects its boundary). Using the result of Step 2 (Theorem 6.3.3), we show that it is possible to choose this ball (and the corresponding p and u_0) such that it is contained inside some heart H_{p,u_0} with position p and direction u_0 (see Definition 6.2.6). Then by the result of Step 1 (Theorem 6.2.7), γ must re-intersect the boundary of this heart, so we deduce that it must also re-intersect the boundary of the ball. This is our contradiction. □

  Result of Step 3 (Theorem 6.1.3): Let $(M, [g])$ be a conformal manifold with C^4 conformal metric. Then conformal geodesics on $(M, [g])$ cannot spiral.

6.2 The Exponential Map for Conformal Geodesics

In this section we will complete Step 1 of the proof of Theorem 6.1.3 as outlined in Section 6.1.1.

Step 1: Define an exponential map adapted to conformal geodesics and identify a domain and range on which it is a homeomorphism.

For any $(p, u_0) \in S(TM)$, we define the following analogue of the exponential map appropriate to conformal geodesics (see [58, Definition 1.10] for a definition of the exponential map for metric geodesics):

Definition 6.2.1 (The Exponential Map)**.**

$$\begin{aligned} \exp_{p,u_0} : T_{u_0}\left(S\left(T_pM\right)\right) &\to M \\ A &\mapsto \begin{cases} \gamma_{p,u_0,A_\perp/|A|^2}\left(2\pi|A|\right) & \text{if } A \neq 0 \\ p & \text{if } A = 0 \end{cases} \end{aligned} \tag{6.2.1}$$

where $A_\perp := A - g(A, u_0)u_0$ denotes the component of A which is perpendicular to $u_0 \in S(T_pM)$. This map is continuous as a function of A, as we will see in the next section.

6.2.1 The Directional Derivative of The Exponential Map

The exponential map for metric geodesics is usually analysed by considering its directional derivatives. We will do the same thing for the conformal geodesic exponential map in Definition 6.2.1. Calculating these directional derivatives at $A = 0$ will allow us to understand this map in neighbourhoods of p.

The directional derivative at 0 is

$$\begin{aligned} D\left(\exp_{p,u_0}\right)_0 : T_0(T_{u_0}(S(T_pM))) &\to T_pM \\ A &\mapsto \frac{d}{d\lambda}\exp_{p,u_0}\left(\lambda A\right)|_{\lambda=0^+} \\ &= \frac{d}{d\lambda}\gamma_{p,u_0,A_\perp/\lambda|A|^2}\left(2\pi\lambda|A|\right)|_{\lambda=0^+}. \end{aligned} \tag{6.2.2}$$

To calculate this, we use a power series expansion

$$\gamma_{p,u_0,a_0}(t) = p + \sum_{n=0}^{\infty} \frac{1}{(n+1)!} t^{n+1} \nabla_u^{(n)} u|_{t=0} \tag{6.2.3}$$

where $\nabla_u^{(n)}$ denotes the directional derivative ∇_u applied n times and we recall that $a = \nabla_u u$ (so in particular we set $\nabla_u u|_{t=0} = a_0$). This expression (and subsequent similar expressions) should be understood in terms of co-ordinates.

Equation (6.1.1) allows us to express the power series (6.2.3) in terms of u_0 and a_0 (as well as the Schouten tensor and its derivatives evaluated at p). If the initial acceleration is $a_0 = A_\perp / (\lambda |A|^2)$, then at $t = 0$ we have

$$\nabla_u a|_{t=0} = -\frac{1}{\lambda^2} \frac{|A_\perp|^2}{|A|^4} u_0 + O(1) \tag{6.2.4}$$

where u_0 denotes the initial unit tangent vector and by $O(1)$ we mean terms which are bounded in the limit $\lambda \to 0$. Repeated applications of equation (6.1.1) imply that for a conformal geodesic with initial data $(p, u_0, A_\perp / (\lambda |A|^2))$ we have

$$\nabla_u^{(n)} u|_{t=0} = O(\lambda^{-n}) \tag{6.2.5}$$

as $\lambda \to 0$. In particular all terms involving the Schouten tensor L and its derivatives are $O(\lambda^{2-n})$ (i.e. they are sub-leading in the limit $\lambda \to 0$). To calculate the directional derivative (6.2.2) we must first evaluate the power series (6.2.3) at $t = 2\pi\lambda|A| = O(\lambda)$. We see that the terms in this power series which are first order in λ are exactly those that arise in Euclidean space, where $L \equiv 0$. For the Euclidean metric on $\mathbb{R}^n$, conformal geodesics with initial data (p, u_0, a_0) are circles with equations of the form

$$x(t) = p + u_0 |a_0|^{-1} \sin(|a_0| t) + a_0 |a_0|^{-2} \left(1 - \cos(|a_0| t)\right). \tag{6.2.6}$$

The directional derivative at 0 of the exponential map is therefore

$$D(\exp_{p,u_0})_0 : A \mapsto u_0 \frac{|A|^2}{|A_\perp|} \sin\left(2\pi \frac{|A_\perp|}{|A|}\right) + A_\perp \frac{|A|^2}{|A_\perp|^2} \left(1 - \cos\left(2\pi \frac{|A_\perp|}{|A|}\right)\right). \tag{6.2.7}$$

Note that this expression is finite in the limit $A_\perp \to 0$.

It is clear from the definition of the exponential map that if A and A' are such that $A_\perp = A'_\perp$ and $|A| = |A'|$, then $\exp_{p,u_0}(A) = \exp_{p,u_0}(A')$. Since our aim is to find a region on which the exponential map is a homeomorphism, we therefore restrict our attention to the half space $g(A, u_0) \geq 0$. Based on equation (6.2.7), we define the following quantities related to

$A_\perp, A \in T_{u_0}(T_pM)$

$$\begin{aligned} \sin\theta &:= \frac{|A_\perp|}{|A|},\ \theta \in [0, \pi/2] \\ \hat{a}_0 &:= \frac{A_\perp}{|A_\perp|}. \end{aligned} \tag{6.2.8}$$

We have assumed that $A_\perp \neq 0$ and $A \neq 0$ since this will simplify expressions later on, although these cases can be obtained from the results below by taking the limits $A_\perp \to 0$ and $A \to 0$ respectively.

We see that a vector A in the half space $g(u_0, A) \geq 0$ is uniquely defined by θ, $\hat{a}_0$ and $|A|$. The vectors u_0, $\hat{a}_0$ define a "quarter space" in T_pM by $g(A, \hat{a}_0) \geq 0$ and $g(A, u_0) \geq 0$. The variable θ is the angle between A and the vector[2] u_0.

We can re-write the directional derivative (6.2.7) in terms of $|A|$, θ and $\hat{a}_0$, as

$$D(\exp_{p,u_0})_0 : A \mapsto u_0 \frac{|A|}{\sin\theta} \sin(2\pi \sin\theta) + \hat{a}_0 \frac{|A|}{\sin\theta} (1 - \cos(2\pi \sin\theta)). \tag{6.2.9}$$

We therefore have the following leading order expression for the exponential map:

$$\exp_{p,u_0}(|A|, \theta, \hat{a}_0) = p + u_0 \frac{|A|}{\sin\theta} \sin(2\pi \sin\theta) + \hat{a}_0 \frac{|A|}{\sin\theta} (1 - \cos(2\pi \sin\theta)) + O(|A|^3). \tag{6.2.10}$$

If we hold $\hat{a}_0$ and $\sin\theta/|A|$ fixed while varying $|A|$, we see from Definition 6.2.1 that the image of this curve under the exponential map is a conformal geodesic parameterised by $|A|$. Suppose we extend u_0, $\hat{a}_0$ to obtain an orthonormal basis of T_pM. Using the metric geodesic exponential map, this basis corresponds to a set of geodesic normal co-ordinates for a neighbourhood of $p \in M$. In these co-ordinates, the expression (6.2.10) for the conformal geodesic is the same as the co-ordinate expression for a circle in $\mathbb{R}^n$ to first order in $|A|$, with the $O(|A|^2)$ terms vanishing. Recall that conformal geodesics in Euclidean space are exactly circles (all higher order terms in $|A|$ vanish). By analogy, if we do a power series expansion

[2]For fixed $(u_0, \hat{a}_0)$ we will draw sketches in the $u_0 - \hat{a}_0$ half space defined by $g(A, u_0) \geq 0$. This actually corresponds to considering $\theta \in [0, \pi/2]$ for both $\hat{a}_0$ and -$\hat{a}_0$.

of metric geodesics in these same co-ordinates we also find that the 2nd order term in the expansion parameter vanishes. Recall that metric geodesics in Euclidean space are exactly straight lines (i.e. there exist co-ordinates in which all non-linear terms in the expansion parameter vanish).

6.2.2 The Image of a Ray Under the Exponential Map

In this section we will study the image of a ray in the half space $g(u_0, A) \geq 0$ originating from $A = 0$. Such a ray is defined by fixing θ and $\hat{a}_0$ in (6.2.8).

Lemma 6.2.2. Let $(p, u_0) \in S(TM)$. Under the exponential map at (p, u_0), a ray from $A = 0$ defined by $\hat{a}_0$ and $\theta = \theta_0$ is mapped to a curve in M whose tangent at p lies in the half space of $\text{span}\{u_0, \hat{a}_0\}$ defined by $g(u_0, \hat{a}_0) \geq 0$ and makes an angle of $\theta = \pi \sin\theta_0$ with u_0 (see Figure 6.2).

Proof: The directional derivative at 0 in the direction tangent to a particular ray is given by equation (6.2.9) and is non-zero provided $A \neq 0$ and $\theta \neq \pi/2$ (i.e. $A_\perp \neq A$). This directional derivative gives the tangent direction at p of the curve which is the image of this ray under the exponential map. We see that this image curve lies in the same quarter space as A and that the angle, θ, between the directional derivative and the vector u_0 satisfies

$$\begin{aligned} \tan\theta &= \frac{1 - \cos(2\pi \sin\theta_0)}{\sin(2\pi \sin\theta_0)} \\ &= \tan(\pi \sin\theta_0) \\ \implies \theta &= \pi \sin\theta_0. \end{aligned} \tag{6.2.11}$$

□

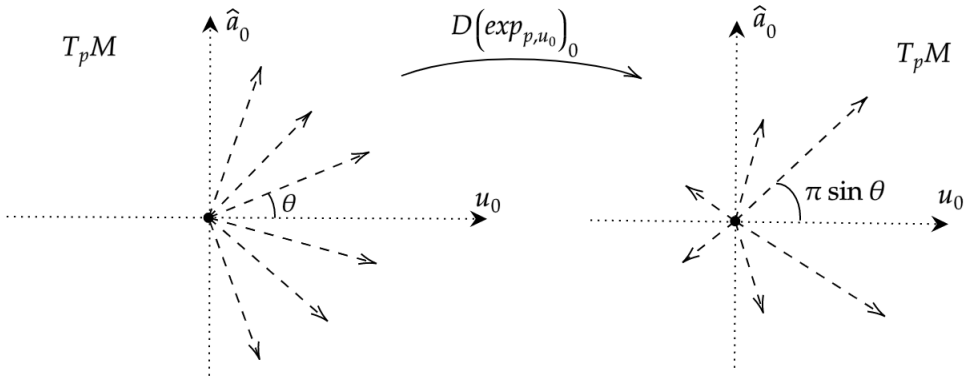

Figure 6.2: The directional derivative along a direction in the $u_0 - \hat{a}_0$ plane which makes an angle of θ with the positive u_0 axis is a vector in the same plane making an angle of $\pi \sin\theta$ with the positive u_0 axis.

6.2.3 The Exponential Map is a Homeomorphism onto a Heart

Lemma 6.2.2 tells us that the exponential map takes distinct rays through the origin in T_pM to curves with distinct tangent directions at p. In this section we will show that, for rays confined to a wedge (defined below) in T_pM, we can find a lower bound on the arc length parameter (or equivalently a lower bound on $|A|$ in Definition 6.2.1) at which these curves can re-intersect. This tells us that the exponential map is a homeomorphism on this wedge. We will then consider a union of such wedges. We find that as we increase the opening angle of the wedge towards π, the lower bound on the arc length parameter we obtain decreases to 0. We conclude that the exponential map is a homeomorphism on some region of the half space $g(A, u_0) \geq 0$ with cross-sections like the one shown on the right of Figure 6.5.

Definition 6.2.3. For any $u_0 \in S(T_pM)$, let $C(u_0, r)$ denote the open ball in $T_{u_0}(T_pM)$ of radius r (defined using the metric g, where we identify $T_{u_0}(T_pM)$ with T_pM) which has u_0 inward pointing and perpendicular to its boundary at p.

Theorem 6.2.4. Let $(p, u_0) \in S(TM)$. Then the exponential map at (p, u_0) is a homeomorphism on $C(u_0, r)$ for some $r > 0$.

Proof: In Section 6.2.1 we calculated an expression for the directional derivative of the exponential map at $A = 0$. We now calculate the derivative at $A \neq 0$. To do this we calculate

the terms in $\exp_{p,u_0}(A+\delta A) - \exp_{p,u_0}(A)$ which are first order in the variation δA.

Recall that for any $u_0 \in S(T_pM)$ and $A \in T_{u_0}(T_pM)$ we can identify $T_{u_0}(T_pM)$ with T_pM and write A as a linear combination of the perpendicular unit vectors u_0 and $\hat{a}_0$ (but note that if A is parallel to u_0 then no such $\hat{a}_0$ is defined or required). It follows that any $\delta A \in T_{u_0}T_pM$ can be written as $\delta A = \alpha u_0 + \beta \hat{a}_0 + \gamma \hat{a}_0'$, where $\hat{a}_0'$ is a unit vector perpendicular to both u_0 and $\hat{a}_0$ and we take $\gamma \geq 0$ without loss of generality. Once again note that if A is parallel to u_0 then $\hat{a}_0$ is not required. Equation (6.2.10), suggests it will be more convenient to express δA in terms of variations in $|A|$ and the quantities $\sin\theta$ and $\hat{a}_0$ introduced in (6.2.8). Similarly to before we assume that $A_\perp \neq 0$ (i.e. $\sin\theta \neq 0$) since this will simplify the expressions, however this case can once again be obtained by taking the limit $A_\perp \to 0$ in the final result and setting β to zero. We have

$$\begin{aligned} \delta|A| &= \alpha\cos\theta + \beta\sin\theta + O(2), \\ \delta\sin\theta &= \frac{\beta\cos^2\theta}{|A|} - \frac{\alpha\sin\theta\cos\theta}{|A|} + O(2), \\ \delta\hat{a}_0 &= \frac{\gamma}{|A|\sin\theta}\hat{a}_0' + O(2). \end{aligned} \tag{6.2.12}$$

where by $O(2)$ we mean terms which are second order in α, β and γ (i.e. second order in δA).

By the chain rule, we have

$$D(\exp_{p,u_0})_A(\delta A) = \frac{\partial \exp_{p,u_0}(A)}{\partial|A|}\delta|A| + \frac{\partial \exp_{p,u_0}(A)}{\partial \sin\theta}\delta\sin\theta + \frac{\partial \exp_{p,u_0}(A)}{\partial \hat{a}_0^\alpha}\delta\hat{a}_0^\alpha. \tag{6.2.13}$$

Since we are interested in calculating $D(\exp_{p,u_0})_A(\delta A)$ we will now drop higher order terms in δA (i.e. the $O(2)$ terms in (6.2.12)). Evaluating each of the three terms in (6.2.13) separately,

we have

$$\begin{aligned}
\frac{\partial \exp_{p,u_0}(A)}{\partial |A|}\delta|A| &= [\alpha\cos\theta + \beta\sin\theta] \times \left[u_0\frac{\sin(2\pi\sin\theta)}{\sin\theta} + \hat{a}_0\frac{(1-\cos(2\pi\sin\theta))}{\sin\theta} + O(|A|^2)\right] \\
\frac{\partial \exp_{p,u_0}(A)}{\partial \sin\theta}\delta\sin\theta &= \left[\beta\cos^2\theta - \alpha\sin\theta\cos\theta\right] \times \left[u_0\left(\frac{2\pi\cos(2\pi\sin\theta)}{\sin\theta} - \frac{\sin(2\pi\sin\theta)}{\sin^2\theta}\right)\right. \\
&\qquad \left. + \hat{a}_0\left(\frac{2\pi\sin(2\pi\sin\theta)}{\sin\theta} - \frac{1-\cos(2\pi\sin\theta)}{\sin^2\theta}\right) + O(|A|^2)\right] \\
\frac{\partial \exp_{p,u_0}(A)}{\partial \hat{a}_0^\alpha}\delta\hat{a}_0^\alpha &= \gamma\hat{a}_0'\left[\frac{1-\cos(2\pi\sin\theta)}{\sin^2\theta} + O(|A|^2)\right].
\end{aligned} \tag{6.2.14}$$

We are interested in when $D(\exp_{p,u_0})_A(\delta A)$ can be zero. It is straightforward to check that if $\theta \in [0,\theta_0)$ for some $\theta_0 \in \left[0,\frac{\pi}{2}\right)$, each of the three terms above are linearly independent at $|A| = 0$ (assuming they are non-zero), and hence also at $|A| < c_1$, for some constant c_1 which depends on θ_0. It follows that $D(\exp_{p,u_0})_A(\delta A)$ can only vanish if each of the three terms above vanish individually. We calculate the norm of each quantity and define functions $f_i(\theta,|A|)$ $(i = 1,2,3)$ as follows.

$$\begin{aligned}
\left|\frac{\partial \exp_{p,u_0}(A)}{\partial |A|}\delta|A|\right| &= 2\left|\alpha\cos\theta + \beta\sin\theta\right| \times \underbrace{\left[\frac{\sin(\pi\sin\theta)}{\sin\theta} + O(|A|^2)\right]}_{f_1(\theta,|A|)} \\
\left|\frac{\partial \exp_{p,u_0}(A)}{\partial \sin\theta}\delta\sin\theta\right| &= 2\left|\beta\cos^2\theta - \alpha\sin\theta\cos\theta\right| \\
&\qquad \times \underbrace{\left[\frac{\sin^2(\pi\sin\theta)}{\sin^4\theta} + \frac{\pi^2}{\sin^2\theta} - \frac{\pi\sin(2\pi\sin\theta)}{\sin^3\theta} + O(|A|^2)\right]^{1/2}}_{f_2(\theta,|A|)} \\
\left|\frac{\partial \exp_{p,u_0}(A)}{\partial \hat{a}_0^\alpha}\delta\hat{a}_0^\alpha\right| &= 2\gamma \times \underbrace{\left[\frac{\sin^2(\pi\sin\theta)}{\sin^2\theta} + O(|A|^2)\right]}_{f_3(\theta,|A|)}
\end{aligned} \tag{6.2.15}$$

Plots of $f_1(\theta,0)$ and $f_2(\theta,0)$ are shown in Figures 6.3 and 6.4 respectively (note that $f_3(\theta,0) = f_1(\theta,0)^2$). We see that $f_i(\theta,0) > 0$ $(i = 1,2,3)$ for $\theta \in [0,\frac{\pi}{2})$, however $f_1(\frac{\pi}{2},0) = f_3(\frac{\pi}{2},0) = 0$. Now suppose we restrict to $\theta \in [0,\theta_0]$ for some $\theta_0 \in \left[0,\frac{\pi}{2}\right)$. Then there exists some constant $c_2 > 0$ (depending on θ_0) such that $f_i(\theta,|A|) > 0$ $(i = 1,2,3)$ for $\theta \in [0,\theta_0]$ and $|A| < c_2$. This means that, for $\theta \in [0,\theta_0]$ and $|A| < c_2$, the three quantities in (6.2.14) all vanish if and

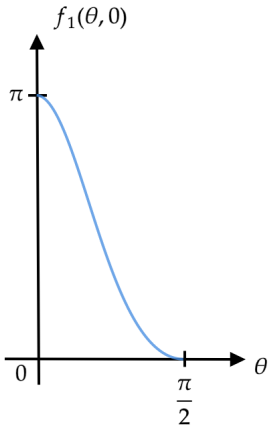

Figure 6.3: Plot of $f_1(\theta, 0)$. We see that $f_1(\theta, 0) > 0$ for $\theta \in [0, \frac{\pi}{2})$.

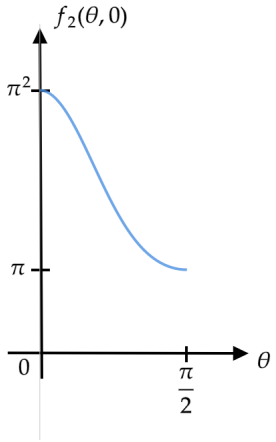

Figure 6.4: Plot of $f_2(\theta, 0)$. We see that $f_2(\theta, 0) > 0$ for $\theta \in [0, \frac{\pi}{2}]$.

only if $\alpha = \beta = \gamma = 0$, or equivalently if and only if $\delta A = 0$. It follows that $D(\exp_{p,u_0})_A$ has non-zero determinant at any A with $\theta \in [0, \theta_0]$ and $|A| < c := \min(c_1, c_2)$. We refer to such a set as a wedge of radius c and opening angle $2\theta_0$.

As we let $\theta_0 \to \frac{\pi}{2}$, we see that $c \to 0$, so the radius of the wedge on which we can guarantee that $D(\exp_{p,u_0})_A$ has non-zero determinant tends to zero. We conclude that $D(\exp_{p,u_0})_A$ has non-zero determinant on a series of wedges whose radii tend to zero as their opening angle tends to π. Taking the union over all such wedges, we find that $D(\exp_{p,u_0})_A$ has non-zero determinant on some set with boundary perpendicular to u_0 at p (see Figure 6.5). Such a set contains an open ball in $T_{u_0}(T_pM)$ which has u_0 inward pointing and perpendicular to its boundary - i.e. it contains $C(u_0, r)$ for some $r > 0$.

Next we show that the exponential map is an injection on this set $C(u_0, r)$. Suppose A, $A' \in C(u_0, r)$. Since $C(u_0, r)$ is an open ball in $T_{u_0}(T_pM)$, it is convex and hence $f(t) := \exp_{p,u_0}(A + t(A' - A)) \in C(u_0, r)$ for any $t \in [0, 1]$. This function is differentiable on $(0, 1)$ so, by the mean value theorem, there exists some $t_* \in (0, 1)$ with

$$\begin{aligned} f'(t_*) &= f(1) - f(0) \\ \implies D(\exp_{p,u_0})_{A+t_*(A'-A)}(A' - A) &= \exp_{p,u_0}(A') - \exp_{p,u_0}(A). \end{aligned} \tag{6.2.16}$$

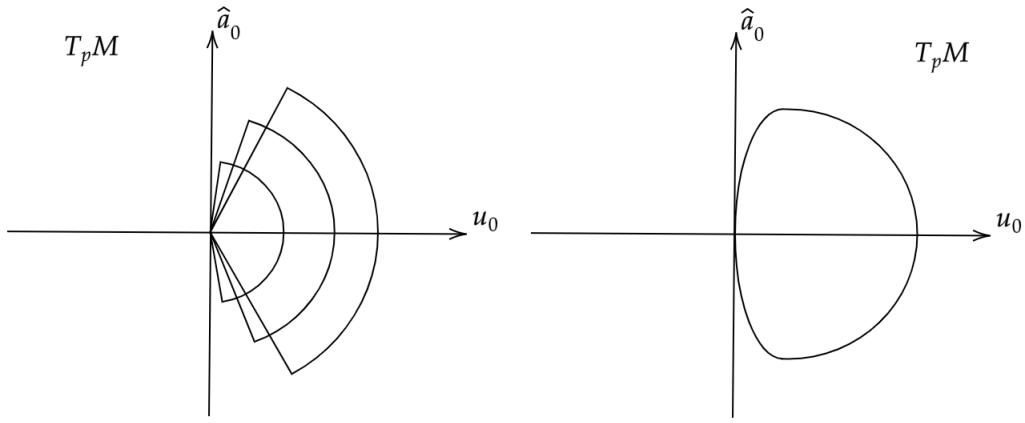

Figure 6.5: The derivative of the exponential map has non-zero determinant on a series of wedges whose radii decrease to 0 as their opening angle increases towards π. Taking the union of such sets gives a set with cross sections like the one shown on the right of this figure. In particular we conclude that the derivative of the exponential map has non-zero determinant on $C(u_0, r)$ for some $r > 0$.

Since $D(\exp_{p,u_0})_{A+t_*(A'-A)}$ has non-zero determinant, it follows that if $\exp_{p,u_0}(A') = \exp_{p,u_0}(A)$ then we must have $A = A'$.

We conclude that the exponential map is injective on $C(u_0, r)$ and hence is a homeomorphism from this set to its image. □

As the radius of a wedge shrinks to 0, so too must the size of the smallest ball which contains its image under the exponential map. Furthermore, by Lemma 6.2.2 we see that as the opening angle of this wedge increases to π, the opening angle of the image set at p must increase to 2π (consider two rays defined by $\pm\hat{a}_0$ and let $\theta_0 \to \pi/2$). In particular, the images of these two rays are both tangent to $-u_0$ at p. Consequently, the image of a ball with u_0 inward pointing and perpendicular to its boundary is a set with cross sections which feature a cusp at p (shown on the right of Figure 6.6). We refer to such a set as a *heart* due to the shape of these cross sections.

Note that if we choose $|A_\perp| = \epsilon^3 < 1$ and $|A| = \epsilon^2$ then the vector A will be mapped to a point on a conformal geodesic which has perpendicular acceleration of size $1/\epsilon$ at p. By choosing ϵ arbitrarily small, this can be made arbitrarily large while simultaneously ensuring that $A \in C(u_0, r)$. As a result, given any $r > 0$, the image set $\exp_{p,u_0}(C(u_0, r))$ will always

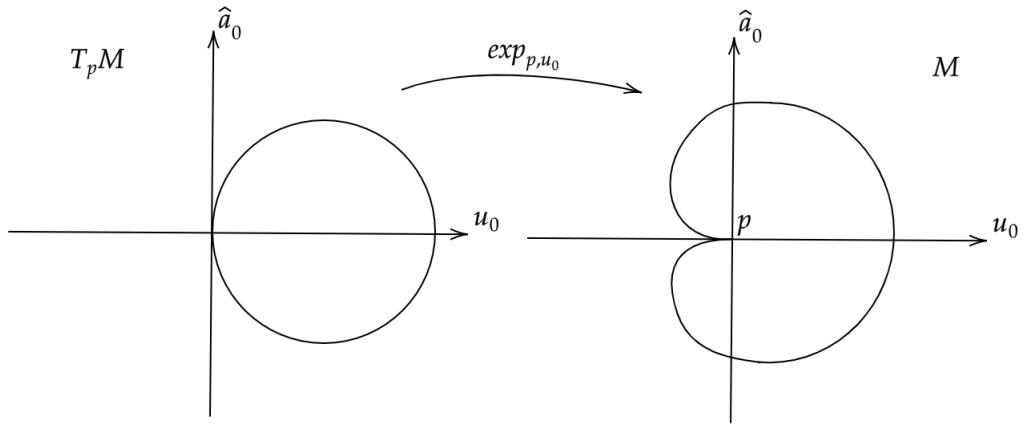

Figure 6.6: The exponential map is a homeomorphism on a ball in T_pM with u_0 perpendicular and inward pointing on its boundary.

contain at least some portion of every conformal geodesic with unit tangent vector u_0 at p, even those with arbitrarily large perpendicular acceleration at this point. This is crucial for the lemma below and for our proof of the no-spiralling theorem (Theorem 6.1.3) in Section 6.4.

Example (the Euclidean metric on $\mathbb{R}^n$): In the case where g is the Euclidean metric on $\mathbb{R}^n$, the $O(|A|^3)$ terms in equation (6.2.10) are identically 0 and conformal geodesics are circles. The images of distinct rays from 0 in the half space $g(u_0, A) > 0$ are also rays. These do not re-intersect, so the exponential map is a homeomorphism (in fact a diffeomorphism) from this half space onto $\mathbb{R}^n$ with the ray from 0 in the direction of $-u_0$ removed. This is essentially the familiar result that we can foliate $\mathbb{R}^n$ by circles tangent to u_0 at p (shown for $n = 2$ in Figure 6.7). Since we have insisted that the conformal geodesic has initial direction u_0 (rather than $-u_0$) we cannot reach points on the $-u_0$ axis. These points correspond to the circle through infinity with initial direction u_0 at p.

If the Schouten tensor is not identically zero then the higher order terms in equation (6.2.10) become important as $|A|$ increases. These terms may cause the images of rays to intersect. This would reduce the size of the domain on which the exponential map is a homeomorphism.

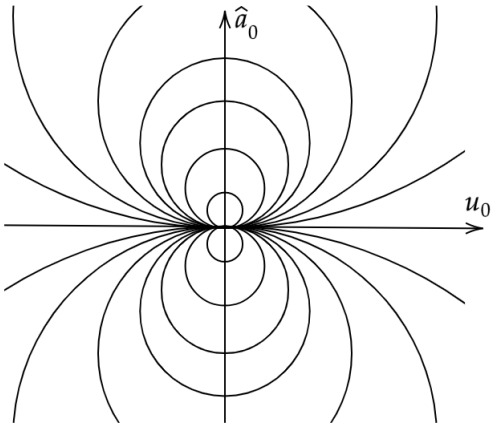

Figure 6.7: $\mathbb{R}^2$ can be foliated by circles which are tangent to u_0 at p.

6.2.4 Conformal geodesics re-intersect the heart boundary

Given any $(p, u_0) \in S(TM)$, we would like to consider the largest open ball $C(u_0, r)$ (see Definition 6.2.3) on which $\exp_{p,u_0}$ is a homeomorphism. It is of course possible this map is a homeomorphism on $C(u_0, r)$ for all $r > 0$, as is the case in Euclidean space (see Section 6.2.3). However, our proof of the no-spiralling theorem in Section 6.4 will be simpler if we work with a finite sized domain with boundary. With this in mind, we make the following definition

Definition 6.2.5. Given any $(p, u_0) \in S(TM)$, define

$$r_{(p,u_0)} := \frac{1}{2} \times \min\{1, \sup\{r : \exp_{p,u_0} \text{ is a homeomorphism on } C(u_0, r)\}\}. \tag{6.2.17}$$

The factor of $1/2$ is included since it will be convenient in the proof of Theorem 6.3.3 for the exponential map to be a homeomorphism onto the heart and its boundary.

Definition 6.2.6. The heart which is the image of the set $C(u_0, r_{(p,u_0)})$ under the exponential map at (p, u_0) is denoted

$$H_{p,u_0} := \exp_{p,u_0}(C(u_0, r_{(p,u_0)}). \tag{6.2.18}$$

For the proof of the no-spiralling theorem (Theorem 6.1.3), we will require the following property of this set.

Theorem 6.2.7. Let $(p, u_0) \in S(TM)$. Then any conformal geodesic with unit tangent u_0 at p re-intersects the boundary of the heart H_{p,u_0}.

Proof: As discussed in Section 6.2.1, a conformal geodesic is the image under the exponential map of a curve in T_pM defined by holding $\hat{a}_0$ and $\sin\theta/|A|$ constant while varying $|A|$. Therefore, a conformal geodesic intersects the boundary of H_{p,u_0} when this curve reaches the boundary of $C(u_0, r_{(p,u_0)}) \subset T_pM$. This occurs at some $|A| \leq 2r_{(p,u_0)}$. $\square$

We therefore see from the definition of the exponential map (Definition 6.2.1) that the arc length parameter distance travelled along the conformal geodesic before it reaches the boundary of H_{p,u_0} is at most $4\pi r_{(p,u_0)}$.

6.3 Size of the Heart

The aim of this section is to follow Step 2 of the proof of Theorem 6.1.3 as outlined in Section 6.1.1.

Step 2: Define a notion of size for a heart and show that given any compact $U \subset M$, there exists $\epsilon > 0$ such that there is a heart at p with direction u_0 which has size at least ϵ, for any $p \in U$ and any $u_0 \in S(T_pM)$.

We begin with the following definitions.

Definition 6.3.1. Let H_{p,u_0} be a heart at p with direction $u_0 \in S(T_pM)$. Define $k(p, u_0, r)$ to be the set of all closed balls in M of radius r with p on their boundary and u_0 pointing into or tangent to the ball.

Crucially, if r is sufficiently small then all balls in $k(p, u_0, r)$ will be contained inside the closure of H_{p,u_0}, which we denote $\bar{H}_{p,u_0}$ (see Figure 6.8).

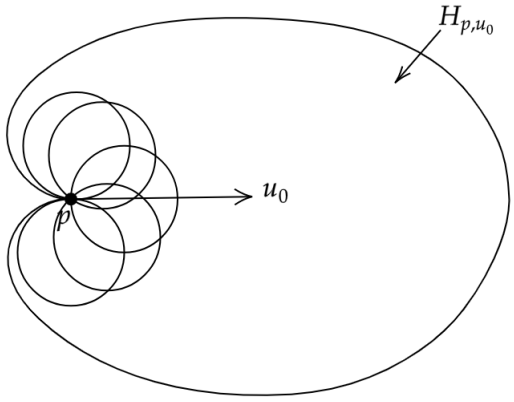

Figure 6.8: This figure shows a sample of balls in the set $k(p, u_0, r)$. We have chosen $r < R(p, u_0)$ which means that all of these balls are contained in the heart H_{p,u_0}.

Definition 6.3.2. At any point $(p, u_0) \in S(TM)$, we define the size of the heart H_{p,u_0} by

$$\begin{aligned} R : S\,(TM) &\to \mathbb{R}_{>0} \\ (p, u_0) &\mapsto \sup\{r : \bar{B} \subset \bar{H}_{p,u_0} \forall \bar{B} \in k(p, u_0, r)\}. \end{aligned} \tag{6.3.1}$$

Theorem 6.3.3. Let $(M, [g])$ be a conformal manifold with C^4 conformal metric and let U be a compact subset of $S(TM)$. Then there exists some $\epsilon > 0$ such that $R(p, u_0) \geq \epsilon$ for any $(p, u_0) \in S(TU)$.

To prove this theorem we begin by considering the following initial value problem

$$y'(t) = f(t, y) \text{ and } y(0) = y_0. \tag{6.3.2}$$

We will require the following theorem (which we do not prove).

Theorem 6.3.4. [42, Section V.3 Corollary 3.3 and Section V.4 Corollary 4.1] Suppose $f(t, y)$ is of class C^m, $m \geq 1$, on an open (t, y)-set. Then (6.3.2) has unique solution $y = \eta(t, y_0)$ which is of class C^m on its domain of existence.

From this we can establish the following corollary.

Corollary 6.3.5. Suppose the metric g is C^4. Then the heart boundary is a C^2 surface away from the cusp.

Proof: We will parameterise conformal geodesics $x^\alpha(t)$ by their arc length, t. The conformal geodesic equation can then be written as three separate 1st order ODEs on some co-ordinate patch

$$\begin{aligned}\frac{dx^\beta}{dt} &= u^\beta \\ \frac{du^\beta}{dt} &= a^\beta - \Gamma^\beta_{\gamma\delta} u^\gamma u^\delta \\ \frac{da^\beta}{dt} &= -\Gamma^\beta_{\gamma\delta} u^\gamma a^\delta - \left(g_{\gamma\delta} a^\gamma a^\delta + L_{\gamma\delta} a^\gamma a^\delta\right) u^\beta + L^\beta_\gamma u^\gamma.\end{aligned} \tag{6.3.3}$$

Since the metric is C^4, the Christoffel symbols $\Gamma^\beta_{\gamma\delta}$, the Schouten tensor L and the corresponding endomorphism $L^\#$ are all C^2. Theorem 6.3.4 therefore implies that the solution $x^\alpha = \eta^\alpha(t, x_0, u_0, a_0)$ is also C^2. This tells us that, away from $A = 0$, the exponential map considered as a function of (p, u_0, A) is C^2. We conclude that the heart boundary is C^2 away from the cusp. □

Next we define the following function.

Definition 6.3.6.

$$\begin{aligned}R_1(p, u_0) := \sup\{r : &\text{ any open ball in } M \text{ of radius } r \text{ with } u_0 \text{ tangent to} \\ &\text{its boundary is contained in } H_{p,u_0}\}\end{aligned} \tag{6.3.4}$$

Note that, unlike Definition 6.3.2, this definition only considers balls which have u_0 tangent to their boundary at p.

Lemma 6.3.7. For any compact $U \subset S(TM)$, there exists $\epsilon > 0$ such that $R_1(p, u_0) \geq \epsilon$ for any $(p, u_0) \in U$.

Proof: Let $U \subset S(TM)$ be compact and let $(p, u_0) \in U$. This specifies a value $r_{(p,u_0)}$ such that the exponential map at (p, u_0) is a homeomorphism from the open ball $C(u_0, r_{(p,u_0)})$ to

the heart H_{p,u_0}. Next we choose a unit vector $\hat{a}_0$ which is perpendicular to u_0. By restricting to elements of $C(u_0, r_{(p,u_0)}) \subset T_{u_0}(T_pM)$ which lie in $\text{span}\{u_0, \hat{a}_0\}$, we obtain a curve through $0 \in T_{u_0}(T_pM)$. This circle is mapped by the exponential map to a curve, $\lambda_{p,u_0,\hat{a}_0}$, which passes through p and lies on the boundary of the heart H_{p,u_0}. Finally, we choose some value $x \in (-\pi/2, \pi/2)$. By considering the angle between A and u_0, this uniquely specifies a point on this circle. The exponential map takes this point to a point on the curve $\lambda_{p,u_0,\hat{a}_0}$. Note that choosing $x \in (-\pi/2, \pi/2)$ means we do not consider the problem point at 0 which is mapped to the cusp at p.

By Corollary 6.3.5, $\lambda_{p,u_0,\hat{a}_0}$ is an endless C^2 curve. This allows us to consider its curvature. For any $x \in (-\pi/2, \pi/2)$ we define the following real–valued function

$$F(p, u_0, \hat{a}_0, x) \mapsto \left| \frac{d^2}{dx^2} \lambda_{p,u_0,\hat{a}_0}(x) \right|. \tag{6.3.5}$$

From Corollary 6.3.5, we see that F is a continuous function.

There is a subtlety at the point p, where the boundary of the heart contains a cusp and directional derivatives have discontinuities. However, if we approach p in either of the two directions along $\lambda_{p,u_0,\hat{a}_0}$ then the function F tends to a finite limit. Note that the two limits taken in opposite directions may not be equal. Attaching endpoints to $\lambda_{p,u_0,\hat{a}_0}$ at p, these two limits correspond to the two values we get for the magnitude of the curvature of $\lambda_{p,u_0,\hat{a}_0}$ at p if we use one-sided derivatives in either direction.

This means that for fixed $(p, u_0, \hat{a}_0)$, the function $F(p, u_0, \hat{a}_0, x)$ is bounded. Moreover, this bound is itself a continuous function of $(p, u_0, \hat{a}_0)$. We conclude that if we restrict to $(p, u_0) \in U$, with any choice of $\hat{a}_0$ and $x \in (-\pi/2, \pi/2)$, then $F(p, u_0, \hat{a}_0, x)$ is bounded.

In short, given any $(p, u_0) \in U$ and any circle of radius $r_{(p,u_0)}$ in $T_{u_0}(T_pM)$ with u_0 perpendicular to its boundary, the magnitude of the sectional curvature at a point on the image of this circle, taken in the direction of the circle's image, is bounded by $1/\epsilon > 0$, for some $\epsilon > 0$, where we understand that at p itself we consider two different sectional curvatures corresponding to the different directions along the image of the circle.

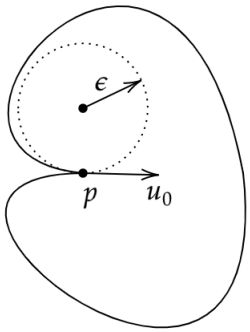

Figure 6.9: If every sectional curvature at every point on the heart boundary is bounded above by $\epsilon > 0$, then any ball of radius $1/\epsilon$ with u_0 tangent to its boundary at p is contained inside the heart.

As a result, for any $(p, u_0) \in U$, the heart H_{p,u_0} must contain every open ball in M of radius ϵ which has u_0 tangent to its boundary at p, i.e. $R_1(p, u_0) \geq \epsilon$ (see Figure 6.9). $\square$

Next we consider balls in M with u_0 pointing inwards on the boundary. We make the following definitions.

Definition 6.3.8.

$$B_{1/2}(r, p, u_0) := B(r, p) \cap \{q : g(\exp_p^{-1}(q), u_0) \geq 0.\} \tag{6.3.6}$$

Here $\exp_p$ denotes the metric geodesic map at p (we can restrict ourselves to sufficiently small r so that this map is invertible on $B(p, r)$ for all $(p, u_0) \in W$). The set we have defined consists of points in the half ball with boundary perpendicular to u_0 at p which have non-negative u_0 co-ordinate, where these co-ordinates are defined using the metric geodesic map applied to an orthonormal basis of T_pM (see Figure 6.10).

Definition 6.3.9.

$$R_2(p, u_0) := \sup\{r : B_{1/2}(r, p, u_0) \subset H_{p,u_0}.\} \tag{6.3.7}$$

Lemma 6.3.10. For any compact $U \subset S(TM)$, there exists $\epsilon > 0$ such that $R_2(p, u_0) > \epsilon$ for any $(p, u_0) \in U$.

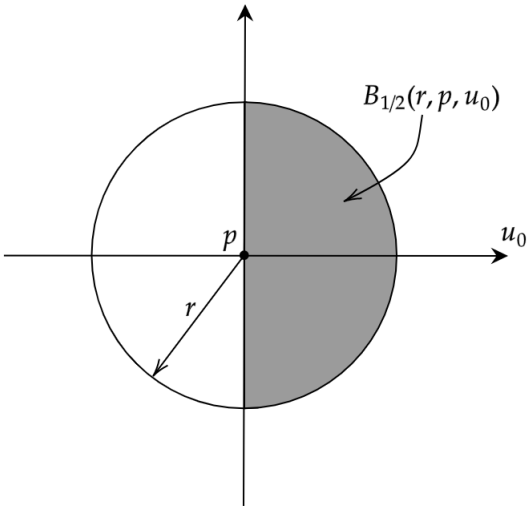

Figure 6.10: $B_{1/2}(r, p, u_0)$ is the half ball in M of radius r centred on p consisting of points q such that $g(\exp_p^{-1}(q), u_0) \geq 0$.

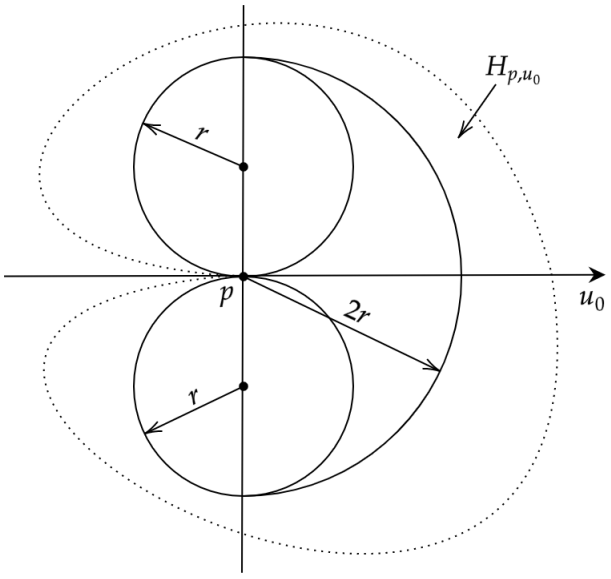

Figure 6.11: If $R_1(p, u_0) > r$ and $R_2(p, u_0) > 2r$ then $R(p, u_0) > r$.

Proof: Let $U \subset S(TM)$ be compact. From Corollary 6.3.5, $\exp_{p,u_0}(A)$ regarded as a function of (p, u_0, A) is continuous (in fact C^2) away from the cusp. We also saw in Section 6.2.2 that the boundary of H_{p,u_0} is continuous (including at p). We conclude that the boundary of H_{p,u_0} varies continuously with (p, u_0) and hence $R_2(p, u_0)$ is also continuous. The result follows since $R_2(p, u_0)$ is strictly positive and a continuous function on a compact set is bounded and attains its bounds. □

Combining these two lemmas, we are able to prove Theorem 6.3.3.

Proof of Theorem 6.3.3: By Lemmas 6.3.7 and 6.3.10, for any compact $U \subset S(TM)$, there exists $\epsilon > 0$ such that $R_1(p, u_0) \geq \epsilon$ and $R_2(p, u_0) \geq 2\epsilon$.

The result follows by observing that $R(p, u_0) > R_1(p, u_0)$ and $R(p, u_0) > R_2(p, u_0)$ (Figure 6.11). □

6.4 No-Spiralling Theorem

The aim of this section is to follow Step 3 of the proof of Theorem 6.1.3 as outlined in Section 6.1.1.

The theorem we will prove is the following.

Step 3: Using the fact that a conformal geodesic with unit tangent u_0 at p must re-intersect the boundary of H_{p,u_0}, deduce that conformal geodesics cannot spiral.

Theorem 6.1.3. Let $(M, [g])$ be a conformal manifold with C^4 conformal metric. Then conformal geodesics on $(M, [g])$ cannot spiral.

Proof: Suppose there is a conformal geodesic, γ, which spirals towards some point $p_* \in M$. We will show that there exists $r > 0$ such that $\bar{B}(p_*, r) \subset \bar{H}_{p,u_0}$, where p and u_0 are the point and unit tangent at which γ enters $\bar{B}(p_*, r)$ for the final time (i.e. it remains trapped in $B(p_*, r)$ thereafter). This would then contradict Theorem 6.2.7 since if γ does not leave

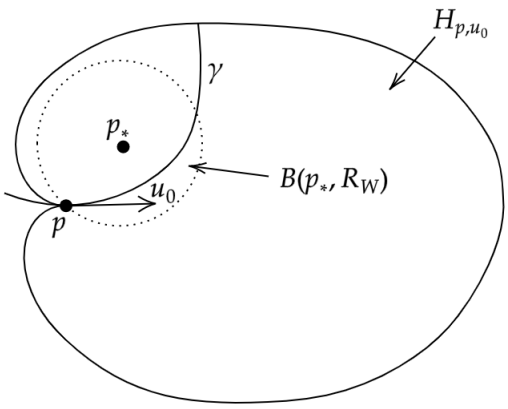

Figure 6.12: If γ enters $B(p_*, R_W) \subset H_{p,u_0}$, then in order to reach the boundary of H_{p,u_0} it must leave $B(p_*, R_W)$.

$B(p_*, r)$ then it cannot re-intersect the boundary of H_{p,u_0}. This is illustrated in Figure 6.12.

Define a compact subset of $S(TM)$ by $W := \{(p, u_0) \subset S\,(TM) : p \in \bar{B}(p_*, 1)\}$. Invoking Theorem 6.3.3, we can then define:

$$R_W := \inf\{R(p, u_0) : (p, u_0) \in W\} > 0. \tag{6.4.1}$$

So for any $(p, u_0) \in S\,(TM)$ with $d(p, p_*) \leq 1$, any closed ball in M of radius at most R_W with u_0 inward pointing or tangent to its boundary at p is contained inside $\bar{H}_{p,u_0}$.

Let p denote the point at which γ enters $\bar{B}(p_*, R_W)$ for the final time and let u_0 denote its unit tangent at this point (so u_0 is either inward pointing or tangent to the boundary of $\bar{B}(p_*, R_W)$ at p). By construction we then have $\bar{B}(p_*, R_W) \subset \bar{H}_{p,u_0}$. But since γ remains trapped in $B(p_*, R_W)$, it cannot re-intersect the boundary of H_{p,u_0}. This contradicts Theorem 6.2.7. $\square$

Chapter7

Summary and Outlook

The primary aim of this thesis was the study of conformally invariant properties of spacetime. In Chapter 2 we considered two versions of the Penrose property which were shown to be equivalent in asymptotically flat spacetimes. If a spacetime satisfies the Penrose property then this can be thought of as suggesting that its asymptotics near spatial infinity are fundamentally different from those of Minkowski. As a result, it was argued that the existence of a physically relevant spacetime satisfying the Penrose property provides evidence against a "Lorentz covariant" quantum gravity construction. We studied the Penrose property in positive and negative mass Schwarzschild spacetime in various dimensions and found that it held only in the positive mass case in 3 and 4 dimensions. We concluded that this provides evidence against a "Lorentz covariant" quantum gravity construction in 3 or 4 spacetime dimensions, but we found no such evidence in higher dimensions. Although we found a necessary and sufficient condition on the metric for the Penrose property to be satisfied in static, spherically symmetric spacetimes, the more general case remains open.

Next we broadened the definition of the Penrose property to include spacetimes which are not asymptotically flat. In the asymptotically de Sitter case we found, as for asymptotically flat spacetimes, that the two versions of the Penrose property were equivalent. We also found that the Penrose property is not satisfied in pure de Sitter spacetime, although it is satisfied in positive mass Schwarzschild-de Sitter of dimension 4 or higher. This provides evidence against an "$SO(d+1,1)$ covariant" construction of quantum gravity in 4 or more

spacetime dimensions. We also observed that the Penrose property in asymptotically de Sitter spacetimes appears to be more complicated than in the asymptotically flat case, since it is no longer a property purely of the metric asymptotics. For this reason it seems that obtaining a general result regarding the Penrose property will be more challenging.

In the asymptotically anti-de Sitter case, we found that one version of the Penrose property (the "finite version") does not generalise to an interesting property (in fact we showed that it is never satisfied). However, by understanding the Penrose property in asymptotically flat spacetime as a statement about the ability of causal curves to connect points on $\mathscr{I}^{\pm}$ which can only by connected by null curves on the conformal boundary, we are able to generalise the "non-timelike boundary version of the Penrose property" to the asymptotically AdS setting. We call this new property the "timelike boundary version of the Penrose property" and observe that it was previously considered by Gao and Wald in [39]. We find an interesting difference between the timelike and non-timelike boundary versions of the Penrose property. In the former, the results of [39] show that the property fails in spacetimes which satisfying a focusing theorem. However, in the asymptotically flat and asymptotically dS cases, we find that a necessary condition for the Penrose property to be satisfied in Schwarzschild (respectively Schwarzschild-de Sitter) spacetime of mass m is $m > 0$. We had previously argued in the asymptotically flat case that the positive point mass at i^0 provided the focusing and retarding of null rays necessary for the Penrose property to be satisfied. However, this does not appear to be the case in the asymptotically AdS setting. Although the results of Gao and Wald [39] provide conditions under which the timelike boundary version of the Penrose property is guaranteed to fail, it remains an open problem to determine general conditions under which the property holds. Another possible approach for the study of the Penrose property is through the use of conformally isometric embeddings (see for example [32]).

The link between positivity of mass and the focusing and retarding of null geodesics discussed previously for asymptotically flat spacetimes is strengthened by the positive mass theorem, and in particular the version proved in Chapter 4. This proof uses arguments inspired by Penrose, Sorkin and Woolgar [61] who showed that asymptotically flat spacetimes with negative ADM mass necessarily contain a null line. Negative mass can then be ruled out if

the spacetime is assumed to satisfy a focusing theorem which forbids the existence of such a line. If the Einstein equations are assumed to hold then the conditions of these focusing theorems often have the interpretation of imposing some sort of local non-negative energy condition on spacetime. In [61], it is argued that a null line can be constructed in a negative mass 3+1 dimensional spacetime by taking the limit (in a suitable topology) of a sequence of "faster and faster" causal curves connecting antipodal generators of $\mathscr{I}^{\pm}$. The key step is to show that these curves cannot "escape to infinity" and hence tend to a limit curve which enters the interior of the spacetime. It is then argued that this limit curve is necessarily a null line. The key step relied on the opposite result to the one shown by Penrose for positive mass Schwarzschild in [59]. Indeed, it is shown that if the curves do "escape to infinity" then their time of flight must diverge to $+\infty$. This contradicts the sequence as consisting of faster and faster curves. However, this divergence is no longer present in higher dimensions and is precisely the reason Penrose's arguments in [59] do not generalise. This was noted in [61] and as a result it was necessary to alter the argument in order to prove a version of the positive mass theorem in higher dimensions. This alteration involved using a comparison argument of the type used in Chapter 2 to prove the failure of the Penrose property in Schwarzschild spacetime of negative mass in 3+1 dimensions and positive mass in higher dimensions. This argument involved considering multiple metrics defined on the same manifold and comparing the causal properties of both. It was shown that near conformal infinity the lightcones of a negative mass asymptotically Schwarzschildean spacetime are contained inside the lightcones of some Minkowski metric. From this fact we are able to construct a causal curve between antipodal generators of $\mathscr{I}^{\pm}$ which has negative time of flight. This curve is used as the starting point for our sequence of faster and faster causal curves which we show converges towards a null line through the interior spacetime.

Alternative versions of the positive mass theorem [64–66, 72] contain a rigidity statement which says that $m = 0$ if and only if the spacetime is isometric to a subset of Minkowski. In [61] (and also in [33]), the authors were unable to prove such a result. They argue that any attempt to do so would contradict known asymptotically flat solutions with non-zero ADM mass in higher dimensions. We have been able to prove a higher dimensional version of

the positive mass theorem using global causality arguments of the sort found in [61], however we have once again been unable to prove a rigidity statement. If $m = 0$, the behaviour of the metric near conformal infinity would now be governed by the next leading order terms (i.e. the $o\left(|m|r^{-(d-2)}\right)$ terms in (4.2.3)), over which we have no control. It remains an open problem to determine a suitable set of assumptions under which a rigidity result can be proved using global causality arguments.

It was argued in [61] that the Penrose property is a conformally invariant property of spacetimes near spatial infinity. This observation lead us to consider more generally the nature of possible conformal completions at this point. Another motivation has been the desire to use limiting arguments for curves near i^0. The problem with such arguments was that it was unclear when they would be valid since the nature of the metric at i^0 was not understood in general. It was already known that Minkowski spacetime admitted a smooth completion at spatial infinity, while the standard completion of the Schwarzschild spacetime in $3+1$ dimensions is continuous but not C^1. We have shown in Chapter 5 that $(d+1)$-dimensional Myers-Perry metrics admit a conformal completion at i^0 which is $C^{d-3,1}$. Furthermore, we have shown that this result is optimal in even spacetime dimensions in the sense that no C^{d-2} completion exists unless the ADM mass vanishes. In particular, if $d \geq 4$ then the metric can be chosen to be at least $C^{1,1}$. This means that the geodesic equations have a unique solution which depends continuously on the initial point p and initial unit tangent direction, u, at p. However, several major results from causality theory (such as Theorem 4.5.1 and results in [58]) cannot be applied since they require the metric to be C^2. If $d \geq 5$ then the conformal metric is at least C^2 and all standard results on causality can be applied at i^0. In particular, one can define an exponential map which is C^{d-4}.

Our results in Chapters 2 to 5 have primarily focused on conformally compactified spacetimes. It has been suggested in [37] that the analysis of such spacetimes, particularly near the conformal boundary, may be aided by the use of conformal geodesics. It was proposed that these curves be used to construct conformally invariant co-ordinate systems which may be extended across the conformal boundary. However, if this is to be done in a useful manner then we would expect conformal geodesics to satisfy certain regularity conditions.

In particular, we hope to rule out the possibility that they spiral towards a point on the manifold, since this would lead to another type of co-ordinate singularity which we would need to guard against. In Chapter 6 we proved a no-spiralling theorem for conformal geodesics on Riemannian manifolds. This proof required an improved understanding of the local properties of these curves, in particular through the definition of a conformal geodesic analogue of the exponential map. We were able to construct an alternative proof of the no-spiralling proof for metric geodesics and show how this could be adapted to the conformal geodesic case. It should be noted that this method was fairly general and in particular does not rely on the conformal invariance of solutions. It therefore appears that we may be able to use these methods to prove no-spiralling results for solutions to other systems of ODEs. In the Lorentzian case, our proof fails from the very beginning. In particular, the exponential map (Definition (6.2.1)) is not well defined since it is now possible to have $|A| = 0$ for $A \neq 0$. If these curves are to be used to study the conformal properties of spacetime then the Lorentzian case should also be considered.

It would also be interesting to investigate further the similarities and differences between metric and conformal geodesics. For example, it is a standard result that given any $p \in M$, there exists a neighbourhood $U \ni p$ such that for any $q \in U$ there is a unique metric geodesic from p to q contained entirely in U. This is the statement that the exponential map has non-zero injectivity radius at every $p \in M$. It is not clear if this result can be adapted to the conformal geodesic setting. Since the equations are now third order, one may hope that an analogous result can be proved regarding conformal geodesics connecting three sufficiently nearby points. This appears to be complicated by the fact that there are now different orderings in which the points may be connected. Another possibility is to investigate whether conformal geodesics can be specified uniquely by, for example, two sufficiently nearby points and an initial unit tangent vector. We leave this for future work.

Appendices

A1 Compactness of Causal Curves Following [67]

In this appendix we summarise how the convergence of the sequence of causal curves $(\gamma_i)_{i=0}^{\infty}$ discussed in Section 4.4 should be defined. To understand this convergence, we follow [48] and make the following definitions.

Definition A1.1. The sequence of causal curves $(\gamma_i)_{i=0}^{\infty}$ converges to γ in the *upper topology* iff the γ_i are eventually included in every open set which includes γ.

Definition A1.2. The sequence of causal curves $(\gamma_i)_{i=0}^{\infty}$ converges to γ in the *lower topology* iff the γ_i eventually meet every open set which meets γ.

Definition A1.3. The sequence of causal curves $(\gamma_i)_{i=0}^{\infty}$ converges to γ in the *Vietoris topology* iff it converges in both the upper and lower topologies.

The *fastest causal curve* γ in Section 4.4 is defined to be the limit of the sequence $(\gamma_i)_{i=0}^{\infty}$ in the Vietoris topology [67]. Since we have assumed that $\mathcal{D} \cup \mathscr{I}$ is globally hyperbolic, if we were also to assume that the metric were C^2 (as in Theorem 4.5.1) then the three definitions above would coincide (see [67] Alternative Definition 26 and comments after the proof of Lemma 28).

Bibliography

[1] L.F. Abbott and S. Deser, *Stability of gravity with a cosmological constant*, Nuclear Physics B **195** (1982), no. 1, 76–96.

[2] S. Alexakis, V. Schlue, and A. Shao, *Unique continuation from infinity for linear waves*, Advances in Mathematics **286** (2013), 481–544.

[3] R. Arnowitt, S. Deser, and Charles W. Misner, *Republication of: The dynamics of general relativity*, General Relativity and Gravitation **40** (2008), no. 9, 1997–2027.

[4] A. Ashtekar, *Logarithmic ambiguities in the description of spatial infinity*, Found. Phys. **15** (1985), 419–431. MR 811916

[5] A. Ashtekar and R.O. Hansen, *A unified treatment of null and spatial infinity in general relativity. I. Universal structure, asymptotic symmetries and conserved quantities at spatial infinity*, Jour. Math. Phys. **19** (1978), 1542–1566.

[6] A. Ashtekar and J.D. Romano, *Spatial infinity as a boundary of spacetime*, Class. Quantum Grav. **9** (1992), 1069–1100. MR 1158130

[7] R. Beig and P. T. Chruściel, *The asymptotics of stationary electro-vacuum metrics in odd spacetime dimensions*, Class. Quantum Grav. **24** (2007), 867–874. MR MR2297271

[8] R. Beig and J. M. Heinzle, *CMS-slicings of Kottler-Schwarzschild-de Sitter cosmologies*, Commun. Math. Phys. **260** (2005), 673–709.

[9] R. Beig and B.G. Schmidt, *Einstein's equations near spatial infinity*, Commun. Math. Phys. **87** (1982/83), 65–80. MR 680648

[10] R. Beig and W. Simon, *On the multipole expansion for stationary spacetimes*, Proc. Roy. Soc. London A **376** (1981), 333–341.

[11] A Borde, *Geodesic focusing, energy conditions and singularities*, Classical and Quantum Gravity **4** (1987), no. 2, 343–356.

[12] J. D. Brown and J. W. York, *Quasilocal energy and conserved charges derived from the gravitational action*, Phys. Rev. D **47** (1993), 1407–1419.

[13] X. O. Camanho, J. D. Edelstein, J. Maldacena, and A. Zhiboedov, *Causality constraints on corrections to the graviton three-point coupling*, Journal of High Energy Physics **2016** (2016), no. 2.

[14] P. Cameron, *The Penrose property with a cosmological constant*, Classical and Quantum Gravity **39** (2022), no. 11, 115002.

[15] ———, *Positivity of mass in higher dimensions*, Annales Henri Poincaré (2022), arXiv:2010.05086.

[16] P. Cameron and P. T. Chruściel, *Asymptotic flatness in higher dimensions*, Journal of Mathematical Physics **63** (2022), no. 3, 032501.

[17] P. Cameron and M. Dunajski, *On Schwarzschild causality in higher dimensions*, Classical and Quantum Gravity **37** (2020).

[18] P. Cameron, M. Dunajski, and K. P. Tod, *Conformal geodesics cannot spiral*, 2022, arXiv:2205.07978.

[19] M. P. do. Carmo, *Riemannian geometry.*, Mathematics. Theory and applications, Birkhäuser, Boston, 1992 (eng).

[20] P. T. Chruściel, *On the Invariant Mass Conjecture in General Relativity*, Commun. Math. Phys. **120** (1988), 233.

[21] ———, *On the structure of spatial infinity. I. The Geroch structure*, Jour. Math. Phys. **30** (1989), 2090–2093. MR 1009923

[22] ———, *On the structure of spatial infinity. II. Geodesically regular Ashtekar-Hansen structures*, Jour. Math. Phys. **30** (1989), 2094–2100. MR 1009924

[23] ———, *A poor man's positive energy theorem: II. null geodesics*, Classical and Quantum Gravity **21** (2004), no. 18, 4399–4415.

[24] ———, *Elements of causality theory*, (2011), arXiv:1110.6706.

[25] P. T. Chruściel and E. Delay, *On mapping properties of the general relativistic constraints operator in weighted function spaces, with applications*, Mém. Soc. Math. de France. **94** (2003), 1–103.

[26] P. T. Chruściel and G. J. Galloway, *A poor man's positive energy theorem*, Classical and Quantum Gravity **21** (2004), no. 9, L59–L63.

[27] P. T. Chruściel, G. J. Galloway, and Y. Potaux, *Uniqueness and energy bounds for static AdS metrics*, Phys. Rev. D **101** (2020), 064034.

[28] P. T. Chruściel and J. Grant, *On Lorentzian causality with continuous metrics*, Class. Quantum Grav. **29** (2012), 145001.

[29] J. Corvino and R.M. Schoen, *On the asymptotics for the vacuum Einstein constraint equations*, Jour. Diff. Geom. **73** (2006), 185–217.

[30] S Deser, R Jackiw, and G 't Hooft, *Three-dimensional Einstein gravity: Dynamics of flat space*, Annals of Physics **152** (1984), no. 1, 220–235.

[31] M. Dunajski and W. Kryński, *Variational principles for conformal geodesics*, Lett. Math. Phys. **111** (2021), 127.

[32] M. Dunajski and K. P. Tod, *Conformally isometric embeddings and Hawking temperature*, Classical and Quantum Gravity **36** (2019), no. 12, 125005.

[33] M. Eichmair, L.-H. Huang, D. A. Lee, and R. Schoen, *The spacetime positive mass theorem in dimensions less than eight*, Journal of the European Mathematical Society **18** (2016), 83–121.

[34] R. O. Emparan and H. S. Reall, *Black holes in higher dimensions*, Living Reviews in Relativity **11** (2008), no. 1.

[35] F. G. Friedlander, *Radiation fields and hyperbolic scattering theory*, Mathematical Proceedings of the Cambridge Philosophical Society **88** (1980), no. 3, 483–515.

[36] H. Friedrich, *Gravitational fields near space-like and null infinity*, Jour. Geom. Phys. **24** (1998), 83–163.

[37] H. Friedrich and B. G. Schmidt, *Conformal geodesics in general relativity*, Proceedings of the Royal Society of London. Series A, Mathematical and Physical Sciences **414** (1987), no. 1846, 171–195.

[38] G. J. Galloway, *Maximum Principles for Null Hypersurfaces and Null Splitting Theorems*, Annales Henri Poincaré **1** (2000), no. 3, 543–567.

[39] S. Gao and R. M Wald, *Theorems on gravitational time delay and related issues*, Classical and Quantum Gravity **17** (2000), no. 24, 4999–5008.

[40] R. Geroch, *Structure of the Gravitational Field at Spatial Infinity*, Journal of Mathematical Physics **13** (1972), no. 7, 956–968.

[41] R.O. Hansen, *Multipole moments of stationary spacetimes*, Jour. Math. Phys. **15** (1974), 46–52.

[42] P. Hartman, *Ordinary differential equations*, Volume 38 of Classics in Applied Mathematics, Society for Industrial and Applied Mathematics, 2002.

[43] S. W. Hawking, *Gravitational radiation in an expanding universe*, J. Math. Phys. **9** (1968), 598–604.

[44] S. W. Hawking and G. F. R. Ellis, *The large scale structure of space-time*, Cambridge Monographs on Mathematical Physics, Cambridge University Press, 1973.

[45] S. W. Hawking and R. Penrose, *The singularities of gravitational collapse and cosmology*, Proceedings of the Royal Society of London. A. Mathematical and Physical Sciences **314** (1970), 529 – 548.

[46] J. Holland and G. Sparling, *Complex null geodesics in the extended Schwarzschild universe*, General Relativity and Gravitation **50** (2018), no. 7, 86.

[47] G. T. Horowitz and N. Itzhaki, *Black holes, shock waves, and causality in the AdS/CFT correspondence*, Journal of High Energy Physics **1999** (1999), no. 02, 010–010.

[48] E. Kein and A. Thompson, *Theory of correspondences*, Wiley, New York, 1984.

[49] C.-C. M. Liu and S.-T. Yau, *Positivity of quasilocal mass*, Phys. Rev. Lett. **90** (2003), 231102.

[50] Juan Martin Maldacena, *The Large N limit of superconformal field theories and supergravity*, Adv. Theor. Math. Phys. **2** (1998), 231–252.

[51] L. J. Mason and J-P Nicolas, *Conformal scattering and the Goursat problem*, Journal of Hyperbolic Differential Equations **01** (2004), no. 02, 197–233.

[52] E. Minguzzi, *Lorentzian causality theory*, Living Rev. Rel. **22** (2019).

[53] N. Ó Murchadha, L. B. Szabados, and K. P. Tod, *Comment on "positivity of quasilocal mass"*, Phys. Rev. Lett. **92** (2004), 259001.

[54] R. C. Myers and M. J. Perry, *Black holes in higher dimensional spacetimes*, Ann. Phys. **172** (1986), 304–347.

[55] R. Penrose, *Asymptotic properties of fields and space-times*, Phys. Rev. Lett. **10** (1963), 66–68.

[56] ———, *Conformal treatment of infinity*, General Relativity and Gravitation (1964), 565–586.

[57] ———, *Perspectives in geometry and relativity*, Hlavaty Festschrift, ed. B. Hoffmann, p. 252, Bloomington: Indiana University Press, 1966.

[58] ———, *Techniques in differential topology in relativity*, Society for Industrial and Applied Mathematics, 1972.

[59] ———, *On Schwarzschild causality—a problem for "Lorentz covariant" general relativity*, 1980.

[60] ———, *Quasi-local mass and angular momentum in general relativity*, Proceedings of the Royal Society of London. A. Mathematical and Physical Sciences **381** (1982), 53 – 63.

[61] R. Penrose, R. D. Sorkin, and E. Woolgar, *A positive mass theorem based on the focusing and retardation of null geodesics*, 1993.

[62] K. Prabhu, *Conservation of asymptotic charges from past to future null infinity: supermomentum in general relativity*, Jour. High Energy Phys. (2019), 148, 47. MR 3940857

[63] B. G. Schmidt, *Conformal geodesics*, Conformal Groups and Related Symmetries Physical Results and Mathematical Background (Berlin, Heidelberg) (A. O. Barut and H. D. Doebner, eds.), Springer Berlin Heidelberg, 1986, pp. 135–137.

[64] R. Schoen and S.-T. Yau, *On the proof of the positive mass conjecture in general relativity*, Communications in Mathematical Physics **65** (1979), no. 1, 45 – 76.

[65] ———, *Proof of the positive mass theorem. II*, Communications in Mathematical Physics **79** (1981), no. 2, 231 – 260.

[66] ———, *The energy and the linear momentum of space-times in general relativity*, Communications in Mathematical Physics **79** (1981), no. 1, 47 – 51.

[67] R. D. Sorkin and E. Woolgar, *A causal order for spacetimes with C^0 Lorentzian metrics: proof of compactness of the space of causal curves*, Classical and Quantum Gravity **13** (1996), no. 7, 1971–1993.

[68] A. Staruszkiewicz, *Gravitation theory in three-dimensional space*, Acta Phys. Polon. **24** (1963), 735–740.

[69] K. P. Tod, *Some examples of the behaviour of conformal geodesics*, Journal of Geometry and Physics **62** (2012), no. 8, 1778–1792.

[70] R. M Wald, *General relativity*, Chicago Univ. Press, Chicago, IL, 1984.

[71] M.-T. Wang, *Four lectures on quasi-local mass*, 2015.

[72] E. Witten, *A new proof of the positive energy theorem*, Communications in Mathematical Physics **80** (1981), no. 3, 381–402.

[73] ———, *Anti-de Sitter space, thermal phase transition, and confinement in gauge theories*, Adv. Theor. Math. Phys. **2** (1998), 505–532.

[74] ———, *Light rays, singularities, and all that*, Reviews of Modern Physics **92** (2020), no. 4.